ORTA DOĞU TEKNİK ÜNİVERSİTESİ
FEN BİLİMLERİ ENSTİTÜSÜ MÜDÜRLÜĞÜ

TEZ ŞABLONU ONAY FORMU
THESIS TEMPLATE CONFIRMATION FORM

1. Şablonda verilen yerleşim ve boşluklar değiştirilmemelidir.
2. **Jüri tarihi** Başlık Sayfası, İmza Sayfası, Abstract ve Öz'de ilgili yerlere yazılmalıdır.
3. İmza sayfasında jüri üyelerinin unvanları doğru olarak yazılmalıdır. Tüm imzalar **mavi pilot kalemle** atılmalıdır.
4. **Disiplinlerarası** programlarda görevlendirilen öğretim üyeleri için jüri üyeleri kısmında tam zamanlı olarak çalıştıkları anabilim dalı başkanlığının ismi yazılmalıdır. Örneğin: bir öğretim üyesi Biyoteknoloji programında görev yapıyor ve biyoloji bölümünde tam zamanlı çalışıyorsa, İmza sayfasına biyoloji bölümü yazılmalıdır. İstisnai olarak, disiplinler arası program başkanı ve tez danışmanı için disiplinlerarası program adı yazılmalıdır.
5. Tezin **son sayfasının sayfa** numarası Abstract ve Öz'de ilgili yerlere yazılmalıdır.
6. Bütün chapterlar, referanslar, ekler ve CV sağ sayfada başlamalıdır. Bunun için **kesmeler** kullanılmıştır. **Kesmelerin kayması** fazladan boş sayfaların oluşmasına sebep olabilir. Bu gibi durumlarda paragraf (¶) işaretine tıklayarak kesmeleri görünür hale getirin ve yerlerini **kontrol edin**.
7. Figürler ve tablolar kenar boşluklarına taşmamalıdır.
8. Şablonda yorum olarak eklenen uyarılar dikkatle okunmalı ve uygulanmalıdır.
9. Tez yazdırılmadan önce PDF olarak kaydedilmelidir. Şablonda yorum olarak eklenen uyarılar PDF dokümanında yer almamalıdır.
10. Tez taslaklarının kontrol işlemleri tamamlandığında, bu durum öğrencilere METU uzantılı öğrenci e-posta adresleri aracılığıyla duyurulacaktır.
11. Tez yazım süreci ile ilgili herhangi bir sıkıntı yaşarsanız, Sıkça Sorulan Sorular (SSS) sayfamızı ziyaret ederek yaşadığınız sıkıntıyla ilgili bir çözüm bulabilirsiniz.

1. Do not change the spacing and placement in the template.
2. Write **defense date** to the related places given on Title page, Approval page, Abstract and Öz.
3. Write the titles of the examining committee members correctly on Approval Page. **Blue ink** must be used for all signatures.
4. For faculty members working in **interdisciplinary programs**, the name of the department that they work full-time should be written on the Approval page. For example, if a faculty member staffs in the biotechnology program and works full-time in the biology department, the department of biology should be written on the approval page. Exceptionally, for the interdisciplinary program chair and your thesis supervisor, the interdisciplinary program name should be written.
5. Write **the page number of the last page** in the related places given on Abstract and Öz pages.
6. All chapters, references, appendices and CV must be started on the right page. **Section Breaks** were used for this. **Change in the placement** of section breaks can result in extra blank pages. In such cases, make the section breaks visible by clicking paragraph (¶) mark and **check their position.**
7. All figures and tables must be given inside the page. Nothing must appear in the margins.
8. All the warnings given on the comments section through the thesis template must be read and applied.
9. Save your thesis as pdf and Disable all the comments before taking the printout.
10. This will be announced to the students via their METU students e-mail addresses when the control of the thesis drafts has been completed.
11. If you have any problems with the thesis writing process, you may visit our Frequently Asked Questions (FAQ) page and find a solution to your problem.

☒ **Yukarıda bulunan tüm maddeleri okudum, anladım ve kabul ediyorum. / I have read, understand and accept all of the items above.**

Name : Selime
Surname : Çelik
E-Mail : selime.celik@metu.edu.tr
Date : 14.06.2024
Signature : _____

GENOME-WIDE ASSOCIATION STUDY IN COMMON BEAN UNDER IRON DEFICIENCY

A THESIS SUBMITTED TO
THE GRADUATE SCHOOL OF NATURAL AND APPLIED SCIENCES
OF
MIDDLE EAST TECHNICAL UNIVERSITY

BY

SELİME ÇELİK

IN PARTIAL FULFILLMENT OF THE REQUIREMENTS
FOR
THE DEGREE OF MASTER OF SCIENCE
IN
MOLECULER BIOLOGY AND GENETICS

JUNE 2024

Approval of the thesis:

GENOME-WIDE ASSOCIATION STUDY IN COMMON BEAN UNDER IRON DEFICIENCY

submitted by **SELİME ÇELİK** in partial fulfillment of the requirements for the degree of **Master of Science** i**n Molecular Biology and Genetics, Middle East Technical University** by,

Prof. Dr. Naci Emre Altun
Dean, **Graduate School of Natural and Applied Sciences** _____

Prof. Dr. Mesut Muyan
Head of the Department, **Biological Sciences, METU** _____

Assist. Prof. Dr. Emre Aksoy
Supervisor, **Biological Sciences, METU** _____

Examining Committee Members:

Prof. Dr. Sertaç Önde
Biological Sciences, METU _____

Assist. Prof. Dr. Emre Aksoy
Biological Sciences, METU _____

Assoc. Prof. Dr. Ceyhun Kayıhan
Molecular Biology and Genetics, Başkent University _____

Date: 03.06.2024

I hereby declare that all information in this document has been obtained and presented in accordance with academic rules and ethical conduct. I also declare that, as required by these rules and conduct, I have fully cited and referenced all material and results that are not original to this work.

Name Last name : Selime Çelik

Signature :

ABSTRACT

GENOME-WIDE ASSOCIATION STUDY IN COMMON BEAN UNDER IRON DEFICIENCY

Çelik, Selime
Master of Science, Molecular Biology and Genetics
Supervisor: Assist. Prof. Dr. Emre Aksoy

June 2024, 103 pages

Common bean is one of the most important legume crops in the world. Its production and yield are highly affected by iron deficiency in the soil. Despite its significance, there is a gap in the literature regarding the genetic mechanisms underlying iron deficiency tolerance in common beans. This thesis aims to fill this gap by evaluating the root and above-ground characteristics of a pool of common bean accessions under iron deficiency conditions and identifying significant genetic markers linked to iron deficiency tolerance. In this study, 133 common bean landraces and 3 commercial cultivars from 19 provinces in Türkiye were grown in hydroponic systems under iron-deficient conditions for 13 days. Various root and above-ground traits were measured to assess the impact of iron deficiency. Using the GAPIT package in R Studio, these phenotypic data were associated with genotypic data obtained from 7900 DArT-seq markers. Through genome-wide association studies (GWAS), seven significant markers were identified significantly associated with FCR activity, root fresh weight, and total root area. Then, several potential candidate genes near these markers were identified and subsequent gene ontology analysis was done. Besides, five of the most tolerant and five of the most sensitive common bean accessions were identified, therefore, this study offers a foundation for developing

more resilient common bean cultivars, which could significantly enhance productivity in iron-deficient soils.

Keywords: Common Bean, Iron Deficiency, Genome-wide Association Study, Root Characteristics, Above-soil Characteristics

ÖZ

DEMİR EKSİKLİĞİNDE FASULYEDE GENOM ÇAPINDA İLİŞKİLENDİRME ÇALIŞMASI

Çelik, Selime
Yüksek Lisans, Moleküler Biyoloji ve Genetik
Tez Yöneticisi: Dr. Öğr. Üyesi Emre Aksoy

Haziran 2024, 103 sayfa

Fasulye, dünyadaki önemli baklagil bitkilerinden biridir. Üretimi ve verimi topraktaki demir eksikliğinden oldukça etkilenmektedir. Önemine rağmen, fasulyede demir eksikliği toleransının altında yatan genetik mekanizmalar konusunda literatürde bir boşluk bulunmaktadır. Bu tez, demir eksikliği koşulları altında bir fasulye genotip havuzunun kök ve toprak üstü özelliklerini değerlendirerek ve demir eksikliği toleransıyla bağlantılı önemli genetik markörleri belirleyerek bu boşluğu doldurmayı amaçlamaktadır. Bu çalışmada, Türkiye'nin 19 ilinden 133 yerel fasulye çeşidi ve 3 ticari çeşit, 13 gün boyunca demir eksikliği koşullarında topraksız sistemde yetiştirilmiştir. Demir eksikliğinin etkisini değerlendirmek için çeşitli kök ve yeşil aksam özellikleri ölçülmüştür. R Studio'da GAPIT paketi kullanılarak bu fenotipik veriler, 7900 DArT-seq marköründen elde edilen genotipik verilerle ilişkilendirilmiştir. Genom çapında ilişkilendirme çalışması (GWAS) aracılığıyla, FCR aktivitesi, kök taze ağırlığı ve toplam kök alanı ile yüksek ilişkili yedi önemli markör belirlenmiştir. Ardından bu markörlerin yakınındaki potansiyel aday genler belirlenmiş ve gen ontoloji analizi yapılmıştır. Ayrıca, bu çalışma kapsamında, demir eksikliğine en toleranslı ve en hassas beşer fasulye aksesyonu belirlenmiştir;

dolayısıyla bu çalışma, demir eksikliği görülen topraklarda üretimi önemli ölçüde artırabilecek daha dayanıklı fasulye çeşitlerinin geliştirilmesi için bir temel sunmaktadır.

Anahtar Kelimeler: Fasulye, Demir Eksikliği, Genom Çapında İlişkilendirme Çalışması, Kök Özellikleri, Yeşil Aksam Özellikleri

So long, and thanks for all the fish.

ACKNOWLEDGMENTS

I extend my deepest gratitude to my supervisor, Assist. Prof. Dr. Emre Aksoy, for his exceptional mentorship and support. His guidance, insightful feedback, and dedication to my growth as a researcher have been invaluable, and I am grateful for the opportunity to learn from him.

I want to thank the thesis examining committee, Prof. Dr. Sertaç Önde and Assoc. Prof. Dr. Ceyhun Kayıhan. I would like to thank Prof. Dr. Faheem Shahzad Baloch and Assoc. Prof. Dr. Muhammad Azhar for providing the seeds.

I want to express my sincere appreciation to my colleagues. Utku Deniz, Zeynep Burcu Durmaz, Damla Söbe, Fatih Kaya, Berk Yanlız, Ece Fidan, Aytuğ Ulutaş, Aleyna Çilingir, İmran Çolak, and Zahit Kaya—together, we formed a cohesive team and achieved remarkable results.

I want to acknowledge the support and encouragement of my dear family. My mother, Nursel Çelik, my father, Ahmet Çelik, and my brother, Altan Çelik. Their love, understanding, and belief in me have been a constant source of motivation.

I would like to extend my heartfelt gratitude to my fiancée, Utku Deniz, for his encouragement and support. His assistance, both as a colleague and a partner, has been invaluable in navigating the challenges of this journey. I am also grateful to our beloved cats, Nohut and Karamel Macchiato, who provided companionship during long hours of writing and research.

I would like to express my appreciation to my friends, Fatih Kaya, Berfin Kalali, and Anna Jasmine Kokino, for their kindness and care in looking after our cats. I trusted them wholeheartedly, and their presence and support have made this journey manageable.

I would like to acknowledge the financial support provided by TUBITAK BIDEB, where I was a 2210A scholarship recipient.

This work was supported by Research Fund of the Middle East Technical University. Project Number: TEZ-YL-108-2023-11059.

TABLE OF CONTENTS

LIST OF TABLES

TABLES

LIST OF FIGURES

FIGURES

LIST OF ABBREVIATIONS

ABBREVIATIONS

GWAS	Genome-wide association study
SNP	Single nucleotide polymorphism
DArT	Diversity arrays technology
FCR	FERRIC CHELATE REDUCTASE or FCR activity in the roots
RFCR	Relative FCR enzyme activity in the roots
CHL	Chlorophyll concentration
RCHL	Relative chlorophyll concentration
LA	Leaf area
RLA	Relative leaf area
LFW	Leaf fresh weight
RLFW	Relative leaf fresh weight
RFW	Root fresh weight
RRFW	Relative root fresh weight
FWR	Fresh weight ratio
RFWR	Relative fresh weight ratio
RDW	Root dry weight
RRDW	Relative root dry weight
LDW	Leaf dry weight
RLDW	Relative leaf dry weight

DWR	Dry weight ratio
RDWR	Relative dry weight ratio
MRN	Main root number
RMRN	Relative main root number
RTN	Root tip number
RRTN	Relative root tip number
TRL	Total root length
RTRL	Relative total root length
MRL	Maximum root length
RMRL	Relative maximum root length
TRA	Total root area
RTRA	Relative total root area
TRV	Total root volume
RTRV	Relative total root volume

CHAPTER 1

INTRODUCTION

1.1 Origin and Importance of Common Bean

Legumes have played a significant role in human diets for thousands of years, offering a rich source of nutrients and serving as staple crops in many cultures. The Fabaceae family, commonly known as the Leguminosae, encompasses a diverse array of approximately 20,000 species spanning 700 genera. Despite this vast diversity, only a select few legumes have been extensively cultivated as staple crops, including peas, chickpeas, soybeans, peanuts, and common beans (Allen, 2013). These leguminous plants are characterized by their distinctive pods, protective structures that encase the seeds during growth. While the primary use of legumes is as seed foods, their pods, leaves, roots, and tubers also contribute valuable dietary components. Renowned for their high protein content, often surpassing that of cereal seeds by double or more, legumes play a crucial role in meeting global nutritional needs (Maphosa & Jideani, 2017).

One of the remarkable features of legumes is their ability to access atmospheric nitrogen through symbiotic relationships with specific microbial species, facilitated by specialized structures known as root nodules. This process allows legumes to convert atmospheric nitrogen into usable forms, such as amino acids, which are then transported to developing seeds for storage and subsequent utilization (Q. Wang et al., 2018). Additionally, legume seeds provide a diverse array of essential nutrients, including iron, thiamin, riboflavin, phytochemicals, oils, and starch, all vital for supporting the growth and development of emerging seedlings (Mullins & Arjmandi, 2021).

Phaseolus vulgaris L., commonly known as the common bean, holds significant importance as a grain legume consumed worldwide for its edible seeds and pods. Its versatility is evident as immature pods, consumed as vegetables like snap beans and French beans, offer a nutritious addition to meals, while mature seeds, harvested as dry beans such as black beans, pinto beans, and kidney beans, serve as both staple foods and potential protein substitutes for meats. Researchers are particularly interested in beans due to their rich nutrient profile, affordability compared to animal protein sources, low carbon impact, and long shelf life (Uebersax et al., 2023). Furthermore, due to its association with nitrogen-fixing bacteria, the need for synthetic fertilizer use is reduced in common beans, which is an important factor for sustainable agricultural purposes (Castro-Guerrero et al., 2016).

The common bean is an annual herbaceous plant that exhibits two main growth habits: bush-type (pseudo-determinate), reaching heights of 20-60 cm, or vining (indeterminate), climbing up to 2-5 meters with support. Along its stem, the plant bears rounded trifoliate leaves, often pubescent and ranging in color from green to purple. The taproot features numerous adventitious roots for anchorage and nutrient uptake. Its inflorescence produces striking white, pale purple, or reddish-purple papilionaceous flowers, extending up to 35 cm in length. The ensuing pods, varying in color from green to yellow, may be straight or curved and measure up to 20 centimeters long, each containing 4 to 12 seeds. These kidney-shaped or round seeds, reaching lengths of 2 cm, display a diverse array of colors including brown, red, green, yellow, purple, and black, with patterns ranging from solid to speckled or flecked (Smith & Rao, 2021).

Common beans play a crucial role in nutrition in Türkiye as well, being one of the main sources of calories, protein, and minerals after cereals. Türkiye stands as the top producer of common beans in the Mediterranean region and the third largest producer globally, with an estimated 279,518 tons of fresh or dried common beans produced annually (Baloch et al., 2022a). Most recent data show that in 2022, 28,346,198.86 tons of dry beans were produced worldwide, with China, Brazil, and Myanmar being the top three producers. 23,340,915.7 tons of green beans were

produced worldwide in 2022. The top producer of green beans was by far China (Mainland) followed by Indonesia and Türkiye (FAO, 2023). Given the significance of common beans in diets worldwide and their essential role in Turkish agriculture, breeding cultivars resilient to Fe deficiency is imperative for sustaining food security and promoting agricultural sustainability.

The cultivation of every current bean variety traces back to two distinct domestication processes of wild populations, occurring at distinct pre-Columbian dates in central Peru and Western Mexico. Following its introduction to South-Western Europe in 1492, the common bean was further disseminated to the Mediterranean region, parts of Asia, and Africa, and eventually reintroduced to the Americas (Pathania et al., 2014).

Domestication, the process of transforming wild plants into crops, is complex. Some scientists suggest multiple domestication events, while others argue for a single event. Domestication led to the formation of two gene pools: Mesoamerican and Andean (Chacón S et al., 2005). The Andean gene pool spans from Southern Peru to Northwestern Argentina, while the Mesoamerican gene pool extends from Colombia to Northern Mexico. After being introduced throughout the 15th and 16th centuries by Columbus and Pizarro, Europe is thought to be a secondary center of diversification for the common bean. First to arrive in Europe in 1506, the gene pool from Mesoamerica was followed in 1528 by the gene pool from the Andes. The subsequent spread of common bean to other European nations was complicated, including multiple introductions from various American locations as well as integrated trade with Mediterranean and European countries. Common beans are currently grown as distinct gene pools or as hybrid forms between the two gene pools all over the world, including Türkiye, for their edible dry seeds or unripe fruit (Nadeem et al., 2018).

The challenge of ensuring food security for present and future generations has emerged as a paramount concern in the twenty-first century, exacerbated by the impacts of climate change and adverse environmental conditions. Genetic diversity

is essential for ensuring food security by enabling crops to adapt to changing environmental conditions, resist pests and diseases, improve nutritional content, and promote sustainable agricultural practices (Esquinas-Alcázar, 2005). Türkiye, which is recognized as one of the world's biodiversity hotspots and a center of origin for many crops, has played a crucial role in preserving genetic diversity, including that of common beans. The introduction of common beans into Türkiye by Asian traders from Europe has led to the proliferation of hundreds of local landraces across different regions. These landrace varieties, inherently heterogeneous and adapted to diverse environments, offer a rich source of genetic variation essential for enhancing crop quality. Harnessing the genetic diversity of common bean landraces through Genome-Wide Association Studies (GWAS) holds promise for identifying genes associated with key agronomic traits, facilitating targeted breeding efforts to develop resilient and high-yielding varieties capable of meeting the challenges of modern agriculture (Nadeem et al., 2018).

The population of common beans used in this study comprises 133 diverse accessions collected from 19 distinct geographic regions across Türkiye and 3 commercial cultivars. Utilizing a mixed linear model (Q + K), marker-trait association analysis was conducted using a comprehensive dataset consisting of 7,900 DArTseq markers. Prior studies utilizing the same germplasm identified markers associated with various traits, underscoring the genetic diversity and potential utility of this population for genomic studies (Nadeem et al., 2019, 2021; Baloch et al., 2022b; Baloch & Nadeem, 2022; Nadeem & Baloch, 2023). This diverse collection of accessions offers valuable insights into the genetic basis of important agronomic traits and serves as a valuable resource for advancing breeding efforts aimed at enhancing the resilience and productivity of common beans in diverse agroecological settings.

1.2 Significance of Iron for Human Health

Iron (Fe) is an essential micronutrient that is essential for the health and function of both plants and humans. Very few bacteria can replace Fe with other metals, therefore, Fe is a necessary component of almost all living species. Its crucial role stems from its involvement in various biochemical processes (Lasocki et al., 2014). For instance, Fe is a key component of hemoglobin, the protein in red blood cells responsible for transporting oxygen throughout the body. Additionally, it is necessary for the production of myoglobin, which facilitates oxygen storage and release in muscles during physical activity (Sánchez et al., 2017). Beyond its role in oxygen transport, Fe's redox characteristics are vital for numerous biochemical reactions. It participates in electron transport chains and serves as a cofactor for essential enzymes involved in energy production, DNA synthesis, and immune function (Puig et al., 2017). Adequate Fe intake is therefore crucial for maintaining overall health and well-being. However, Fe deficiency remains a prevalent global issue, particularly affecting vulnerable populations such as pregnant women, infants, and young children, as well as those in developing countries (Means, 2020). Fe deficiency can lead to anemia, a condition characterized by insufficient red blood cells or hemoglobin levels, characterized by symptoms like fatigue, weakness, and impaired cognitive function. In severe cases, it can negatively impact growth and development in children and increase the risk of complications during pregnancy (Clark, 2008). Anaemia afflicted 37% (32 million) of pregnant women and 30% (539 million) of non-pregnant women aged 15 to 49 in 2019. In 2019, 40% (269 million) of children aged six months to five suffered from anemia. Dietary Fe deficiency accounted for 66.2% of all occurrences of anemia in 2021, affecting 825 million women and 444 million men worldwide (FAO, 2023).

Given the significance of Fe for both plant and human health, understanding the mechanisms underlying Fe uptake, transport, and regulation in plants is essential for addressing Fe deficiency in crops and improving agricultural productivity, with potential implications for nutritional outcomes worldwide.

1.3 Iron Homeostasis and Its Significance for Plants

In plants, Fe plays a crucial role in various essential biological processes, highlighting its significance for plant growth and development. Fe is intricately involved in key processes such as photosynthesis, protein stability, DNA replication, and respiration. Chloroplasts harbor abundant iron-sulfur (FeS) proteins, including Photosystem I and ferredoxins, which work together to capture light energy, drive the transfer of electrons, and generate reducing power (NADPH), which are essential for powering the synthesis of organic molecules during photosynthesis (Connorton et al., 2017). Fe is also essential for chlorophyll synthesis since it acts as an essential cofactor in the biosynthesis process and is indispensable for maintaining the structure and function of chloroplasts, thereby facilitating efficient photosynthetic activity (Pushnik et al., 1984).

Furthermore, Fe is a vital component of enzymes within mitochondria, another essential organelle involved in cellular respiration. These enzymes, such as respiratory complexes containing FeS and heme (complex III) or heme and copper (complex IV), rely on Fe for their function (Paul et al., 2017). Additionally, haem proteins like cytochrome P450s and peroxidases are present in the endoplasmic reticulum and peroxisomes, contributing to various metabolic processes (Przybyla-Toscano et al., 2021).

Despite its importance, Fe can become toxic when it accumulates to high levels in plant cells. Excess Fe can catalyze the Fenton reaction, generating hydroxyl radicals that cause oxidative damage to lipids, proteins, and DNA (Connolly & Guerinot, 2002). Consequently, plants must regulate Fe levels carefully to avoid both deficiency and overload stress. Therefore, plants have developed sophisticated mechanisms to maintain Fe homeostasis, enabling them to respond effectively to fluctuations in Fe availability. These mechanisms involve intricate signaling pathways, transporters, and storage proteins that orchestrate Fe uptake, transport, distribution, and storage within plant cells. Understanding these mechanisms is

crucial for developing strategies to enhance Fe acquisition and utilization in plants, thereby improving crop productivity and resilience to environmental stresses.

1.3.1 Iron Uptake

Fe, which is one of the most prevalent elements in soil, comprising around 5.6% of the Earth's crust and belonging to the five most abundant elements, is primarily obtained from the rhizosphere, although its availability is often limited by soil pH and redox conditions (Naranjo-Arcos & Bauer, 2016). In aerobic or alkaline soils, Fe exists mainly as insoluble ferric oxides, hindering root absorption. In soils with pH values between 7.4 and 8.5, Fe solubility is further reduced, exacerbating Fe deficiency. This condition is exacerbated in calcareous soils due to higher bicarbonate concentrations, impeding Fe uptake by plants (Lucena & Hernandez-Apaolaza, 2017). This scarcity of bioavailable Fe can lead to Fe deficiency chlorosis, characterized by yellowing leaves and stunted growth, adversely affecting crop yield and quality (J. Li et al., 2021). Therefore, the bioavailability of Fe in these soils is often insufficient for optimal plant growth, necessitating interventions to alleviate Fe deficiency and enhance crop productivity.

Plants have evolved distinct strategies to cope with Fe deficiency and acquire Fe from soil. All dicots and non-graminaceous monocots utilize Strategy I, characterized by rhizosphere acidification through proton extrusion which is mediated by proton-ATPases, such as the H+-ATPase 2 (AHA2) in model plant *Arabidopsis thaliana*, promoting Fe solubility. This strategy involves ferric chelate reductases such as FRO2 (FERRIC REDUCTION OXIDASE 2) converting Fe^{3+} into Fe^{2+}, which is the form of Fe that can be taken up by plant roots, thus, facilitating the uptake of ferrous Fe by root cells. The more soluble ferrous Fe is readily taken up by plant roots through specific Fe transporters, such as IRT1 (IRON-REGULATED TRANSPORTER 1) in the following steps (Morrissey & Guerinot, 2009). In contrast, Strategy II, employed by graminaceous species, involves the release of phytosiderophores, which are small organic molecules that have a high affinity for

Fe, to chelate Fe3+ in the rhizosphere, followed by uptake of Fe-phytosiderophore complexes via specific transporters such as YELLOW STRIPE 1 (YS1)/YS1-LIKE (YSL) transporter. The oxidation state of Fe that the plant absorbs while using either strategy—ferrous Fe^{2+} for Strategy I and ferric Fe^{3+} for Strategy II—distinguishes the two approaches primarily (Connorton et al., 2017).

Up to 75% of the Fe in plant roots has been observed to be bound to the apoplast, where negatively charged carboxyl groups in the cell walls serve as a cation sink. During periods of Fe deficiency, this apoplastic pool diminishes, indicating mobilization into the symplast, the living cell interior. Although the mechanism of absorption remains unknown, recent research has revealed that phenolics released by roots in response to Fe shortage aid in utilizing apoplastic Fe and recovering from deficiency (Morrissey & Guerinot, 2009).

Additionally, plants employing Strategy I for Fe uptake release secondary compounds such as coumarins via the ATP-binding cassette (ABC) transporter ABCG37, also known as PLEIOTROPIC DRUG RESISTANCE 9 (PDR9), to enhance Fe mobility in the rhizosphere. Coumarins play a significant role, particularly in alkaline soils, where they may form complexes with Fe^{3+}, potentially increasing direct absorption by roots and maximizing Fe uptake efficiency (Spielmann et al., 2023).

Understanding the mechanisms of Fe uptake and transport in plants is critical for developing strategies to mitigate Fe deficiency and ensure sustainable agriculture. By elucidating the molecular pathways involved in Fe homeostasis, researchers can devise targeted approaches to enhance Fe uptake efficiency and improve crop resilience to environmental stresses.

1.3.2 Regulation of Iron Uptake in Plants

The efficient regulation of Fe homeostasis in plants is crucial for ensuring optimal Fe distribution without reaching toxic levels. Plants adapt their root morphology in

Fe-limiting conditions by increasing root hair density and lateral root numbers, facilitating greater soil contact. The mechanisms linking Fe availability to root morphology changes remain unclear. Over the past 15 years, significant progress has been made in identifying transcriptional regulators of Fe homeostasis, primarily basic Helix-Loop-Helix (bHLH) transcription factors. These factors, including FER and FIT, regulate the expression of Fe uptake genes in tomato (Ling et al., 2002) and Arabidopsis (Colangelo & Guerinot, 2004), respectively. Additionally, other transcription factor families such as MYB and WRKY have been implicated in the Fe deficiency response (Naranjo-Arcos & Bauer, 2016). In monocotyledonous plants like rice, transcription factors like IDEF1 and IDEF2 control phytosiderophore biosynthesis and Fe uptake. Post-transcriptional mechanisms, including protein degradation and turnover, help regulate Fe uptake to prevent overload. Recent studies suggest hemerythrin E3 ligases like BTS in *Arabidopsis* and HRZ in rice may act as negative regulators of Fe deficiency response, although many questions about their function remain unanswered (Connorton et al., 2017). These findings deepen our understanding of plant Fe regulation mechanisms, with potential applications in crop improvement and Fe biofortification.

1.3.3 Transportation and Distribution of Iron

The majority of Fe enters the plant through the roots, where it is then transported to sink tissues for use in Fe-dependent enzymes and other metabolic processes. IRT1 is a specialized Fe transporter involved in the symplastic pathway, the main mechanism by which roots absorb Fe from the soil. It facilitates the initial uptake of Fe from the soil into root cells, primarily localized to the outward-facing membrane of epidermal cells. During Fe deficiency, IRT1 serves as the primary high-affinity transporter for Fe uptake, whereas under abundant Fe conditions, it collaborates with the low-affinity metal transporter Natural Resistance-Associated Macrophage Protein 1 (NRAMP1) for Fe absorption (Spielmann et al., 2023).

For efficient translocation and to prevent harmful redox reactions Fe needs to be complexed with chelators. Fe is assumed to be transferred within the symplast as Fe^{2+}-nicotianamine (NA) complexes (Kumar et al., 2017). Besides, NA chelates Zn^{2+} and other divalent cations and is a precursor of a pyhtosiderophore, mugineic acid (Connorton et al., 2017). These complexes are vital for Fe transport within the plant.

Once Fe has entered the symplast of the epidermal root cells, it diffuses across the plasmodesmata in order to reach the vascular tissues. Fe is loaded into the xylem by IREG1/FPN1. Citrate chelates Fe^{3+}, whose efflux into the xylem is mediated by FRD3. Then, the Fe^{3+}-citrate complex is transported to the upper tissues of the plants (Paul et al., 2017).

Leaves are major sites of Fe demand for photosynthesis. Fe returns to the symplast in leaves, where it is reduced to Fe^{2+} by the FCR enzyme and turns into Fe^{2+}-NA once more before being remobilized via the phloem to other sink organs. In *Arabidopsis*, the oligopeptide transporter family protein OPT3 mediates Fe remobilization via the phloem (Morrissey & Guerinot, 2009).

Fe is distributed to various tissues, with seeds being significant storage sites. During germination, Fe reserves in seeds are crucial before seedlings develop a root system for nutrient absorption. Fe loading in seeds involves transporters like YSL, and studies have demonstrated the delivery of Fe to pea embryos as a Fe^{3+}-citrate/malate complex (Connorton et al., 2017).

1.3.4 Storage of Iron

Fe must be stored in cell compartments where usage and storage must be synchronized as soon as it reaches the target tissue. A significant amount of Fe is needed for photosynthesis, the electron transport chain, and chlorophyll synthesis. Consequently, the chloroplasts receive the majority of the Fe. Before Fe can be transported into the chloroplast, it must first be reduced by FRO7 and then transported by the transporter PERMEASE IN CHLOROPLAST 1 (PIC1) (Krohling

et al., 2016). The two main ways that Fe can be stored that have been suggested are sequestration into vacuoles and ferritin. Fe is imported into the vacuole by the Fe-transporter FPN2 and VACUOLAR IRON TRANSPORTER 1 (VIT1), and it is exported through the mediation of NATURAL RESISTANCE-ASSOCIATED MACROPHAGE PROTEIN 3 and 4 (NRAMP3 AND NRAMP4) (Kim & Guerinot, 2007). Ferritin (FER), a macroprotein complex found in all kingdoms of life that can hold up to 4500 Fe atoms, is where Fe gets sequestered in the chloroplast (Zielińska-Dawidziak, 2015). Different species store different amounts of total Fe in their ferritin; for example, peas store about 60% of their total Fe, while *Arabidopsis* seeds store less than 5%. Ferritin is mostly found in the plastids of plants. The majority of Fe in cereal grains like wheat and rice is found in vacuoles in the aleurone layer, which is frequently eliminated during grain processing (Connorton et al., 2017).

1.4 Iron Deficiency in Common Bean

In order to absorb Fe from the soil solution, the common bean (*Phaseolus vulgaris L.*) employs Strategy I. Here, the action of H^+-ATPase causes a proton outflow that acidifies the rhizosphere, enabling ferric reductase oxidase to convert insoluble Fe^{3+} into absorbable Fe^{2+}. Next, a Fe-regulated transporter imports Fe^{2+} into the root cell from the surrounding soil. The growth of yellow leaves with dark green veins is one of the indications of ferric chlorosis, a Fe shortage since chlorophyll is what gives leaves their green color. Fe is known to play a role in the formation of carotenoids and chlorophyll, and any reduction in the quantity of these pigments would first manifest as visible symptoms on immature leaves. This is because young leaves are the first to exhibit signs of a Fe deficit because Fe has limited mobility in plants (Nsiri & Krouma, 2023). Plants with Fe deficiency have further physiological, biochemical, and even molecular metabolic alterations that are specific to species, genotypes, and cultivars.

In a previous study, Fe deficiency resistance of four different common bean cultivars was assessed based on the following parameters: chlorosis symptoms, plant growth,

root Fe reduction activity, and rhizosphere acidification of the external medium, and it was shown that FCR activity was increased in response to Fe deficiency. Also, different degrees of Fe- chlorosis and significant decreases in biomass were seen in all common bean plants that are exposed to Fe deficiency, and cultivars showed different degrees of acidification (Krouma et al., 2003).

In another study, it was shown that common bean plants grown in Fe-deficient conditions displayed morphological abnormalities after a 7-day treatment period. Interveinal chlorosis first appeared in immature leaves, mostly in the tips of the leaves. The biomass output of all plant organs was impacted by the Fe shortage. Root and stem Fe levels decreased in cases of Fe insufficiency. All of the photosynthetic gas exchange metrics were negatively impacted by the Fe shortage. Finally, it can be concluded that Fe deficiency significantly impaired nutrient absorption, altered photosynthetic behavior, interfered with Fe buildup, and hindered plant development (Idoudi et al., 2024).

1.4.1 Treatment of Iron Deficiency

Treating Fe deficiency in plants can be approached through agronomic, genetic, and transgenic methods, each with its unique advantages and disadvantages. Agronomic methods involve adjusting soil pH, improving drainage, and using Fe chelates or fertilizers to enhance Fe availability. While agronomic approaches are relatively simple, they may not be sustainable in the long term, particularly in large-scale agricultural systems, and can result in environmental impacts such as leaching. Alternatively, genetic, and transgenic approaches aim to enhance plants' ability to acquire and utilize Fe efficiently. Genetic methods focus on breeding or selecting plant varieties with improved Fe uptake or tolerance to low-Fe conditions. This approach offers more lasting solutions but requires significant time and effort for breeding programs and may face limitations due to the genetic variability within plant species. Transgenic methods involve introducing genes responsible for Fe uptake or tolerance from other organisms into target plants. Transgenic approaches

offer precise control over gene expression but raise concerns about ecological impact, consumer acceptance, and regulatory hurdles. Overall, each method provides a range of solutions for addressing Fe deficiency in plants, but their efficacy, sustainability, and acceptability vary depending on the specific context and goals of plant production (Krishna et al., 2023; Lucena & Hernandez-Apaolaza, 2017).

Genetic solutions may require extensive screening and breeding efforts, making them time-consuming and resource-intensive. GWAS is a powerful tool used in genetics to identify genetic variations associated with particular traits or diseases across the entire genome of an organism (Brachi et al., 2011). In the context of Fe deficiency in plants or any organism, a GWAS project involves analyzing the genomes of a large and diverse population to identify genetic markers or variants linked to traits related to Fe uptake, transport, or utilization. By pinpointing specific genetic variations associated with traits relevant to Fe metabolism, such as increased Fe uptake efficiency or enhanced tolerance to low-Fe conditions, candidate genes can be identified and further could be manipulated through breeding or genetic engineering to develop Fe-efficient or Fe deficiency-tolerant crop varieties. This way GWAS can enable targeted breeding efforts to develop Fe-efficient crop varieties without the need for genetic modification (Tibbs Cortes et al., 2021). The insights gained from a GWAS project can provide valuable information for plant breeders and geneticists to select or engineer plants with improved Fe nutrition, ultimately contributing to more sustainable and resilient agricultural systems. The diverse population of common bean accessions collected from 19 different Turkish geographic regions provides an invaluable resource for Genome-Wide Association Studies (GWAS), offering a rich genetic diversity that enhances the power and robustness of genetic analyses to unravel the complex genetic architecture underlying traits of agronomic importance.

1.5 Genome-Wide Association Study

Genome-wide association studies (GWAS) are very important for uncovering the genetic basis of complex traits and diseases across an organism's entire genome. The primary purpose of GWAS is to identify associations between genetic variants, known as markers, and specific phenotypic traits or diseases. Markers serve as signposts along the genome, indicating areas where variations may influence traits of interest. Among the various types of markers used in GWAS, Single Nucleotide Polymorphisms (SNPs) are the most common. However, Diversity Arrays Technology (DArT) markers, such as DArTseq markers, have gained prominence for their ability to capture genetic variation across a broad range of organisms, including plants. DArT markers offer advantages over SNPs by being relatively cost-effective and providing high-throughput genotyping capabilities (Mace et al., 2008). They differ from SNPs in their methodology, as DArT markers are based on detecting presence or absence variations (PAVs) rather than single nucleotide changes (Adu et al., 2021). This diversity in marker types allows researchers to comprehensively explore genetic variation and its association with traits of interest, contributing to advancements in fields such as agriculture, medicine, and ecology.

Genome-wide association studies (GWAS) can be instrumental in understanding the genetic basis of Fe deficiency in plants. By analyzing the genomes of diverse plant populations, GWAS can identify genetic variants associated with traits related to Fe uptake, transport, and utilization. In the context of Fe deficiency studies, GWAS can help pinpoint genes and genomic regions involved in plant responses to low Fe availability, including mechanisms for enhancing Fe uptake efficiency, increasing tolerance to low-Fe conditions, and regulating Fe homeostasis. These genetic insights can inform the development of Fe-efficient crop varieties through marker-assisted breeding or genetic engineering approaches. Additionally, GWAS can uncover candidate genes and pathways for further functional characterization, providing valuable knowledge for improving plant nutrient management strategies and enhancing agricultural productivity in Fe-deficient soils. Overall, GWAS serves

as a powerful tool for unraveling the complex genetic architecture underlying Fe deficiency in plants, ultimately contributing to sustainable and resilient crop production systems.

Understanding which plants exhibit resistance to Fe deficiency and identifying the genomic regions associated with this resistance is crucial for enhancing agricultural productivity and sustainability. By identifying naturally resistant plants, breeders can develop improved crop varieties with enhanced tolerance to Fe deficiency, leading to higher yields and better crop performance. This approach not only reduces the need for chemical fertilizers but also promotes sustainable agricultural practices and resilience to environmental stressors, such as alkaline soils. Moreover, the development of Fe-efficient crop varieties provides economic benefits to farmers by lowering production costs and enhancing resilience to market fluctuations. While Fe deficiency resistance may not directly impact human health, its importance in ensuring food security, promoting sustainable agriculture, and supporting rural livelihoods cannot be understated.

A series of studies conducted by the same research group focused on different properties of Turkish common bean germplasm using genomic approaches, all utilizing the same germplasm collection and marker set of 7900 DArTseq markers. These studies have revealed significant associations between genetic markers and various traits, facilitating marker-assisted breeding efforts. One study aimed to investigate seed traits including seed width, seed yield/plant (SYP), and hundred seed weight, while another focused on exploring magnesium (Mg) content diversity in common bean seeds across different regions of Türkiye (Baloch et al., 2022b; Nadeem & Baloch, 2023). Similarly, another study focused on seed protein contents, identifying 11 markers associated with this trait, providing valuable insights for marker-assisted breeding (Baloch & Nadeem, 2022). Additionally, a comprehensive study investigated markers associated with days to flowering, predicting five candidate genes associated with days to flowering (Nadeem et al., 2021). Finally, a fifth study evaluated seed antioxidant activity in a diverse set of common bean landraces and commercial cultivars collected from various regions of Türkiye,

identifying markers associated with antioxidant activity and predicting candidate genes linked to these markers (Nadeem et al., 2019). These collective findings underscore the importance of genomic approaches and marker-trait associations in enhancing common bean breeding programs, addressing various agronomic challenges, and improving crop resilience and nutritional value.

1.6 Aim of the Study

Fe is vital for plant growth, yield, and overall well-being, making it crucial for agricultural productivity and food security. This study aims to investigate how common bean genotypes respond to Fe deficiency stress, focusing on root and above-soil characteristics. By identifying significant markers and potential candidate genes linked with Fe deficiency tolerance, the study seeks to contribute insights into developing more resilient common bean cultivars. Additionally, the study aims to identify the most tolerant and sensitive common bean accessions to Fe deficiency, as they can offer valuable insights for improving agricultural practices. Ultimately, this research aims to enhance our understanding of plant responses to nutrient deficiencies and support sustainable agricultural practices.

CHAPTER 2

MATERIALS AND METHODS

2.1 Plant Material

A total of 133 common bean landraces and 3 commercial cultivars (Akman, Karacasehir, Goksun) were used as plant material in this study (Table A.1). The landraces were collected from fields of various farmers in 19 different provinces of Türkiye, most of them being the main common bean-growing provinces in Türkiye. This collection panel was established by Prof. Dr. Faheem Shehzad Baloch in 2014, at Bolu Abant Izzet Baysal University (BAIBU). From each landrace, one plant was chosen and cultivated in an augmented design in the field, and a single plant selection was performed for two years in a row, in 2014 and 2015. Later, the collection panel was used as plant material in several studies (Nadeem et al., 2019; Baloch et al., 2022; Baloch & Nadeem, 2022; Nadeem & Baloch, 2023). The common bean accessions used in this study represent a highly diverse population. This diversity is evidenced by previous studies utilizing the same panel of common bean genotypes, which have demonstrated significant variation in magnesium (Mg) content among these accessions (Baloch et al., 2022b). Such genetic diversity is crucial for identifying traits associated with Fe deficiency tolerance, as it provides a broad genetic base from which to uncover significant markers and potential candidate genes.

2.2 Growth Conditions

The study was set up as a complete randomized design. The experiment was carried out under hydroponics conditions in order to assess the responses of genotypes to Fe

deficiency in terms of root characteristics. The genotypes were evaluated in controlled greenhouse conditions in the Department of Biological Sciences: Biology/Molecular Biology, Middle East Technical University, Ankara, Türkiye, during the years of 2022-23. The experiments were completed in a total of eight sets. The experiments were conducted in eight separate sets due to the large number of plants involved. To ensure uniformity and minimize potential differences among sets, three genotypes were randomly selected for measurements and experiments within each set. Subsequently, statistical analysis was performed to assess if there were any significant differences among the sets, and the results indicated no statistically significant variations between the sets. The greenhouse conditions were (22°C/18°C (±3°C) with 16-h light/8-h dark cycle, 60% humidity) and 1200 µmol $m^{-2}s^{-1}$ photosynthetic active radiation. In the greenhouse environment, halogen plant growth lamps were used as the light sources.

The hydroponic system utilized in this experiment comprised ten opaque plastic boxes measuring 35 x 50 x 15 cm each. Two separate systems were established to simulate Fe-sufficient and Fe-deficient growth conditions. In each system, five plastic boxes were interconnected using 22 mm diameter pipes, while one box was linked to a main tank equipped with an aquarium pump. This setup created a continuous circulation system, ensuring proper aeration throughout. Both the main tank and the plastic boxes were filled with a nutrient solution, with the main tank accommodating 40 liters and each plastic box holding 26 liters of the solution. To support plant growth on the liquid surface, opaque insulation foams measuring 33 x 48 cm were utilized. These foams were drilled with 15 mm holes spaced 4 cm apart, providing 80 holes per foam for the plantlets.

Seeds were initially planted in separate plastic cups filled with perlite and nutrient medium and covered with aluminum foil. Additional plastic cups with small openings on top were stacked on these cups, with opaque black bags placed over them. The opaque bags were removed on Day 4, followed by the removal of the cups with openings on Day 5. On Day 8, ten plantlets from each genotype were selected and carefully transferred to the hydroponic system for stress induction. The transfer

process involved wrapping the plantlets in sponges to secure them in the holes on the foam, ensuring the roots were submerged in the nutrient solution while the rest of the plantlets remained above the foam. Physiological and biochemical measurements were conducted on Day 21, encompassing a 13-day period of exposure to Fe deficiency stress from Day 8 to Day 21.

As a nutrient medium, Hoagland solution (Hoagland & Arnon, 1950) in half concentrations was used in this experiment, with slight changes. The contents of the nutrient solution were as follows: 2 mM KNO_3, 2 mM $Ca(NO_3)$, 1 mM NH_4HCO_3, 0.5 mM $MgSO_4$, 0.25 mM KH_2PO_4, 50 µM KCl, 25 µM H_3BO_3, 2 µM $MnSO_4$, 2 µM $ZnCl_2$, 0.5 µM $CuSO_4$, and 0.15 µM $CoCl_2$, 0.075 µM $(NH_4)_6Mo_7O_{24}$ and 30 µM Fe-EDTA (3 µM Fe-EDTA for Fe deficiency). The pH of the nutrient solutions was initially adjusted to 5.7 and monitored twice a week to ensure it remained stable. To compensate for evaporation, fresh nutrient solution was added to the main tank or boxes as needed to maintain the liquid level. Additionally, every 3 days, 4 ml of ReeFlowers Rem Algae were introduced into the main tanks to prevent algae formation within the system.

2.3 Biochemical Analyses

2.3.1 Total Chlorophyll Concentration Measurement

For each accession, 5 samples were taken. The middle leaf of the first trifoliate of the plant was taken, and a piece of it was detached with the help of a 1000 µl pipette tip, placed in a 1.5 ml Eppendorf tube, and crushed using 200 µl of 80% (v/v) acetone. Then, 800 µl of 80% (v/v) acetone was added to each Eppendorf tube, and the samples were placed at 4°C for 48 hours. After, the samples were centrifuged at 13,000 g for 5 minutes at 4°C, and the supernatant was taken for absorbance reading at 470, 646.8, and 663.2 nm using a spectrophotometer, using 80% (v/v) acetone as blank. Total chlorophyll concentration (chlorophyll a and b) (mg total chlorophyll/g leaf FW) was calculated by the formula (1).

$$\frac{((A_{663,2}x7{,}15)+(A_{646,8}x18{,}71))(\mu g/ml)\ x\ Volume\ (ml)}{1000\ x\ Leaf\ FW\ (g)} \quad (1)$$

2.3.2 FCR Enzyme Activity Measurement

For each accession, 5 samples were taken. The root of the plant was taken, it was gently dried by dabbing with a paper towel, and its fresh weight was measured and transferred into 50 ml falcon tubes containing 30 ml of assay solution of 0.33 mM Fe (III)-EDTA and 1 mM ferrozine (Aksoy & Koiwa, 2013). The samples were immediately placed into a dark container to ensure they were not exposed to light while the experiment was still going on for the other samples. They were incubated for 20-24 hours at room temperature in the dark. At the end of the incubation, the samples were taken for absorbance reading at 562 nm, by using the assay solution without a sample as blank. The FCR enzyme activity level (μmol Fe (II)/g root FW/h) was calculated by the formula (2).

$$\frac{(A_{562}/28{,}6)\ x\ Volume\ (ml)\ x\ 1000}{Root\ FW\ (g)\ x\ incubation\ time\ (h)} \quad (2)$$

2.4 Physiological Analyses

2.4.1 Chlorophyll Index (SPAD)

For each accession, 5 samples were taken. The difference between the transmittance of a red (650 nm) and an infrared (940 nm) light through the leaf was measured by The Soil Plant Analysis Development (SPAD) chlorophyll meter device, and a SPAD value was obtained for each sample. The measurements were taken from the 1/3 parts of the middle leaf of the first trifoliate of each plant three times, and the mean value of these three measurements was used as the SPAD value of that plant.

2.4.2 Leaf Area Measurement

For each accession, 5 samples were taken. The first trifoliate of the plant was taken and placed on the scanner and then scanned at a resolution of 300 dpi in 24-bit color on an Epson Perfection V850 Pro Scanner. In order to calculate the leaf area (cm^2) of the scanned leaves, Easy Leaf Area software was used (Easlon & Bloom, 2014). In Figure 2.1, a leaf sample is depicted alongside its corresponding output, generated using the Easy Leaf Area software, demonstrating the results obtained from the analysis.

Figure 2.1. Investigation of leaf area with Easy Leaf Area software.

2.4.3 Root Structure Profiling

For each accession, 5 samples were taken. The root of the plant was taken and placed in a transparent container containing water on the scanner with its entire surface exposed and scanned at a resolution of 300 dpi in 16-bit grayscale on an Epson Perfection V850 Pro Scanner. Rhizo Vision Explorer was used to examine the root characteristics, with the following settings: root type option as whole root, image

threshold level as 75, keep largest component option as true, edge smoothing option as enabled and threshold level as 2, root pruning option as enabled and threshold level as 2, convert pixels to physical unit option as enabled and dots per inch as 300 (Seethepalli et al., 2021). In Figure 2.2, an illustration is presented featuring a root sample alongside the corresponding output generated using the specified options in the Rhizo Vision Explorer.

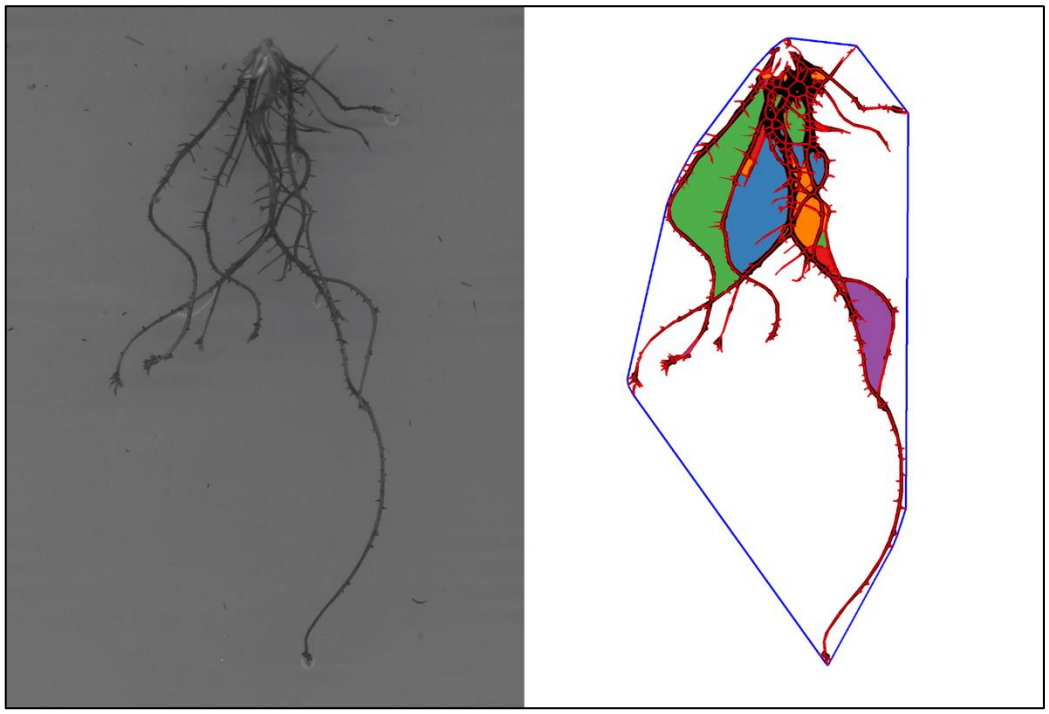

Figure 2.2. Root morphology analysis using Rhizo Vision Explorer software.

In this study, the examined root traits included the following:

1. Maximum root number: This metric was defined as the maximum number of roots observed in each row of the segmented image. It was determined by performing a horizontal line scan that recorded pixel transitions from a background to a root pixel. These pixel transitions were sorted, and the maximum number of roots was noted.

2. Number of root tips: This metric was defined as the pixels in the identified root topology that had only one neighboring skeletal pixel.
3. Total root length: This metric was defined as the sum of Euclidean distances between connected skeletal pixels throughout the entire root topology in the plant root image.
4. Main root length: This metric referred to the maximum vertical distance that the root crown had grown at the time of imaging.
5. Total root area: This metric was defined as the network area of the root system that lay below the skeletal pixel with the maximum radius.
6. Volume: This metric was defined as the product of the length of the pixel and the cross-sectional area of the root at that pixel.

2.4.4 Root and Leaf Fresh and Dry Weight Measurements

After the scanning, the roots were gently dried by dabbing with a paper towel and weighed and recorded as fresh weight. Similarly, leaves were weighed after the scanning as well, for fresh weight. Then, root and leaf samples were placed between two sheets of paper individually and kept in an oven at a temperature of 60°C for 48 hours. The dried samples were weighed again and recorded as dry weight.

2.5 Statistical Analysis

2.5.1 Phenotypic Data Analysis

Using XLSTAT software, descriptive statistics, two-way ANOVA tests, and Pearson's correlation tests of the data were performed. Following two-way ANOVA, Fisher's LSD test was performed for investigated traits according to the randomized block design model, at a significance level of 5%. Relative trait values were calculated by the formula (3), with C being the value from the measurement taken

from plants that grew in control conditions, S being the value from the measurement taken from plants that grew in stress conditions.

$$\%Relative\ measurement = \frac{S-C}{C} \times 100 \quad (3)$$

XLSTAT software was utilized to conduct correlation tests between different variables, including Pearson's correlation test at a significance level of 5%.

To assess the distribution of the data, normal distribution graphs were generated in Microsoft Excel. Histograms were created for each trait to visualize the distribution of the data. The histogram data was then used to plot normal distribution curves to verify if the data approximated a normal distribution. Finally, the normal distribution was statistically tested with the Shapiro-Wilk test with a p-value greater than 0.05 indicating that the data was normally distributed.

2.5.2 GWAS Analysis

The Iteratively Nested Keyway (BLINK) model was employed by using the R package GAPIT (Genomic Association and Prediction Integrated Tool, Version 3) to conduct a Genome-Wide Association Study (GWAS) on R Studio (Huang et al., 2019; J. Wang & Zhang, 2021). The BLINK model was employed for GWAS due to its effective control of false positives through iterative updates of marker effects and its computational efficiency in processing large datasets. A Manhattan Plot was generated by using GAPIT in order to visualize GWAS results.

The significance threshold of the Manhattan plot was automatically assigned as 5.6 by GAPIT, determined using the Benjamini-Hochberg cut-off. Additionally, a Bonferroni correction was applied, setting a significance threshold of 0.0071. DArTseq markers that met the significance thresholds of Bonferroni were considered significantly associated with the studied traits. Significant markers were further analyzed for their association with these traits, and possible candidate genes were identified based on their proximity (within ± 100 kb) and by exploring the *P. vulgaris*

genome utilizing the KEGG Genome Browser on GenomeNet (Kanehisa et al., 2023). Sequences containing the significant DArT markers were aligned to the *P. vulgaris* reference version 2.1.

Using the BLASTP tool, nucleotide sequences of potential candidate genes were translated into the corresponding proteins and used as queries against the *Arabidopsis thaliana* protein database (Altschul et al., 1990). Orthologs were identified with an E-value lower than 1e-5. Gene ontology analysis of the *Arabidopsis thaliana* orthologs of the potential candidate genes identified from significant markers was conducted using Ensembl Biomart (Kinsella et al., 2011).

CHAPTER 3

RESULTS

3.1 Evaluation of Phenotypic Diversity

To verify the assumption of normality, scatter plots of the data were generated for each trait. Microsoft Excel was utilized for creating these visualizations. The normality of the data sets was assessed using the Shapiro-Wilk test, a widely recognized method for evaluating the normal distribution of data. For each trait measured in the study, including SPAD, CHL, LA, FRO, RFW, RDW, LFW, LDW, FWR, DWR, MRN, RTN, TRL, MRL, TRA, and TRV, the p-values obtained from the Shapiro-Wilk test were carefully examined, which were 0.0828, 0.0518, 0.2973, 0.6657, 0.1233, 0.0576, 0.0587, 0.9050, 0.1607, 0.1340, 0.0803, 0.0576, 0.2959, 0.1480, and 0.0505, respectively. The p-values ranged from 0.0505 (for TRV) to 0.9050 (for LDW), affirming the normality of the data across different traits. Notably, all p-values were found to be greater than the conventional significance level of 0.05, indicating that the data for each trait followed a normal distribution. Additionally, the scatter plots depicting the normal distributions for each trait can be referenced in Figure B.1 and Figure B.2.

According to the descriptive statistics (Table 3.1) of the phenotypic data, there was a significant 21.8% decrease in chlorophyll content, a significant 10.2% decrease in SPAD, a significant 21.5% decrease in leaf area, a significant 27.2% decrease in leaf fresh weight, a significant 21.3% decrease in leaf dry weight, a significant 39.2% decrease in root fresh weight and a significant 26.5% decrease in root dry weight in Fe deficiency conditions compared to control.

For chlorophyll content, the minimum value was 0.2, the maximum value was 1.5, and the mean value was 1.0 for control conditions; for Fe deficiency conditions, the minimum value was 0.2, the maximum value was 1.3, and the mean value was 0.7.

SPAD value ranged from a minimum of 36.5 to a maximum of 51, with a mean of 44.3 for control conditions; whereas for Fe deficiency conditions, the SPAD value ranged from a minimum of 29.1 to a maximum of 49.2, with a mean of 39.8. FCR activity showed a minimum value of 12, a maximum value of 58.7, and a mean of 24 for control conditions; in Fe deficiency conditions, FCR activity ranged from a minimum of 11.5 to a maximum of 80.4, with a mean of 28. Regarding leaf area, the minimum value was 20.3, the maximum value was 100.8, and the mean value was 49.3 for control conditions; whereas for Fe deficiency conditions, the minimum value was 13.6, the maximum value was 70.9, and the mean value was 38.7.

For leaf fresh weight, the minimum value was 235, the maximum value was 1953.3, and the mean value was 705.1 for control; whereas for Fe deficiency conditions, the minimum value was 65, the maximum value was 940, and the mean value was 513.1. Leaf dry weight exhibited a minimum value of 28.8, a maximum value of 208, and a mean of 77.2 for control conditions; in Fe deficiency conditions, the leaf dry weight ranged from a minimum of 17.7 to a maximum of 128, with a mean of 60.8.

For root fresh weight, the minimum value was 266.7, the maximum value was 4566.7, and the mean value was 904.1 under control conditions; under Fe deficiency conditions, the root fresh weight ranged from a minimum of 236.7 to a maximum of 1256.7, with a mean of 549.8. Root dry weight had a minimum value of 17, a maximum value of 163.9, and a mean of 56.1 for control conditions; in Fe deficiency conditions, the root dry weight ranged from a minimum of 16.7 to a maximum of 71.5, with a mean of 41.2. The fresh weight ratio showed a minimum value of 0.3, a maximum value of 4.9, and a mean of 1.3 for control conditions; in Fe deficiency conditions, the fresh weight ratio ranged from a minimum of 0.4 to a maximum of 6.9, with a mean of 1.2. Similarly, the dry weight ratio exhibited a minimum value of 0.2, a maximum value of 2.2, and a mean of 0.7 for control conditions; under Fe deficiency conditions, the dry weight ratio ranged from a minimum of 0.2 to a maximum of 1.6, with a mean of 0.7.

The maximum root number ranged from a minimum of 10.4 to a maximum of 68.5, with a mean of 21.4 under control conditions; in Fe deficiency conditions, the range was from 9.7 to 21.5, with a mean of 15.2. For root tip number, the minimum value was 56.3, the maximum value was 1413, and the mean value was 262.3 under control conditions; whereas for Fe deficiency conditions, the minimum was 62, the maximum was 277.4, and the mean was 147.8. Total root length exhibited a minimum value of 53.4, a maximum value of 1171.1, and a mean of 216.5 under control conditions; in Fe deficiency conditions, the total root length ranged from a minimum of 50.5 to a maximum of 277.2, with a mean of 104.8. The main root length had a minimum value of 4.7, a maximum value of 22.6, and a mean of 10.1 for control conditions; in Fe deficiency conditions, the main root length ranged from a minimum of 4 to a maximum of 13.7, with a mean of 7.8. The total root area showed a minimum value of 1.7, a maximum value of 42.6, and a mean of 10.2 for control conditions; under Fe deficiency conditions, the total root area ranged from a minimum of 2.1 to a maximum of 10.9, with a mean of 5.0. Similarly, total root volume exhibited a minimum value of 0.6, a maximum value of 31, and a mean of 5 for control conditions; in Fe deficiency conditions, the total root volume ranged from a minimum of 0.4 to a maximum of 7.7, with a mean of 1.7.

Table 3.1 Descriptive statistics of the studied traits in common bean accessions.

Traits	Control					Fe Deficiency					RL. (%)
	Min.	Max.	Mean	SD	CV%	Min.	Max.	Mean	SD	CV%	
CHL (mg/g LFW)	0.2	1.5	1.0	0.3	31.3	0.2	1.3	0.7	0.2	32.8	-21.8
SPAD	36.5	51.0	44.3	3.3	7.4	29.1	49.2	39.8	3.9	9.7	-10.2
FCR (µmol Fe(II)/g RFW/h)	12.0	58.7	24.0	7.0	29.3	11.5	80.4	28.0	8.5	30.5	16.6
LA (cm^2)	20.3	100.8	49.3	17.5	35.5	13.6	70.9	38.7	11.5	29.8	-21.5
LFW (mg)	235.0	1953.3	705.1	329.0	46.7	65.0	940.0	513.1	167.1	32.6	-27.2
LDW (mg)	28.8	208.0	77.2	33.9	43.9	17.7	128.0	60.8	18.0	29.6	-21.3
RFW (mg)	266.7	4566.7	904.1	723.8	80.1	236.7	1256.7	549.8	187.7	34.1	-39.2
RDW (mg)	17.0	163.9	56.1	31.2	55.6	16.7	71.5	41.2	12.0	29.0	-26.5
FWR	0.3	4.9	1.3	0.6	50.2	0.4	6.9	1.2	0.8	66.5	-1.6
DWR	0.2	2.2	0.7	0.3	37.2	0.2	1.6	0.7	0.2	33.9	-3.1
MRN	10.4	68.5	21.4	10.2	47.8	9.7	21.5	15.2	2.1	13.7	-29.1
RTN	56.3	1413.0	262.3	238.1	90.8	62.0	277.4	147.8	43.0	29.1	-43.6
TRL (cm)	53.4	1171.1	216.5	211.9	97.9	50.5	277.2	104.8	35.0	33.4	-51.6
MRL (cm)	4.7	22.6	10.1	4.3	42.8	4.0	13.7	7.8	2.3	29.4	-22.4
TRA (cm^2)	1.7	42.6	10.2	9.6	93.6	2.1	10.9	5.0	2.0	40.7	-50.8
TRV (cm^3)	0.6	31.0	5.0	6.5	130.9	0.4	7.7	1.7	1.4	83.1	-65.3

CHL, total chlorophyll concentration; SPAD, chlorophyll index; FCR, ferric chelate reductase enzyme activity; LA, leaf area; LFW, leaf fresh weight; LDW, leaf dry weight; RFW, root fresh weight; RDW, root dry weight; FWR, root fresh weight/leaf fresh weight ratio; DWR, root dry weight/leaf dry weight ratio; MRN, maximum root number; RTN, root tip number; TRL, total root length; MRL, main root length; TRA, total root area; TRV, total root volume; SD, standard deviation; CV, coefficient of variation; RL, relative change.

ANOVA results (Table 3.2) depicted that these traits among common bean accessions were significant within genotypes, treatments, and genotype x treatment interaction: CHL, SPAD, LA, LFW, LDW, RFW, RDW, MRN, RTN, TRL, MRL, TRA, and TRV. ANOVA results demonstrate that there was a significant genetic diversity for FCR between genotypes and treatments, yet, genotype x treatment interaction was not significant, with a p-value of 0.930. ANOVA results also indicate that the fresh weight ratio was not statistically significant within treatments with a p-value of 0.146, and the dry weight ratio was not statistically significant within treatments and genotype x treatment interactions, with p-values of 0.184 and 0.101, respectively.

Table 3.2 ANOVA of the traits under control and Fe-deficient conditions.

Traits	Source	Mean Square	F	Pr > F
	Treatment	9.0	399.3	**<0,0001**
CHL	Genotype	0.4	19.4	**<0,0001**
	Treatment*Genotype	0.0	2.1	**<0,0001**
	Treatment	5766.8	948.1	**<0,0001**
SPAD	Genotype	81.0	13.3	**<0,0001**
	Treatment*Genotype	26.5	4.4	**<0,0001**
	Treatment	3582.3	61.5	**<0,0001**
FCR	Genotype	387.2	6.6	**<0,0001**
	Treatment*Genotype	47.1	0.8	0.930
	Treatment	37811.0	252.1	**<0,0001**
LA	Genotype	1024.6	6.8	**<0,0001**
	Treatment*Genotype	799.4	5.3	**<0,0001**
	Treatment	10146967.8	267.7	**<0,0001**
LFW	Genotype	279019.0	7.4	**<0,0001**
	Treatment*Genotype	226573.0	6.0	**<0,0001**
	Treatment	85604.9	81.3	**<0,0001**
LDW	Genotype	3517.2	3.3	**<0,0001**
	Treatment*Genotype	2160.5	2.1	**<0,0001**
	Treatment	25388614.8	596.2	**<0,0001**
RFW	Genotype	1073599.2	25.2	**<0,0001**
	Treatment*Genotype	654459.8	15.4	**<0,0001**
	Treatment	59385.8	139.4	**<0,0001**
RDW	Genotype	2384.8	5.6	**<0,0001**
	Treatment*Genotype	1424.3	3.3	**<0,0001**
	Treatment	0.4	2.1	0.146
FWR	Genotype	2.4	12.4	**<0,0001**
	Treatment*Genotype	0.7	3.5	**<0,0001**
	Treatment	0.4	1.8	0.184
DWR	Genotype	0.6	2.9	**<0,0001**
	Treatment*Genotype	0.2	1.2	0.104
	Treatment	9562.1	454.9	**<0,0001**
MRN	Genotype	173.7	8.3	**<0,0001**
	Treatment*Genotype	180.6	8.6	**<0,0001**
	Treatment	3343441.3	294.8	**<0,0001**
RTN	Genotype	106426.4	9.4	**<0,0001**
	Treatment*Genotype	88912.3	7.8	**<0,0001**

Table 3.2 Cont'd

TRL	Treatment	3174068.3	133.2	**<0,0001**
	Genotype	96906.1	4.1	**<0,0001**
	Treatment*Genotype	69856.9	2.9	**<0,0001**
MRL	Treatment	1288.9	250.0	**<0,0001**
	Genotype	74.2	14.4	**<0,0001**
	Treatment*Genotype	17.8	3.4	**<0,0001**
TRA	Treatment	6731.6	288.6	**<0,0001**
	Genotype	204.8	8.8	**<0,0001**
	Treatment*Genotype	134.1	5.8	**<0,0001**
TRV	Treatment	2525.6	215.2	**<0,0001**
	Genotype	117.2	10.0	**<0,0001**
	Treatment*Genotype	59.0	5.0	**<0,0001**

CHL, total chlorophyll concentration; SPAD, chlorophyll index; FCR, ferric chelate reductase enzyme activity; LA, leaf area; LFW, leaf fresh weight; LDW, leaf dry weight; RFW, root fresh weight; RDW, root dry weight; FWR, root fresh weight/leaf fresh weight ratio; DWR, root dry weight/leaf dry weight ratio; MRN, maximum root number; RTN, root tip number; TRL, total root length; MRL, main root length; TRA, total root area; TRV, total root volume.

Violin plots shown in Figure 3.1 and Figure 3.2 further represent that there was a decrease in total chlorophyll content, SPAD value, leaf area, leaf fresh weight, leaf dry weight, root fresh weight, root dry weight, maximum root number, root tip number, total root length, main root length, total root area, and total root volume, in response to Fe deficiency treatment.

In control conditions, the total chlorophyll content exhibited a distribution mainly clustered around the middle range, although there were some outliers observed near values lower than 0.5. Conversely, in Fe deficiency conditions, the distribution of values appeared more normally distributed, as depicted in the violin plots shown in Figure 3.1 and Figure 3.2. The SPAD values displayed a more normal distribution in control conditions, although, in Fe deficiency conditions, there were some outliers observed above 45 and below 35, which gave the plot a slightly atypical appearance compared to a typical normal distribution. In Fe deficiency conditions, the values were mostly clustered around the middle range, similar to the control conditions, as depicted in the violin plots. Regarding FCR activity, both plots exhibited a clustering around the middle range, yet there were some outliers observed above 40 in the Fe deficiency conditions. For the leaf area, the plot shape appeared normally distributed in Fe deficiency conditions. However, in control conditions, there were outliers observed above 75, resulting in a slightly atypical appearance with a longer upper tail.

The leaf fresh weight plot in Fe deficiency conditions appeared normal, while in control conditions, there were outliers above 1000, leading to an elongated upper tail. Similar patterns were observed in the leaf dry weight plots, with outliers above 1000 in control conditions. The plots for root fresh weight and root dry weight showed similarities, with both plots exhibiting a mostly normal distribution. However, there were outliers above 1000 in root fresh weight and above 100 in root dry weight, contributing to elongated upper tails in both plots.

The plots for both the fresh weight ratio and dry weight ratio exhibited similarities, with clustering around the middle range and some outliers observed above 2 for fresh

weight ratio in both conditions, and above 1.25 for dry weight ratio in both conditions.

Similarly, the plots for maximum root number, root tip number, total root length, main root length, total root area, and total root volume displayed similarities. Plots representing plants grown in control conditions showed numerous outliers above the mean value, resulting in a long tail above. Conversely, the plots in Fe deficiency conditions demonstrated a relatively more normal distribution around the middle, with some outliers in total root volume observed above 2.5.

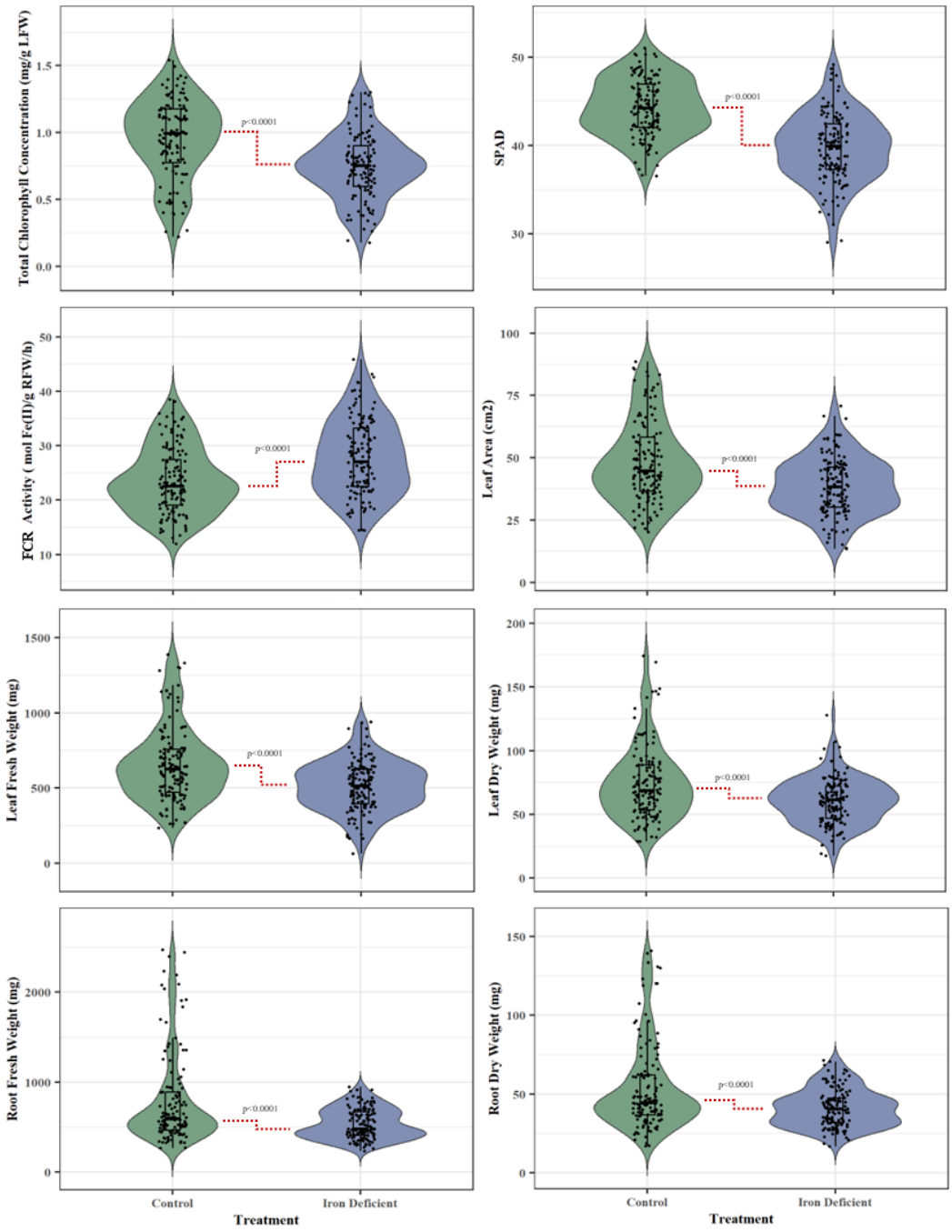

Figure 3.1 Plots of the studied traits under control and Fe-deficient conditions.

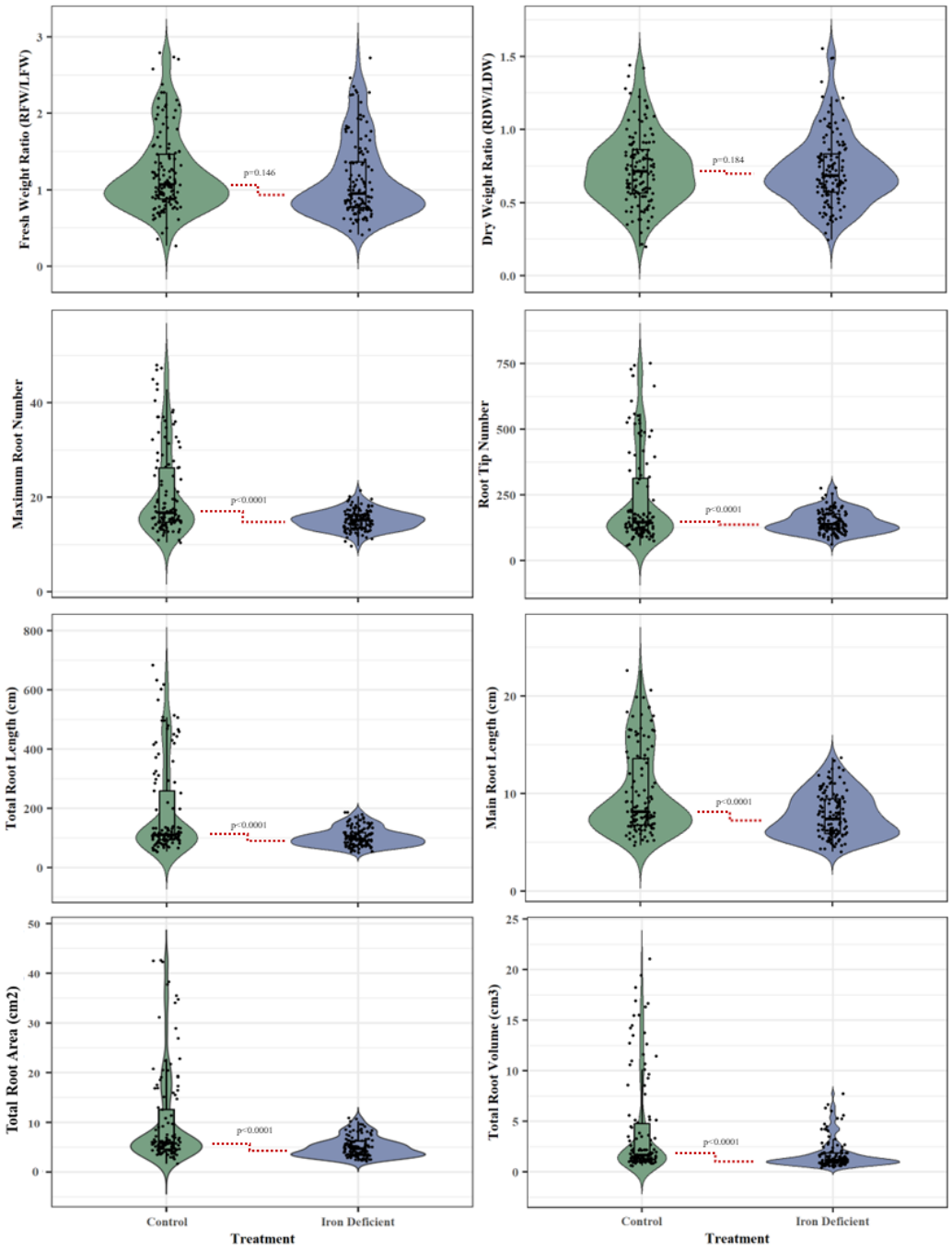

Figure 3.2 Plots of the studied traits under control and Fe-deficient conditions.

The correlation analysis (Table 3.3) revealed several significant relationships among the examined traits. Notably, a strong positive linear relationship was observed between total chlorophyll content and SPAD value (r=0.64). Similarly, strong positive linear correlations were observed between leaf area and several traits, such as root fresh weight (r=0.71), root dry weight (r=0.65), maximum root number (r=0.69), root tip number (r=0.74), total root length (r=0.71), main root length (r=0.55), total root area (r=0.58), and total root volume (0.62). The leaf area showed stronger correlations with various morphological parameters as well, including leaf fresh weight (r=0.97), and leaf dry weight (r=0.97). There was a stronger linear correlation between root fresh weight and root dry weight (r=0.92). Additionally, strong correlations were found between root fresh weight and various traits, such as leaf fresh weight (r=0.64), leaf dry weight (0.69), and several root characteristics such as maximum root number (r=0.72), root tip number (r=0.76), total root length (r=0.76), main root length (r=0.64), total root area (r=0.72), and total root volume (r=0.72). Similarly, there were strong correlations between root dry weight and leaf fresh weight (r=0.65), leaf dry weight (r=0.64), maximum root number (r=0.68), root tip number (r=0.74), total root length (r=0.72), main root length (r=0.64), total root area (r=0.69), and total root volume (r=0.72). There was a stronger correlation between leaf fresh weight and leaf dry weight (r=0.96), and strong correlations between leaf fresh weight and several root traits, which are maximum root number (r=0.70), root tip number (r=0.73), total root length (r=0.72), main root length (r=0.55), total root area (r=0.58), and total root volume (r=0.63). Between leaf dry weight and root characteristics, again, there were several strong correlations, which are, maximum root number (r=0.67), root tip number (r=0.72), total root length (r=0.70), main root length (r=0.56), total root area (r=0.58), and total root volume (r=0.60). There was a strong correlation between the fresh weight ratio and the dry weight ratio (0.62). Between root characteristics, there were stronger correlations as well; maximum root number and root tip number (0.90), total root length (r=0.93), main root length (r=0.71), total root area (r=0.76) and total root volume (r=0.75). There were stronger correlations between root tip number and total root length

(r=0.95), main root length (r=0.78), total root area (r=0.79) and total root volume (r=0.78). There were stronger linear correlations between total root length and main root length (r=0.80), total root area (r=0.83), and total root volume (r=0.81). Between main root length and total root area, there was a stronger correlation (r=0.75). Between total root volume, there were strong correlations between main root length (r=0.74) and total root area (r=0.71).

Table 3.3 Pearson's correlation coefficient values of the traits.

Traits	RCHL	RSPAD	RLA	RFCR	RRFW	RRDW	RLFW	RLDW	RFWR	RDWR	RMRN	RRTN	RTRL	RMRL	RTRA
RSPAD	**0.64***														
RLA	-0.05	0.16													
RFCR	0.05	-0.04	-0.23												
RRFW	0.01	0.25	**0.71***	-0.27											
RRDW	0.02	0.20	**0.65***	-0.35	**0.92***										
RLFW	-0.06	0.17	**0.97***	-0.21	**0.69***	**0.64***									
RLDW	-0.03	0.15	**0.97***	-0.16	**0.69***	**0.64***	**0.96***								
RFWR	-0.20	0.05	0.40	-0.23	0.32	0.31	0.44	0.43							
RDWR	-0.16	0.08	0.32	-0.07	0.19	0.19	0.37	0.29	**0.62***						
RMRN	-0.12	0.24	**0.69***	-0.23	**0.72***	**0.68***	**0.70***	**0.67***	0.43	0.31					
RRTN	-0.08	0.23	**0.73***	-0.30	**0.76***	**0.74***	**0.73***	**0.72***	0.44	0.35	**0.90***				
RTRL	-0.12	0.22	**0.71***	-0.25	**0.76***	**0.72***	**0.72***	**0.70***	0.44	0.32	**0.93***	**0.95***			
RMRL	-0.03	0.20	**0.55***	-0.33	**0.64***	**0.64***	**0.55***	**0.56***	0.38	0.28	**0.70***	**0.78***	**0.80***		
RTRA	-0.13	0.17	**0.58***	-0.25	**0.72***	**0.69***	**0.58***	**0.58***	0.37	0.30	**0.76***	**0.79***	**0.83***	**0.75***	
RTRV	-0.09	0.15	**0.62***	-0.26	**0.72***	**0.72***	**0.63***	**0.60***	0.40	0.27	**0.74***	**0.78***	**0.81***	**0.74***	**0.70***

RCHL, relative total chlorophyll concentration; RSAPD, chlorophyll index; RLA, relative leaf area; RFCR, relative ferric chelate reductase enzyme activity; RRFW, relative root fresh weight; RRDW, relative root dry weight; RLFW, relative leaf fresh weight; RLDW, relative leaf dry weight; RFWR, relative root fresh weight/leaf fresh weight ratio; RDWR, relative root dry weight/leaf dry weight ratio; RMRN, relative maximum root number; RRTN, relative root tip number; RTRL, relative total root length; RMRL, relative main root length; RTRA, relative total root area; RTRV, relative total root volume; *Significant level under 0.0001 for Pearson correlation test.

Out of the 133 common bean landraces and 3 commercial cultivars studied, the top 5 most tolerant and the top 5 most sensitive to Fe deficiency were identified after evaluation of their responses. The following traits were considered to classify common bean accessions as tolerant or sensitive to Fe deficiency to cover both above-soil and root characteristics: SPAD, total chlorophyll content, leaf area, leaf dry weight, root dry weight, FCR activity, maximum root number, root tip number, total root length, main root length, total root area, and total root volume. Based on each of these traits, the 5 most tolerant and the 5 most sensitive accessions were selected. Accessions that were classified as tolerant or sensitive according to at least six of these traits were subsequently identified as overall tolerant or sensitive, respectively. Table 3.4 presents the most tolerant and sensitive common bean accessions, as well as the traits that were key determinants of their tolerance. The most sensitive accessions were Bitlis-35, Hakkari-49, Bingol-1, Hakkari-11, and Hakkari-23, while the most tolerant accessions were Duzce-9, Nigde-Derinkuyu, Duzce-1, Nigde-Dermason and Elazig.

Table 3.4 Most tolerant and sensitive common bean accessions.

	Genotype	Traits	# of Traits
SENSITIVE	Bitlis-35	FCR, LDW, RDW, MRN, RTN, TRL, MRL, TRA	8
	Hakkari-39	LA, LDW, RDW, MRN, RTN, TRL, TRA	7
	Bingol-1	CHL, LA, LDW, RDW, MRL, TRV	6
	Hakkari-11	LA, MRN, RTN, TRL, MRL, TRA	6
	Hakkari-23	SPAD, FCR, LA, MRN, RTN, TRA	6
TOLERANT	Duzce-9	LA, LDW, RDW, MRN, RTN, TRL, TRA, TRV	8
	Nigde-Derinkuyu	CHL, SPAD, RDW, MRN, RTN, MRL, TRA, TRV	8
	Duzce-1	FCR, LA, LDW, RDW, RTN, TRA, TRV	7
	Nigde-Dermason	LA, LDW, MRN, RTN, TRL, TRA	6
	Elazig	RDW, RTN, TRL, MRL, TRA, TRV	6

CHL, total chlorophyll concentration; SPAD, chlorophyll index; FCR, ferric chelate reductase enzyme activity; LA, leaf area; LDW, leaf dry weight; RDW, root dry weight; MRN, maximum root number; RTN, root tip number; TRL, total root length; MRL, main root length; TRA, total root area; TRV, total root volume.

Figure 3.3 represents the leaves from the common bean accessions that are most tolerant and sensitive to Fe deficiency. Images (a) to (e) show the most sensitive accessions, while images (f) to (j) show the most tolerant ones. The roots of the 2 most tolerant and 2 most sensitive genotypes are represented in Figure C.1.

Bitlis-35 was considered sensitive to Fe deficiency based on FCR activity, leaf dry weight, root dry weight, and other root characteristics, but not according to chlorophyll content or SPAD value. As seen in Figure 3.3 (a), the chlorosis on the leaves is not visible. Hakkari-39 was considered sensitive in terms of leaf area and leaf dry weight, which is evident in Figure 3.3 (b). It was also sensitive in terms of root dry weight and other root characteristics, but not according to chlorophyll content or SPAD value. It is evident from Figure 3.3 (b) that there is no visible chlorosis on the leaves of Hakkari-39 plants grown under Fe deficiency. Bingol-1 was classified as sensitive to Fe deficiency in terms of chlorophyll content and leaf area, as seen in Figure 3.3 (c). It was also considered sensitive in terms of leaf dry weight, root dry weight, main root length, and total root volume. Hakkari-11 was classified as sensitive to Fe deficiency according to leaf area and several root characteristics, but not chlorophyll content. The lack of chlorosis on the leaves of Hakkari-11 plants grown under Fe deficiency is visible in Figure 3.3 (d). Hakkari-23 was considered sensitive in terms of SPAD value and leaf area, both of which can be seen in Figure 3.3 (e). It was also sensitive in terms of FCR activity and several root characteristics.

Duzce-9 was classified as tolerant to Fe deficiency in terms of leaf area and leaf dry weight, as evidenced in Figure 3.3 (f). It was also tolerant in terms of several root characteristics. Nigde-Derinkuyu was considered tolerant based on chlorophyll content and SPAD value, but not leaf area. This is visible in Figure 3.3 (g), where there is no visible chlorosis, but a slight decrease in leaf area can be seen in the leaves of the Nigde-Derinkuyu plants grown under Fe deficiency compared to those grown under control conditions. It also exhibited tolerance in several root characteristics. Duzce-1 was identified as tolerant in terms of leaf area, as illustrated in Figure 3.3 (h), as well as FCR activity and several root characteristics. Nigde-Dermason was

found to be tolerant in terms of leaf area, as shown in Figure 3.3 (i). It was also classified as tolerant based on several root characteristics. Elazig exhibited tolerance in several root characteristics but was not tolerant in terms of leaf area, as depicted in Figure 3.3 (j). The leaf area was visibly reduced in response to Fe deficiency treatment.

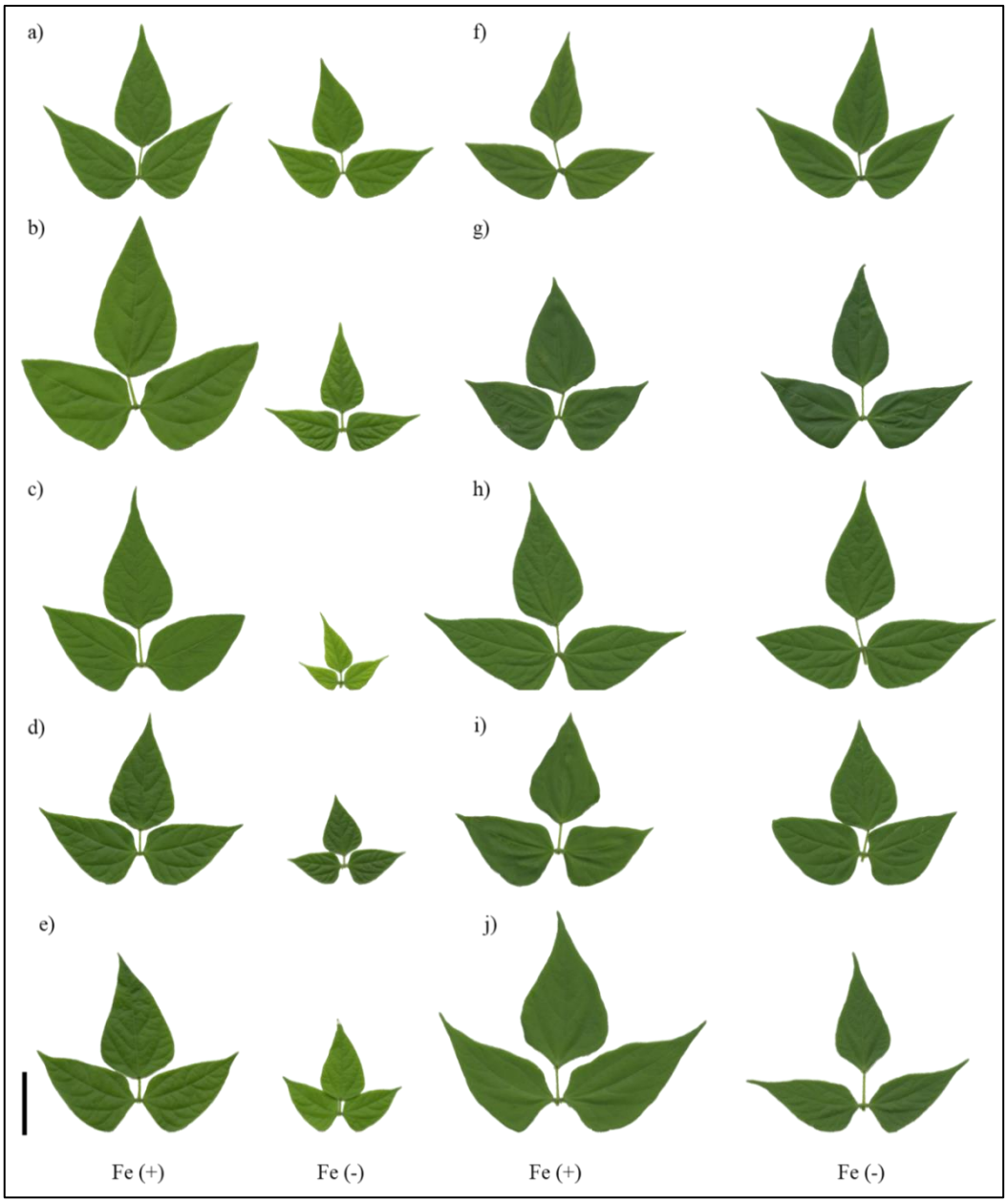

Figure 3.3. Leaves of the most sensitive and tolerant common bean accessions to Fe deficiency treatment. The most sensitive accessions are a) Bitlis-35, b) Hakkari-39, c) Bingol-1, d) Hakkari-11, e) Hakkari-23. The most tolerant accessions are f) Duzce-9, g) Nigde-Derinkuyu, h) Duzce-1, i) Nigde-Dermason, j) Elazig. Bar represents 5 cm.

3.2 Genome-Wide Association Study

The results of the GWAS were visualized in a Manhattan plot with a threshold level of 5.4, which can be seen in Figure 3.4. The threshold line (green) in the Manhattan plots was automatically assigned by GAPIT using the Benjamini-Hochberg cut-off. Furthermore, a Bonferroni correction was applied, and the significance threshold was adjusted to 0.0071, and all markers continued to be significant. In total, 7 SNPs were significantly associated with FCR, RFW, and TRA. Other markers were also identified in association with various traits including chlorophyll content, SPAD values, and leaf fresh weight. However, these markers were not considered significantly associated with the mentioned traits as they fell below the established threshold. Additional information about the SNPs that are significantly associated with FCR, RFW and TRA can be seen in Table 3.5. Markers significantly associated with FCR activity were located on chromosomes 1, 7, and 8, with p values 3.33E-16, 2.18E-06 and 3.92E-06, respectively, as depicted in Figure 3.4. and detailed in Table 3.5. Moreover, markers significantly linked with total root area were identified on chromosomes 4, 7, and 11, with p values 1.19E-09, 1.05E-06, and 2.63E-06, respectively. Notably, a single marker significantly associated with root fresh weight was found on chromosome 4, with a p-value of 4.18E-09. In GWAS results, minor allele frequency (MAF) indicates how common or rare an allele is within the population, while the effect size quantifies the magnitude of the allele's influence on the trait, with larger effect sizes suggesting a stronger association.

After significant markers were identified, the potential candidate genes were identified based on their proximity to the markers, specifically within a range of ± 100 kb. Three distinct significant markers were identified on different chromosomes, leading to the discovery of a total of 89 potential candidate genes related to FCR activity in the roots. The potential candidate genes are elaborated in Table 3.6, Table 3.7, and Table 3.8, providing their NCBI-GeneID, NCBI-ProteinID, AT number of their *Arabidopsis thaliana* orthologs, as well as the name and full name of the

Arabidopsis thaliana ortholog genes; and the positions of the markers and potential candidate genes can be visualized in Figure 3.5 (a), (b), and (c).

Additionally, from a significant marker located on chromosome 4, a single potential candidate gene was pinpointed: a ubiquitin carboxyl-terminal hydrolase family protein. Further information about this potential candidate gene, including its NCBI-GeneID, NCBI-ProteinID, AT number of its *Arabidopsis thaliana* ortholog, name, and full name of the *Arabidopsis* ortholog gene, can be accessed in Table 3.9. Its genomic position is depicted in Figure 3.5 (d).

From three different significant markers identified on three different chromosomes, a total of 68 potential candidate genes were identified related to total root area under Fe deficiency. Additional details about these potential candidate genes, including their NCBI-GeneID, NCBI-ProteinID, AT numbers of their *Arabidopsis thaliana* orthologs, names, and full names of the *Arabidopsis* ortholog genes, can be found in Table 3.10, Table 3.11, and Table 3.12. Their chromosomal positions are visualized in Figure 3.5 (e), (f), and (g).

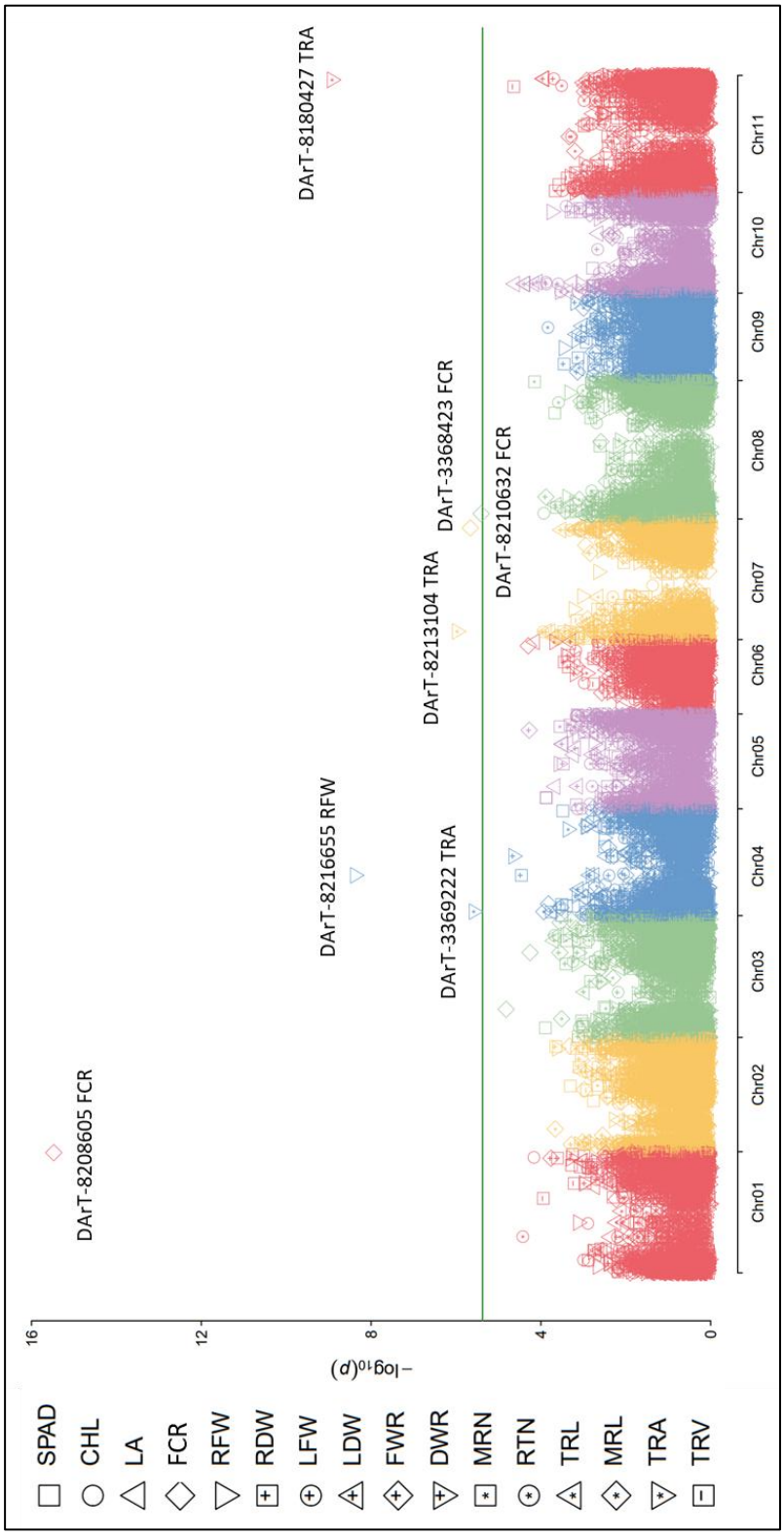

Figure 3.4 Manhattan plot of the studied traits.

Table 3.5 Chromosomal regions associated with studied traits.

Trait	Marker	Chr	Position (bp)	p-value	-log(p)	MAF	Effect
FCR	DArT-8208605	1	51,872,044	3.33E-16	15.5	0.06	-6.5
FCR	DArT-3368423	7	47,814,993	2.18E-06	5.7	-0.05	2.8
FCR	DArT-8210632	8	2,175,532	3.92E-06	5.4	0.02	-2.4
RFW	DArT-8216655	4	17,337,717	4.18E-09	8.4	0.19	-11.0
TRA	DArT-8180427	11	48,115,094	1.19E-09	8.9	-0.01	-17.0
TRA	DArT-8213104	7	3,383,362	1.05E-06	6.0	-0.17	3.0
TRA	DArT-3369222	4	1,656,590	2.63E-06	5.6	-0.43	-3.1

FCR, ferric chelate reductase enzyme activity; RFW, root fresh weight; TRA, total root area; MAF, Minor allele frequency.

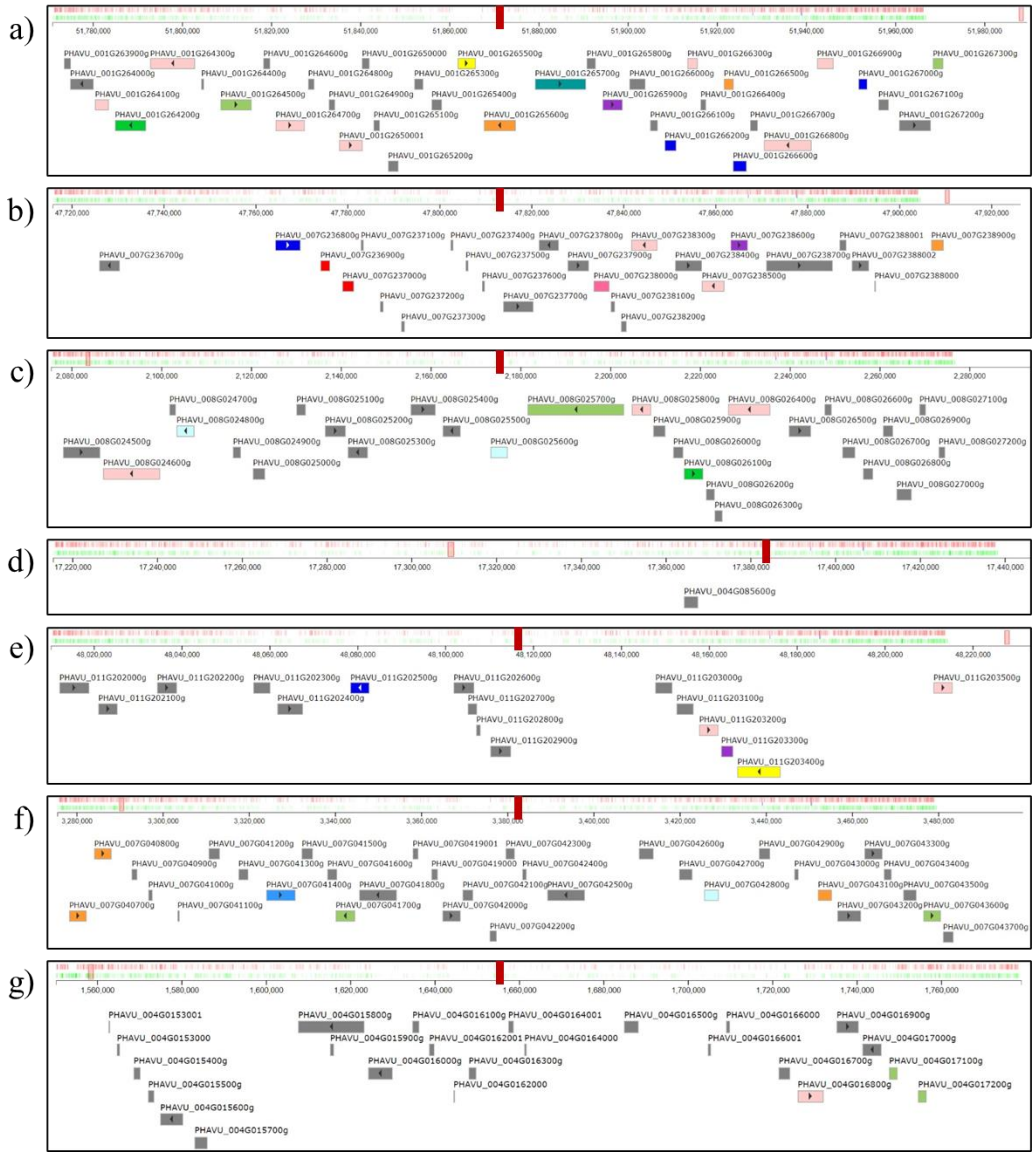

Figure 3.5 Possible candidate genes and their positions on the common bean genome for the markers a) DArT-8208605 (FCR), b) DArT-3368423 (FCR), c) DArT-8210632 (FCR), d) DArT-8216655 (RFW), e) DArT-8180427 (TRA), f) DArT-8213104 (TRA), and g) DArT-3369222 (TRA). The positions of the significant markers are indicated with red lines on the genome.

Table 3.6 Possible candidate genes for the marker DArT-8208605 (FCR).

Entry	GeneID	ProteinID	AGI Number	Gene Name Abbreviation	Arabidopsis Ortholog Gene Name
PHAVU_001G263900	18642630	XP_007163785	AT1G05510	*OBAP1a, DUF1264*	*OIL BODY-ASSOCIATED PROTEIN 1A*, naphthalene 1,2-dioxygenase subunit alpha
PHAVU_001G264000	18642631	XP_007163786	AT3G23700	*SRRP1*	*S1 RNA-BINDING RIBOSOMAL PROTEIN 1*
PHAVU_001G264100	18642632	XP_007163788	AT3G26560		ATP-dependent RNA helicase
PHAVU_001G264200	18642633	XP_007163789	AT4G14210	*PDS3, PDE226*	*PHYTOENE DESATURASE 3, PIGMENT DEFECTIVE 226*
PHAVU_001G264300	18642634	XP_007163790	AT2G32000		DNA topoisomerase, type IA, core
PHAVU_001G264400	18642635	XP_007163791	AT2G31980	*CYS2*	*PHYTOCYSTATIN 2*
PHAVU_001G264500	18642636	XP_007163792	AT3G23670	*PAKRP1L*	*PHRAGMOPLAST-ASSOCIATED KINESIN-RELATED PROTEIN*
PHAVU_001G264600	18642637	XP_007163793	AT4G12240		Zinc finger (C2H2 type) family protein
PHAVU_001G264700	18642638	XP_007163794	AT3G23660	*SEC23E*	Sec23/Sec24 protein transport family protein
PHAVU_001G264800	18642639	XP_007163795	AT4G12560	*CPR1, CPR30*	*CONSTITUTIVE EXPRESSER OF PR GENES 1, CONSTITUTIVE EXPRESSER OF PR GENES 30*
PHAVU_001G264900	18642640	XP_007163796	AT1G30790		F-box and associated interaction domains-containing protein
PHAVU_001G2650001	18642641	XP_007163797	AT4G14180	*PRD1, MEI1*	*PUTATIVE RECOMBINATION INITIATION DEFECT 1, MEIOSIS DEFECTIVE 1*
PHAVU_001G2650000	18642642	XP_007163798	AT4G14180	*PRD1, MEI1*	*PUTATIVE RECOMBINATION INITIATION DEFECT 1, MEIOSIS DEFECTIVE 1*
PHAVU_001G265100	18642643	XP_007163799	AT5G49610		F-box family protein
PHAVU_001G265200	18642644	XP_007163800	AT4G14190		Pentatricopeptide repeat (PPR) superfamily protein
PHAVU_001G265300	18642645	XP_007163801	AT4G14130	*XTH15, XTR7*	*XYLOGLUCAN ENDOTRANSGLUCOSYLASE/HYDROLASE 15, XYLOGLUCAN ENDOTRANSGLYCOSYLASE 7*
PHAVU_001G265400	18642646	XP_007163802	AT4G15550	*IAGLU*	*INDOLE-3-ACETATE BETA-D-GLUCOSYLTRANSFERASE*
PHAVU_001G265500	18642647	XP_007163803	AT3G23750	*BARK1, TMK4*	*BAK1-ASSOCIATING RECEPTOR-LIKE KINASE 1, TRANS-MEMBRANE KINASE 4*
PHAVU_001G265600	18642648	XP_007163804	AT4G19710	*AK-HSDH*	*ASPARTATE KINASE-HOMOSERINE DEHYDROGENASE*
PHAVU_001G265700	18642649	XP_007163805	AT3G23790	*AAE16*	*ACYL ACTIVATING ENZYME 16*
PHAVU_001G265800	18642650	XP_007163806	AT4G14050	*MEF35*	*MITOCHONDRIAL EDITING FACTOR 35*
PHAVU_001G265900	18642651	XP_007163807	AT4G14040	*SBP2, EDA38*	*SELENIUM-BINDING PROTEIN 2, EMBRYO SAC DEVELOPMENT ARREST 38*
PHAVU_001G266000	18642652	XP_007163808	AT4G14000		Putative methyltransferase family protein
PHAVU_001G266100	18642653	XP_007163809	AT4G13990	*MBGT1*	*MANNAN BETA-GALACTOSYLTRANSFERASE 1*
PHAVU_001G266200	18642654	XP_007163810	AT5G17200		Pectin lyase-like superfamily protein
PHAVU_001G266300	18642655	XP_007163811	AT4G13980	*HSFA5*	*HEAT SHOCK TRANSCRIPTION FACTOR A5*

Table 3.6 Cont'd

Entry	GeneID	ProteinID	AGI Number	Gene Name Abbreviation	Arabidopsis Ortholog Gene Name
PHAVU_001G266400	18642656	XP_007163812	AT3G23805	*RALFL24*	*RALF-LIKE 24*
PHAVU_001G266500	18642657	XP_007163813	AT4G13940	*HOG1, SAHH1, SAH1, EMB1395,*	*HOMOLOGY-DEPENDENT GENE SILENCING 1, S-ADENOSYL-L-HOMOCYSTEIN HYDROLASE 1, EMBRYO DEFECTIVE 1395, MATERNAL EFFECT EMBRYO ARREST 58*
PHAVU_001G266600	18642658	XP_007163814	AT4G13930	*SHM4*	*SERINE HYDROXYMETHYLTRANSFERASE 4*
PHAVU_001G266700	18642659	XP_007163815	AT1G09220		Pentatricopeptide repeat (PPR) superfamily protein
PHAVU_001G266800	18642660	XP_007163816	AT2G31970	*RAD50*	*DNA REPAIR-RECOMBINATION PROTEIN*
PHAVU_001G266900	18642661	XP_007163817	AT4G13870	*WEX, WRNEXO*	*WERNER SYNDROME-LIKE EXONUCLEASE*
PHAVU_001G267000	18642662	XP_007163818	AT3G23820	*GAE6*	*UDP-D-GLUCURONATE 4-EPIMERASE 6*
PHAVU_001G267100	18642663	XP_007163819	AT4G13850	*GRP2, GR-RBP2, RBGA5*	*GLYCINE RICH PROTEIN 2, GLYCINE-RICH RNA-BINDING PROTEIN 2, RNA-BINDING GLYCINE-RICH PROTEIN A5*
PHAVU_001G267200	18642664	XP_007163820	AT3G59780		Rhodanese/Cell cycle control phosphatase superfamily protein
PHAVU_001G267300	18642665	XP_007163821	AT4G13800	*ENOR3L3*	Magnesium transporter NIPA (DUF803)

Table 3.7 Possible candidate genes for the marker DArT-3368423 (FCR).

Entry	GeneID	ProteinID	AGI Number	Gene Name Abbreviation	Arabidopsis Ortholog Gene Name
PHAVU_007G236700	18626842	XP_007145411	AT1G04690	*KAB1, KV-BETA1*	*POTASSIUM CHANNEL BETA SUBUNIT 1, K+ CHANNEL BETA SUBUNIT PROTEIN*
PHAVU_007G236800	18626843	XP_007145412	AT1G04680		Pectin lyase-like superfamily protein
PHAVU_007G236900	18626844	XP_007145413	AT4G13720		Inosine triphosphate pyrophosphatase family protein
PHAVU_007G237000	18626845	XP_007145414	AT4G13720		Inosine triphosphate pyrophosphatase family protein
PHAVU_007G237100	18626846	XP_007145415	AT2G25295	*LCR81*	*LOW-MOLECULAR-WEIGHT CYSTEINE-RICH 81*
PHAVU_007G237200	18626847	XP_007145416	AT3G06985	*LCR44*	*LOW-MOLECULAR-WEIGHT CYSTEINE-RICH 44*
PHAVU_007G237300	18626848	XP_007145417	AT2G25295	*LCR81*	*LOW-MOLECULAR-WEIGHT CYSTEINE-RICH 81*
PHAVU_007G237400	18626849	XP_007145418	AT2G25295	*LCR81*	*LOW-MOLECULAR-WEIGHT CYSTEINE-RICH 81*
PHAVU_007G237500	18626850	XP_007145419	AT5G32619		Defensin-like (DEFL) family protein
PHAVU_007G237600	18626851	XP_007145420	AT2G25295	*LCR81*	*LOW-MOLECULAR-WEIGHT CYSTEINE-RICH 81*
PHAVU_007G237700	18626852	XP_007145421	AT4G13590	*BICAT2, CMT1*	*BIVALENT CATION TRANSPORTER 2, CHLOROPLAST MANGANESE TRANSPORTER1*
PHAVU_007G237800	18626853	XP_007145422	AT3G24040		Core-2/I-branching beta-1,6-N-acetylglucosaminyltransferase family protein
PHAVU_007G237900	18626854	XP_007145423	AT3G22520		Spindle assembly abnormal protein
PHAVU_007G238000	18626855	XP_007145424	AT3G24030		Hydroxyethylthiazole kinase family protein
PHAVU_007G238100	18626856	XP_007145425	AT3G24020	*DIR16*	*DIRIGENT PROTEIN 16*
PHAVU_007G238200	18626857	XP_007145426	AT3G24020	*DIR16*	*DIRIGENT PROTEIN 16*
PHAVU_007G238300	18626858	XP_007145427	AT2G33205		Serinc-domain containing serine and sphingolipid biosynthesis protein
PHAVU_007G238400	18626859	XP_007145429	AT3G24010	*ING1*	*INHIBITOR OF GROWTH 1*
PHAVU_007G238500	18626860	XP_007145430	AT3G23990	*HSP60, HSP60-3B*	*HEAT SHOCK PROTEIN 60, HEAT SHOCK PROTEIN 60-3B*
PHAVU_007G238600	18626861	XP_007145431	AT1G04630	*MEE4*	*MATERNAL EFFECT EMBRYO ARREST 4*
PHAVU_007G238700	18626862	XP_007145432	AT3G23980	*BLI, KOS1*	*BLISTER, KOLD SENSITIV 1*
PHAVU_007G2388001	18626863	XP_007145433	AT1G04620	*HCAR*	*7-HYDROXYMETHYL CHLOROPHYLL A (HMCHL) REDUCTASE*
PHAVU_007G2388002	18626864	XP_007145434	AT1G04620	*HCAR*	*7-HYDROXYMETHYL CHLOROPHYLL A (HMCHL) REDUCTASE*
PHAVU_007G2388000	18626865	XP_007145435	AT1G04620	*HCAR*	*7-HYDROXYMETHYL CHLOROPHYLL A (HMCHL) REDUCTASE*
PHAVU_007G238900	18626866	XP_007145436	AT1G04610	*YUC3*	*YUCCA3*

Table 3.8 Possible candidate genes for the marker DArT-8210632 (FCR).

Entry	GeneID	ProteinID	AGI Number	Gene Name Abbreviation	Arabidopsis Ortholog Gene Name
PHAVU_008G024500	18621634	XP_007139380	AT5G38840		SMAD/FHA domain-containing protein
PHAVU_008G024600	18621635	XP_007139381	AT5G15700		DNA/RNA polymerases superfamily protein
PHAVU_008G024700	18621636	XP_007139382	AT4G32105		Beta-1,3-N-Acetylglucosaminyltransferase family protein
PHAVU_008G024800	18621637	XP_007139383	AT3G30380		Alpha/beta-Hydrolases superfamily protein
PHAVU_008G024900	18621638	XP_007139384	AT4G15733	*SCRL11*	*SCR-LIKE 11*
PHAVU_008G025000	18621639	XP_007139385	AT5G15710		Galactose oxidase/kelch repeat superfamily protein
PHAVU_008G025100	18621640	XP_007139386	AT1G13620	*RGF2, GLV5*	*ROOT MERISTEM GROWTH FACTOR 2, GOLVEN 5*
PHAVU_008G025200	18621641	XP_007139388	AT5G15730	*CRLK2*	*CALCIUM/CALMODULIN-REGULATED RECEPTOR-LIKE KINASE 2*
PHAVU_008G025300	18621642	XP_007139389	AT2G03890	*PI4K GAMMA 7, UBDK GAMMA 7*	*PHOSPHOINOSITIDE 4-KINASE GAMMA 7, UBIQUITIN-LIKE DOMAIN KINASE GAMMA 7*
PHAVU_008G025400	18621643	XP_007139390	AT3G30300		O-fucosyltransferase family protein
PHAVU_008G025500	18621644	XP_007139391	AT1G69010	*BIM2*	*BES1-INTERACTING MYC-LIKE PROTEIN 2*
PHAVU_008G025600	18621645	XP_007139392	AT5G15740	*RRT1*	*RG-I RHAMNOSYLTRANSFERASE 1*
PHAVU_008G025700	18621646	XP_007139393	AT3G02260	*ASA1, BIG, CRM1, DOC1, LPR1, TIR3,*	*ATTENUATED SHADE AVOIDANCE 1, CORYMBOSA1, DARK OVER-EXPRESSION OF CAB 1, LOW PHOSPHATE-RESISTANT ROOT 1, TRANSPORT INHIBITOR RESPONSE 3, UMBRELLA 1*
PHAVU_008G025800	18621647	XP_007139394	AT3G49180	*RID3*	*ROOT INITIATION DEFECTIVE 3*
PHAVU_008G025900	18621648	XP_007139395	AT3G46790	*CRR2*	*CHLORORESPIRATORY REDUCTION 2*
PHAVU_008G026000	18621649	XP_007139396	AT3G23880		F-box and associated interaction domains-containing protein
PHAVU_008G026100	18621650	XP_007139397	AT2G36780		UDP-Glycosyltransferase superfamily protein
PHAVU_008G026200	18621651	XP_007139400	AT2G32235		
PHAVU_008G026300	18621652	XP_007139401	AT5G15780		Pollen Ole e 1 allergen and extensin family protein
PHAVU_008G026400	18621653	XP_007139402	AT5G38880	*AUG5*	*AUGMIN SUBUNIT 5*
PHAVU_008G026500	18621654	XP_007139403	AT3G02290		RING/U-box superfamily protein
PHAVU_008G026600	18621655	XP_007139404	AT3G51550	*FER*	*FERONIA*
PHAVU_008G026700	18621656	XP_007139405	AT3G51550	*FER*	*FERONIA*
PHAVU_008G026800	18621657	XP_007139406	AT5G38900	*PDI*	*PROTEIN DISULFIDE ISOMERASE*

Table 3.8 Cont'd

Entry	GeneID	ProteinID	AGI Number	Gene Name Abbreviation	Arabidopsis Ortholog Gene Name
PHAVU_008G026900	18621658	XP_007139407	AT3G51550	*FER*	*FERONIA*
PHAVU_008G027000	18621659	XP_007139408	AT5G38900	*PDI*	*PROTEIN DISULFIDE ISOMERASE*
PHAVU_008G027100	18621660	XP_007139410	AT3G51550	*FER*	*FERONIA*
PHAVU_008G027200	18621661	XP_007139411	AT3G51550	*FER*	*FERONIA*

Table 3.9 Possible candidate gene for the marker DArT-8216655 (RFW).

Entry	GeneID	ProteinID	AGI Number	Gene Name Abbreviation	Arabidopsis Ortholog Gene Name
PHAVU_004G085600	18632438	XP_007151904	AT1G71850		Ubiquitin carboxyl-terminal hydrolase family protein

Table 3.10 Possible candidate genes for the marker DArT-8180427 (TRA).

Entry	GeneID	ProteinID	AGI Number	Gene Name Abbreviation	Arabidopsis Ortholog Gene Name
PHAVU_011G202000	18616794	XP_007133706	AT2G44480	*BGLU17*	*BETA GLUCOSIDASE 17*
PHAVU_011G202100	18616795	XP_007133708	AT3G14470	*LRR4*	*LEUCINE RICH REPEAT PROTEIN 1*
PHAVU_011G202200	18616796	XP_007133709	AT4G27300		S-locus lectin protein kinase family protein
PHAVU_011G202300	18616797	XP_007133710	AT3G14470	*LRR4*	*LEUCINE RICH REPEAT PROTEIN 1*
PHAVU_011G202400	18616798	XP_007133711	AT3G14470	*LRR4*	*LEUCINE RICH REPEAT PROTEIN 1*
PHAVU_011G202500	18616799	XP_007133712	AT2G44480	*BGLU17*	*BETA GLUCOSIDASE 17*
PHAVU_011G202600	18616800	XP_007133713	AT3G14470	*LRR4*	*LEUCINE RICH REPEAT PROTEIN 1*
PHAVU_011G202700	18616801	XP_007133714			
PHAVU_011G202800	18616802	XP_007133715	AT1G72860	*TNL60*	
PHAVU_011G202900	18616803	XP_007133716	AT3G14460	*LRRAC1*	*LEUCINE-RICH REPEAT (LRR) PROTEIN 1*
PHAVU_011G203000	18616804	XP_007133717	AT3G14470	*LRR4*	*LEUCINE RICH REPEAT PROTEIN 1*
PHAVU_011G203100	18616805	XP_007133718	AT3G14470	*LRR4*	*LEUCINE RICH REPEAT PROTEIN 1*
PHAVU_011G203200	18616806	XP_007133719	AT2G38730		Cyclophilin-like peptidyl-prolyl cis-trans isomerase family protein
PHAVU_011G203300	18616807	XP_007133720	AT3G12260	*NDUFA6*	*NADH-UBIQUINONE OXIDOREDUCTASE SUBUNIT A6*
PHAVU_011G203400	18616808	XP_007133721	AT3G12250	*TGA6, BZIP45*	*TGACG MOTIF-BINDING FACTOR 6*
PHAVU_011G203500	18616809	XP_007133722	AT3G01800		Ribosome recycling factor

Table 3.11 Possible candidate genes for the marker DArT-8213104 (TRA).

Entry	GeneID	ProteinID	AGI Number	Gene Name Abbreviation	Arabidopsis Ortholog Gene Name
PHAVU_007G040800	18624822	XP_007143064	AT1G49820	*MTK, MTK1*	*S-METHYL-5-THIORIBOSE KINASE, 5-METHYLTHIORIBOSE KINASE 1*
PHAVU_007G040900	18624823	XP_007143065	AT2G15220		Plant basic secretory protein (BSP) family protein
PHAVU_007G041000	18624824	XP_007143066	AT2G15220		Plant basic secretory protein (BSP) family protein
PHAVU_007G041100	18624825	XP_007143067			
PHAVU_007G041200	18624826	XP_007143068	AT3G19500		basic helix-loop-helix (bHLH) DNA-binding superfamily protein
PHAVU_007G041300	18624827	XP_007143070	AT2G15220		Plant basic secretory protein (BSP) family protein
PHAVU_007G041400	18624828	XP_007143071	AT4G34260	*AXY8, FUC95A*	*ALTERED XYLOGLUCAN 8*
PHAVU_007G041500	18624829	XP_007143072	AT4G34265		
PHAVU_007G041600	18624831	XP_007143076	AT4G34270	*TIP41*	*TAP42 INTERACTING PROTEIN OF 41 KDA*
PHAVU_007G041700	18624831	XP_007143078	AT4G34270	*TIP41*	*TAP42 INTERACTING PROTEIN OF 41 KDA*
PHAVU_007G041800	18624832	XP_007143079	AT3G19510	*HAT3.1*	Homeodomain-like protein with RING/FYVE/PHD-type zinc finger domain-containing protein
PHAVU_007G0419001	18624833	XP_007143080	AT3G18990	*VRN1, REM39*	*REDUCED VERNALIZATION RESPONSE 1, REPRODUCTIVE MERISTEM 39*
PHAVU_007G0419000	18624834	XP_007143081	AT1G49480	*RTV1*	*RELATED TO VERNALIZATION 1*
PHAVU_007G042000	18624835	XP_007143082	AT2G14910	*DUF760-4*	MAR-binding filament-like protein
PHAVU_007G042100	18624836	XP_007143083	AT3G08820		Pentatricopeptide repeat (PPR) superfamily protein
PHAVU_007G042200	18624837	XP_007143084	AT1G22240	*PUM8*	*PUMILIO 8*
PHAVU_007G042300	18624838	XP_007143085	AT2G18990	*TXND9*	*THIOREDOXIN DOMAIN-CONTAINING PROTEIN 9 HOMOLOG*
PHAVU_007G042400	18624839	XP_007143086	AT2G14900	*GASA7*	Gibberellin-regulated family protein
PHAVU_007G042500	18624840	XP_007143087	AT2G14900	*DHU1*	*DWD HYPERSENSITIVE TO UV-B 1*
PHAVU_007G042600	18624841	XP_007143089	AT3G19540	*BDR4*	*BOUNDARY OF ROP DOMAIN4*
PHAVU_007G042700	18624842	XP_007143090	AT5G02860		Pentatricopeptide repeat (PPR) superfamily protein
PHAVU_007G042800	18624843	XP_007143091	AT4G33920	*APD5*	*ARABIDOPSIS PP2C CLADE D 5*
PHAVU_007G042900	18624844	XP_007143093	AT1G49850		RING/U-box superfamily protein
PHAVU_007G043000	18624845	XP_007143094	AT3G19550		Glutamate racemase
PHAVU_007G043100	18624846	XP_007143095	AT4G33910		2-oxoglutarate (2OG) and Fe(II)-dependent oxygenase superfamily protein

Table 3.11 Cont'd

Entry	GeneID	ProteinID	AGI Number	Gene Name Abbreviation	Arabidopsis Ortholog Gene Name
PHAVU_007G043200	18624847	XP_007143097	AT4G15090	*FAR1*	*FAR-RED IMPAIRED RESPONSE 1*
PHAVU_007G043300	18624848	XP_007143098	AT1G49870		Myosin-2 heavy chain-like protein
PHAVU_007G043400	18624849	XP_007143099	AT2G23090		Uncharacterized protein family SERF
PHAVU_007G043500	18624850	XP_007143100	AT3G43740	*EXLRR11*	*EXTRACELLULAR LEUCINE-RICH REPEAT-CONTAINING-PROTEIN 11*
PHAVU_007G043600	18624851	XP_007143101	AT4G33905		Peroxisomal membrane 22 kDa (Mpv17/PMP22) family protein
PHAVU_007G043700	18624852	XP_007143102	AT4G33890	*ADA1B*	Component of SAGA complex, SPT module subunit, interacts with HAG1

Table 3.12 Possible candidate genes for the marker DArT-3369222 (TRA).

Entry	GeneID	ProteinID	AGI Number	Gene Name Abbreviation	Arabidopsis Ortholog Gene Name
PHAVU_004G0153001	18631704	XP_007151069	ArthCp080	*ndhH*	NADH dehydrogenase subunit 7
PHAVU_004G0153000	18631704	XP_007151069	ArthCp080	*ndhH*	NADH dehydrogenase subunit 7
PHAVU_004G015400	18631705	XP_007151070	AT4G10400		F-box/RNI-like/FBD-like domains-containing protein
PHAVU_004G015500	18631706	XP_007151071	AT5G52460	*EDA41*	*EMBRYO SAC DEVELOPMENT ARREST 41*
PHAVU_004G015600	18631707	XP_007151072	AT3G14470	*LRR4*	*LEUCINE RICH REPEAT PROTEIN 1*
PHAVU_004G015700	18631708	XP_007151073	AT3G14470	*LRR4*	*LEUCINE RICH REPEAT PROTEIN 1*
PHAVU_004G015800	18631709	XP_007151074	AT3G14470	*LRR4*	*LEUCINE RICH REPEAT PROTEIN 1*
PHAVU_004G015900	18631710	XP_007151075	AT3G14470	*LRR4*	*LEUCINE RICH REPEAT PROTEIN 1*
PHAVU_004G016000	18631711	XP_007151076	AT3G14470	*LRR4*	*LEUCINE RICH REPEAT PROTEIN 1*
PHAVU_004G016100	18631712	XP_007151077	AT3G54910		RNI-like superfamily protein
PHAVU_004G0162001	18631713	XP_007151078	AT5G44940		F-box/RNI-like superfamily protein
PHAVU_004G0162000	18631714	XP_007151079	AT5G53640		F-box/FBD/LRR protein
PHAVU_004G016300	18631715	XP_007151080	AT5G53840		F-box/RNI-like/FBD-like domains-containing protein
PHAVU_004G0164001	18631716	XP_007151081	AT1G51370		F-box/RNI-like/FBD-like domains-containing protein
PHAVU_004G0164000	18631717	XP_007151082	AT1G16930		F-box/RNI-like/FBD-like domains-containing protein
PHAVU_004G016500	18631718	XP_007151083	AT3G14470	*LRR4*	*LEUCINE RICH REPEAT PROTEIN 1*
PHAVU_004G0166001	18631719	XP_007151084	AT1G51055		FBD-like domain family protein
PHAVU_004G016500	18631718	XP_007151083	AT3G14470	*LRR4*	*LEUCINE RICH REPEAT PROTEIN 1*
PHAVU_004G0166000	18631720	XP_007151085	AT4G26350		F-box/RNI-like/FBD-like domains-containing protein
PHAVU_004G016700	18631721	XP_007151086	AT3G55250	*PDE329, PSA3*	*PIGMENT DEFECTIVE 329, PHOTOSYSTEM I ASSEMBLY 3*
PHAVU_004G016800	18631722	XP_00715108 7	AT5G40290		HD domain-containing metal-dependent phosphohydrolase family protein
PHAVU_004G016900	18631723	XP_007151088	AT3G22750		Protein kinase superfamily protein
PHAVU_004G017000	18631724	XP_007151089	AT3G01480	*CYP38*	*CYCLOPHILIN 38*
PHAVU_004G017100	18631725	XP_007151090	AT5G62850	*VEX1, SWEET5*	*VEGETATIVE CELL EXPRESSED1*
PHAVU_004G017200	18631726	XP_007151091	AT5G62850	*VEX1, SWEET5*	*VEGETATIVE CELL EXPRESSED1*

The gene ontology analysis uncovered significant biological processes associated with 36 potential candidate genes related to FCR activity under Fe deficiency for the marker DArT-8208605 (Table 3.13). These processes encompassed responses to environmental stimuli and stresses, carbohydrate metabolism, nucleic acid metabolism, protein regulation, and cellular organization and structure maintenance.

Similarly, the gene ontology analysis of 25 potential candidate genes linked to FCR activity under Fe deficiency for the marker DArT-3368423 revealed notable enrichment in biological processes such as ion transport, regulation of plant growth and development, chlorophyll metabolic processes, transcription regulation, phosphorylation, and calcium-mediated signaling (Table 3.14).

Moreover, the gene ontology analysis of 28 potential candidate genes associated with FCR activity in roots under Fe deficiency demonstrated significant enrichment in various biological processes for the marker DArT-8210632 (Table 3.15). These processes included root development, carbohydrate metabolic processes, transcription regulation, defense response, signal transduction, and abscisic acid-activated signaling pathway.

The GWAS analysis focused on root fresh weight identified a single potential candidate gene, although no gene ontology results were obtained specifically for the biological process domain.

Table 3.13 Gene ontology analysis of potential candidate genes from the marker DArT-8208605 (FCR).

GO term accession	GO term name
GO:0000481	maturation of 5S rRNA
GO:0000723	telomere maintenance
GO:0005975	carbohydrate metabolic process
GO:0006139	nucleobase-containing compound metabolic process
GO:0006265	DNA topological change
GO:0006281	DNA repair
GO:0006302	double-strand break repair
GO:0006312	mitotic recombination
GO:0006486	protein glycosylation
GO:0006730	one-carbon metabolic process
GO:0006952	defense response
GO:0006974	cellular response to DNA damage stimulus
GO:0006996	organelle organization
GO:0007049	cell cycle
GO:0007623	circadian rhythm
GO:0008152	metabolic process
GO:0008299	isoprenoid biosynthetic process
GO:0009626	plant-type hypersensitive response
GO:0009737	response to abscisic acid
GO:0010218	response to far red light
GO:0010411	xyloglucan metabolic process
GO:0016117	carotenoid biosynthetic process
GO:0016233	telomere capping
GO:0016567	protein ubiquitination
GO:0019264	glycine biosynthetic process from serine
GO:0031348	negative regulation of defense response
GO:0032508	DNA duplex unwinding
GO:0034337	RNA folding
GO:0035999	tetrahydrofolate interconversion
GO:0042138	meiotic DNA double-strand break formation
GO:0042177	negative regulation of protein catabolic process
GO:0042546	cell wall biogenesis
GO:0044042	glucan metabolic process
GO:0051321	meiotic cell cycle
GO:0071555	cell wall organization

Table 3.14 Gene ontology analysis of potential candidate genes from the marker DArT-3368423 (FCR).

GO term accession	GO term name
GO:0006325	chromatin organization
GO:0006355	regulation of DNA-templated transcription
GO:0006811	monoatomic ion transport
GO:0006813	potassium ion transport
GO:0008150	biological process
GO:0009228	thiamine biosynthetic process
GO:0009229	thiamine diphosphate biosynthetic process
GO:0009908	flower development
GO:0009965	leaf morphogenesis
GO:0015994	chlorophyll metabolic process
GO:0016310	phosphorylation
GO:0019722	calcium-mediated signaling
GO:0033354	chlorophyll cycle
GO:0034220	monoatomic ion transmembrane transport
GO:0036172	thiamine salvage
GO:0040008	regulation of growth
GO:0048316	seed development
GO:0048826	cotyledon morphogenesis
GO:0051781	positive regulation of cell division
GO:0070588	calcium ion transmembrane transport
GO:0071421	manganese ion transmembrane transport

Table 3.15 Gene ontology analysis of potential candidate genes from the marker DArT-8210632 (FCR).

GO term accession	GO term name
GO:0005975	carbohydrate metabolic process
GO:0006004	fucose metabolic process
GO:0006351	DNA-templated transcription
GO:0006355	regulation of DNA-templated transcription
GO:0006390	mitochondrial transcription
GO:0006468	protein phosphorylation
GO:0006952	defense response
GO:0007165	signal transduction
GO:0008150	biological_process
GO:0009451	RNA modification
GO:0009723	response to ethylene
GO:0009738	abscisic acid-activated signaling pathway
GO:0009741	response to brassinosteroid
GO:0009742	brassinosteroid-mediated signaling pathway
GO:0009788	negative regulation of abscisic acid-activated signaling pathway
GO:0009791	post-embryonic development
GO:0009873	ethylene-activated signaling pathway
GO:0010118	stomatal movement
GO:0010214	seed coat development
GO:0010395	rhamnogalacturonan I metabolic process
GO:0010483	pollen tube reception
GO:0016310	phosphorylation
GO:0030308	negative regulation of cell growth
GO:0031425	chloroplast RNA processing
GO:0031426	polycistronic mRNA processing
GO:0031640	killing of cells of another organism
GO:0032922	circadian regulation of gene expression
GO:0045489	pectin biosynthetic process
GO:0046777	protein autophosphorylation
GO:0046854	phosphatidylinositol phosphate biosynthetic process
GO:0048364	root development
GO:0050832	defense response to fungus
GO:0071555	cell wall organization
GO:1902184	negative regulation of shoot apical meristem development

The gene ontology analysis for the 16 potential candidate genes associated with total root area trait under Fe deficiency revealed several significant enrichments in various biological processes, including response to stress, defense response to biotic stress, signal transduction, and protein phosphorylation (Table 3.16).

The gene ontology analysis identified several key biological processes associated with 30 potential candidate genes linked to total root area under Fe deficiency for the marker DArT-8213104 (Table 3.17). These processes include transcription regulation, protein dephosphorylation, protein ubiquitination, phosphoprotein phosphatase activity, and gibberellic acid-mediated signaling pathway.

The gene ontology analysis revealed several significant terms associated with 22 potential candidate genes linked to total root area under Fe deficiency for the marker DArT-8213104, including lateral root morphogenesis, carbohydrate transport, photosystem I and II assembly, and defense response (Table 3.18).

Table 3.16 Gene ontology analysis of potential candidate genes from the marker DArT-8180427 (TRA).

GO term accession	GO term name
GO:0006468	protein phosphorylation
GO:0006950	response to stress
GO:0006952	defense response
GO:0007165	signal transduction
GO:0016310	phosphorylation
GO:0042742	defense response to bacterium
GO:0048544	recognition of pollen
GO:0050832	defense response to fungus
GO:0051707	response to other organism

Table 3.17 Gene ontology analysis of potential candidate genes from the marker DArT-8213104 (TRA).

GO term accession	GO term name
GO:0006355	regulation of DNA-templated transcription
GO:0006417	regulation of translation
GO:0006470	protein dephosphorylation
GO:0008150	biological_process
GO:0009740	gibberellic acid mediated signaling pathway
GO:0010224	response to UV-B
GO:0016567	protein ubiquitination
GO:0031929	TOR signaling
GO:0043666	regulation of phosphoprotein phosphatase activity
GO:0045893	positive regulation of DNA-templated transcription
GO:0071493	cellular response to UV-B

Table 3.18 Gene ontology analysis of potential candidate genes from the marker DArT-3369222 (TRA).

GO term accession	GO term name
GO:0000413	protein peptidyl-prolyl isomerization
GO:0006952	defense response
GO:0008150	biological_process
GO:0008643	carbohydrate transport
GO:0010102	lateral root morphogenesis
GO:0010207	photosystem II assembly
GO:0034219	carbohydrate transmembrane transport
GO:0042549	photosystem II stabilization
GO:0048564	photosystem I assembly
GO:0051260	protein homooligomerization
GO:0051707	response to other organism

CHAPTER 4

DISCUSSION

Nutrient absorption and processing are fundamental processes for all living organisms, including animals and humans, crucial for obtaining energy and essential nutrients vital for growth, tissue repair, and the regulation of essential bodily functions. These nutrients encompass proteins, lipids, carbohydrates, vitamins, and minerals, sourced from various foods such as fruits, vegetables, grains, meats, and dairy products. Insufficient intake of these nutrients can significantly impact immunity and growth, underscoring the importance of a balanced diet for overall health and well-being. Similarly, plants, as living organisms, depend on essential nutrients to thrive and withstand environmental challenges. Among these nutrients, Fe holds particular significance due to its crucial role in numerous physiological processes. However, plants often encounter difficulties in accessing adequate Fe from the soil, leading to conditions of Fe deficiency. Symptoms of Fe deficiency in plants manifest as chlorosis, characterized by yellowing of leaves due to reduced chlorophyll production. This impedes photosynthesis and overall plant growth, ultimately resulting in diminished crop yields and economic losses. Despite these challenges, plants have evolved sophisticated mechanisms to combat Fe deficiency and sustain optimal growth and development. These mechanisms involve the secretion of chelating agents such as coumarins and phenolics, which enhance Fe solubility and uptake from the rhizosphere. Additionally, plants employ specialized Fe transporters to facilitate the absorption and translocation of Fe within the plant. Understanding these mechanisms of Fe acquisition and homeostasis is essential for developing strategies to enhance crop resilience to Fe deficiency and thereby improve agricultural productivity.

Iron deficiency tolerance (IDC) refers to a plant's ability to withstand Fe deficiency stress without compromising yield or overall health. The term "susceptible" is often

used to describe interactions with biotic diseases, which can be misleading in this context. While "sensitivity" to IDC is sometimes used, it is more appropriate for describing reactions to nutrients or substances harmful in excess, such as salt or aluminum in soybeans. Therefore, it is more accurate to describe a soybean genotype's "resistance" to IDC, indicating an active response to Fe stress with varying degrees of severity (Merry et al., 2022).

In our study, Fe deficiency stress led to a reduction in all examined traits except for FCR activity. These traits encompass diverse above-soil characteristics and several root attributes. Collectively, these findings indicate that Fe deficiency treatment resulted in a comparable decrease in both above-soil and root traits.

In most crops, symptoms of Fe chlorosis typically appear during the early stages of growth. Newly formed leaves develop interveinal chlorosis, where the areas between the veins turn light green and eventually yellow as the deficiency progresses. Except in severe cases, where the entire leaf becomes white and translucent and necrosis results in dead brown tissue, the veins usually remain green (Nsiri & Krouma, 2023).

In our study, the 13-day treatment period and emphasis on measurements from the first trifoliate were strategic choices aimed at capturing early responses to Fe deficiency stress while ensuring consistent and comparable data across genotypes. This approach provided valuable insights into the initial adaptive mechanisms and physiological changes in common bean plants under Fe deficiency stress, contributing to a comprehensive understanding of their tolerance mechanisms.

Prior research has utilized SPAD meters as a reliable measure of chlorophyll content and chlorosis severity, as SPAD values are positively correlated with total chlorophyll content (Ruiz-Espinoza et al., 2010; Vasconcelos & Grusak, 2014; Yamamoto et al., 2002). Studies have shown that different common bean cultivars exhibit varying degrees of chlorosis under Fe deficiency, confirmed by SPAD index and chlorophyll pigment measurements (Krouma et al., 2003; Nsiri & Krouma, 2023). In line with prior studies, Fe deficiency treatment resulted in a significantly reduced total chlorophyll content (21.8%) and SPAD values (10.2%) across various

common bean accessions (Table 3.1). This reduction in these two parameters was also considered indicative of sensitivity to Fe deficiency. Consistent with studies conducted in other plant species, there was a strong positive correlation observed between these two values (r=0.64, Table 3.3).

Without sufficient Fe, chlorophyll production is impaired, leading to leaf chlorosis and reduced photosynthetic efficiency. With less chlorophyll, the plant's photosynthetic capability is compromised, reducing the overall energy available for growth, including the development of new leaves and the expansion of existing ones. Fe deficiency often results in stunted overall growth, as the plant reallocates resources to essential survival processes, often at the expense of leaf growth. New leaves that develop under Fe-deficient conditions tend to be smaller and paler compared to those on Fe-sufficient plants (*Marschner's Mineral Nutrition of Higher Plants*, 2012). Previous studies have consistently shown that Fe deficiency leads to reduced crop yield in common bean. Research has demonstrated a marked decrease in biomass production among common bean cultivars under Fe deficiency (Idoudi et al., 2024; Krouma et al., 2003).

In the present study, common bean cultivars exhibited significant limitations in root and leaf growth due to Fe deficiency. This was evidenced by significant reductions in leaf area (21.5%), fresh and dry weights of leaves (27.1% and 21.3%, respectively), as well as fresh and dry weights of roots (39.2% and 26.5%, respectively) in response to Fe deficiency (Table 3.1). These traits also had strong possitive correlations with each other, such as leaf fresh and dry weight (r=0.97), leaf fresh and dry weigth and leaf area (r=0.97), root fresh and dry weight (r=0.92), root fresh and dry weight and leaf area (r=0.71 and r=0.65, respectively) (Table 3.3). Therefore, these traits were also considered indicative of sensitivity to Fe deficiency. The leaves of 5 most tolerant and 5 most sensitive accessions to Fe deficiency were visualized in Figure 3.3 and the roots of 2 most tolerant and 2 most sensitive accessions to Fe deficiency were visualized in Figure C.1.

All tissues in common beans undergo physiological changes due to Fe deficiency; however, nearly all phenotyping of this trait to date has focused on leaf chlorosis. This narrow perspective may explain the prevalent use of foliar Fe treatments, which typically fail to restore yield but may alleviate some chlorosis. Other plant tissues may remain Fe-stressed because most foliar-applied Fe sources are not translocated from the leaves. This issue is particularly significant if foliar-supplied Fe is retained in the leaves rather than being transported to the roots, as a substantial Fe requirement is essential for proper nitrogen fixation in the nodules. Given that common seeds contain approximately 40% protein, yield loss is likely if the Fe deficiency in the nodules persists, even if the leaves show recovery, which highlights the importance of studying root characteristics (Merry et al., 2022).

Plants have developed a variety of strategies to absorb Fe in response to surroundings low in Fe, including altering the morphology of roots and improving Fe uptake by regulating the expression of genes associated with Fe. Depending on the type of plant, roots undergo different morphological and physiological alterations as a result of Fe shortage. With the exception of graminaceous species, Fe deficiency is associated with reduced root extension and increased root hair development in dicotyledonous and monocotyledonous plant species (*Marschner's Mineral Nutrition of Higher Plants*, 2012).

For over a century, the scientific community has focused on studying plant root systems due to their crucial roles in anchoring plants, absorbing water and nutrients, and shaping soil biology. However, roots remain the least understood organ of plants, primarily because their subsurface growth is concealed by the dense soil matrix. To study roots, researchers typically resort to excavation or soil coring, followed by labor-intensive washing processes, due to their subterranean existence. Nevertheless, compelling evidence suggests that different root characteristics directly influence activities such as nitrogen uptake and soil reinforcement, highlighting the significant benefits of measuring and understanding root structures (Seethepalli et al., 2021).

In this study, a hydroponics system was utilized to investigate root system architecture and how it is affected by Fe deficiency treatment. This approach allowed for a controlled environment where root development and responses to Fe deficiency could be observed and analyzed without the challenges posed by soil interference. By focusing on root architecture within a hydroponic setup, insights into how roots adapt and respond to Fe deficiency stress were aimed to be gained, contributing to a deeper understanding of plant physiology under such conditions.

Root characteristics play a crucial role in a plant's response to Fe deficiency, with various adaptations observed between sensitive and tolerant genotypes. Generally, under Fe deficiency, sensitive plants often exhibit shorter shoot lengths, although this observation can be controversial and may vary across different species and environmental conditions. The contrasting root adaptations provide insights into the mechanisms plants use to cope with Fe scarcity.

In tolerant plants, root systems tend to be more extensive, featuring increased root length, higher root hair density, greater root tip number, and expanded root surface area. These adaptations enhance the plant's ability to explore a larger volume of soil, thereby increasing the likelihood of encountering and absorbing the limited available Fe. The longer roots and denser root hairs create more contact points with the soil, facilitating better Fe acquisition through improved access to soil Fe pools. This strategy is particularly effective for plants growing in Fe-deficient conditions, where Fe availability is limited and patchy (Zocchi et al., 2007).

Conversely, some studies suggest that sensitive plants may also develop longer roots under Fe deficiency. This seemingly paradoxical response can be attributed to the lack of effective Fe acquisition mechanisms, necessitating an increased root length to search for Fe more extensively. In this scenario, the longer roots are a compensatory mechanism, driven by the plant's inability to efficiently absorb Fe through other means. Consequently, these plants invest more in root growth at the expense of other physiological processes, potentially leading to suboptimal overall growth and productivity (Jiménez et al., 2019).

Similarly, root hair density, root tip number, and root surface area can vary significantly between sensitive and tolerant plants. Tolerant plants typically exhibit increased root hair density and root tip number, which enhance their ability to mobilize and absorb Fe from the soil. Root hairs secrete organic acids and other compounds that can solubilize Fe, making them more accessible for uptake (Wei Jin et al., 2008). In contrast, sensitive plants, lacking these efficient mechanisms, may also show increased root hair density and root tip number as a compensatory response, although this may not fully offset their overall inefficiency in Fe uptake.

The adaptability of the root system's response appears to provide the adaptive advantage of utilizing Fe patches located away in soils under moderate Fe deficiency; under severe Fe deficiency, on the other hand, acclimation proceeds through a growth-dependent pathway that momentarily stops root elongation and number in order to lower nutrient demand (G. Li et al., 2016).

These differing root adaptations underscore the complexity of plant responses to Fe deficiency. While tolerant plants effectively enhance their root systems to optimize Fe uptake, sensitive plants may exhibit similar morphological changes as a desperate strategy to cope with Fe scarcity. Understanding these mechanisms provides valuable insights into breeding and selecting crop varieties with enhanced tolerance to Fe deficiency, aiming to improve yield and quality in Fe-limited environments.

In our study, a notable trend emerged where most accessions exhibited a decrease in root length (51.6%) and other related root traits under Fe deficiency conditions (Table 3.1). However, intriguingly, among the accessions that appeared tolerant based on other physiological traits, there was a distinct pattern of developing better root systems characterized by longer roots and enhanced root traits, compared to the most sensitive accessions. This observation led us to consider longer roots as a potential indicator of tolerance in this study. The presence of longer roots in these tolerant accessions signifies an adaptive response aimed at improving Fe uptake efficiency and overall plant resilience under Fe deficiency stress. This finding emphasizes the importance of root morphology and adaptation strategies in

determining a plant's tolerance to Fe deficiency and highlights the complex interplay between above-ground and below-ground traits in response to nutrient stress. As expected, there were strong correlations ($r>0.70$) between all root characteristics studied (Table 3.3). These results suggest that besides root length, other root traits such as maximum root number, root tip number total root length, main root length; total root area, and total root volume can also be regarded as key parameters reflecting sensitivity to Fe deficiency.

Another trait investigated in this study was root FCR activity. Previous studies have demonstrated a notable increase in Fe-chelate reductase (FCR) activity over time in plants subjected to Fe deficiency (Krouma et al., 2003; Nsiri & Krouma, 2023). Similarly, in most of the common bean cultivars used in this study, Fe deficiency enhanced the root FCR activity significantly (16.6%, Table 3.1). FCR activity did not show any significant correlation with any other traits (Table 3.3). A prior study revealed no correlations between SPAD values and Fe-chelate reductase (FCR) activity, a finding that aligns with the results of this thesis study (Vasconcelos & Grusak, 2014). Since root and leaf responses to Fe deficiency may be triggered by different signaling pathways, the importance of translocation between organs becomes especially significant. This lack of significant correlation between root FCR activity and leaf SPAD or chlorophyll content values suggests distinct regulatory mechanisms operating in different plant parts.

Some accessions exhibited high FCR activity, indicating their efficient ability to reduce ferric Fe to ferrous Fe and facilitate Fe uptake without extensive root growth. These plants seemed to prioritize FCR activity as a primary mechanism for Fe acquisition, reducing the need for extensive root development. On the other hand, there were accessions with lower FCR activity but exhibited longer roots and enhanced root traits. These plants appeared to rely more on root elongation and exploration to enhance Fe uptake, compensating for lower FCR activity by increasing the surface area for nutrient absorption. Interestingly, some accessions showed a combination of both high FCR activity and extensive root growth, suggesting a synergistic approach where both mechanisms work in tandem to ensure

efficient Fe acquisition under Fe deficiency conditions. This diversity in strategies underscores the complexity of plant responses to Fe deficiency and highlights the multifaceted nature of tolerance mechanisms involving both biochemical and morphological adaptations.

Given the normal distribution of the data sets, there was no necessity to apply any additional transformations or normalization techniques. This statistical validation ensures the reliability and appropriateness of parametric analyses applied to the data, enhancing the robustness of the findings and conclusions drawn from the study.

The non-significant p-values observed in the ANOVA results for treatments in fresh weight ratio, treatments and genotype x treatment interaction in dry weight ratio, and genotype x treatment interaction in FCR; which indicate several interesting aspects of the study. Firstly, the lack of significant differences in fresh weight ratio and dry weight ratio between genotypes and treatments suggests a potential level of genetic homogeneity or limited genetic variability in the specific traits under investigation. This could imply that the genotypes used in this study exhibited similar responses to the applied treatments, highlighting the importance of understanding genetic diversity in stress responses. Secondly, the consistent stress response observed across genotypes, as indicated by the non-significant genotype x treatment interaction, may reflect shared physiological mechanisms or genetic backgrounds influencing the response to Fe deficiency stress. Furthermore, the non-significant findings could also be influenced by factors such as sample size and variability within the dataset, emphasizing the need for larger sample sizes and increased data variability in future studies to enhance the statistical power and robustness of the results.

In general, the violin plots provided a visual representation of the distribution of various traits under both control and Fe deficiency conditions. The plots revealed distinct patterns, with some traits exhibiting more pronounced outliers in control conditions compared to Fe deficiency conditions. This suggests that Fe deficiency

may contribute to a more standardized distribution of certain traits, while control conditions often result in a wider range of values, leading to the presence of outliers.

The correlation analysis (Table 3.3) revealed intriguing relationships among the examined traits, shedding light on the interconnectedness of plant responses to Fe deficiency stress. It's worth mentioning the strong positive linear correlation found between total chlorophyll content and SPAD value ($r = 0.64$), which underscores the effectiveness of SPAD as a surrogate for assessing chlorophyll content. Leaf area exhibited robust correlations with various morphological parameters, demonstrating its crucial role in plant growth under stress conditions. Particularly high correlations were found between leaf area and leaf fresh weight ($r = 0.97$) as well as leaf area and leaf dry weight ($r = 0.97$), underscoring the direct impact of leaf area on biomass accumulation. Furthermore, leaf area showed strong correlations with root parameters, such as root fresh weight ($r = 0.71$) and root dry weight ($r = 0.65$), emphasizing the interconnectedness between above-ground and below-ground biomass allocation strategies in response to Fe deficiency stress. Noteworthy correlations were also observed between root fresh weight and root dry weight ($r = 0.92$), indicating a consistent relationship between water content and structural biomass in the root system. Additionally, strong correlations were evident between root fresh weight and maximum root number ($r = 0.72$) as well as root fresh weight and root tip number ($r = 0.76$), highlighting the importance of root biomass and architecture in nutrient acquisition and stress tolerance. Interestingly, no significant correlations were found between FCR and other investigated traits, suggesting a complex and multifaceted nature of factors influencing ferric chelate reductase activity under Fe deficiency stress conditions.

The most common strategy for preventing Fe deficiency chlorosis (IDC) in crops is through cultivar selection, making it essential to have effective screening tools and comprehensive knowledge of the most tolerant cultivars (Vasconcelos & Grusak, 2014).

Plants have developed various mechanisms to tolerate Fe deficiency, which can involve either shoot/leaf characteristics, root characteristics, or both. Some plants manage Fe deficiency by maintaining chlorophyll production and photosynthetic efficiency, showing less leaf chlorosis and effectively redistributing Fe from older to younger tissues, allowing them to sustain growth and productivity despite low Fe availability. Other plants enhance root mechanisms, such as increasing root length and root hair density, to mobilize and absorb Fe more efficiently. Additionally, some plants release organic compounds from their roots to solubilize Fe in the soil. Plants with both shoot and root tolerance mechanisms can effectively cope with Fe deficiency by combining efficient Fe uptake with strategies that minimize the physiological impact on growth and leaves (Kobayashi & Nishizawa, 2012; Zhang et al., 2019). In light of these mechanisms, several common bean accessions were identified as the most tolerant to Fe deficiency in this study. Two notable examples of sensitive accessions were Bitlis-35 and Hakkari-39. Both Bitlis-35 and Hakkari-39 showed sensitivity in terms of root characteristics, such as root dry weight and FCR activity, but maintained chlorophyll content and SPAD values, with no visible leaf chlorosis. This suggests efficient internal Fe recycling mechanisms, redistributing Fe from older tissues to younger, actively growing leaves. For efficient Fe transport to young leaves which helps prevent chlorosis, NAS genes that chelate Fe and facilitate its transport within the plant might have crucial roles. Similarly, *OPT* transporters such as *OPT3*, are involved in the long-distance transport of Fe, ensuring that young leaves receive adequate Fe to avoid chlorosis. However, the limited root biomass and FCR activity in these accessions imply a compromised ability to mobilize and absorb Fe from the soil, resulting in overall sensitivity to Fe deficiency. The likely molecular mechanisms involved may include insufficient expression or activity of root Fe uptake genes such as *IRT1* and *FRO2* (Zhang et al., 2019). Sensitivity in Bingol-1 was observed in chlorophyll content, leaf area, leaf dry weight, root dry weight, main root length, and total root volume. The visible chlorosis suggests that Bingol-1 has a limited capacity to maintain chlorophyll synthesis and photosynthetic efficiency under Fe deficiency. This could be due to

reduced activity or expression of *FRO2* and Fe transporters in the roots, leading to inadequate Fe uptake and transport to the shoots. Nigde-Derinkuyu demonstrated a unique response to Fe deficiency by maintaining high chlorophyll content and SPAD values while showing reduced leaf area. This suggests that during Fe deficiency, these plants prioritize photosynthesis efficiency over expansive leaf growth. Maintaining chlorophyll content is crucial for sustaining photosynthetic activity, which is essential for energy production and overall plant health. By allocating more Fe towards chlorophyll synthesis rather than expanding leaf area, Nigde-Derinkuyu plants ensure that the existing leaves can effectively capture light and perform photosynthesis, thus optimizing their energy production even under stress conditions. High expression levels of genes related to chlorophyll synthesis and photosynthetic machinery, such as *CHLH (Magnesium Chelatase H Subunit)* and *CAB (Chlorophyll A/B Binding Protein),* might be upregulated in Nigde-Derinkuyu under Fe deficiency, allowing these plants to sustain photosynthetic activity despite limited Fe availability (Sun & Shen, 2024). Nigde-Derinkuyu also exhibited tolerance in root characteristics, which might involve enhanced expression of genes related to root growth and Fe uptake. The apparent prioritization of maintaining chlorophyll content over leaf area expansion could be a strategic adaptation, regulated by signaling pathways involving transcription factors such as *FIT (FER-Like Iron Deficiency-Induced Transcription Factor)* and *PYE (POPEYE).* These factors modulate the expression of Fe uptake and homeostasis genes, ensuring that the limited Fe is utilized where it is most needed for survival. Elazig accession exhibited tolerance in several root characteristics but not leaf area. The reduced leaf area under Fe deficiency indicates some limitations in shoot growth. However, the robust root system suggests efficient Fe acquisition mechanisms, likely involving increased root hair density and activity of Fe uptake genes. This accession may rely more on root adaptations to cope with Fe deficiency. Both Duzce-9 and Nigde-Dermason accessions exhibited tolerance in terms of leaf area and several root characteristics. The maintained leaf biomass indicates effective Fe transport and utilization mechanisms within the shoots, possibly involving efficient Fe chelators

and transporters. The robust root system capable of efficient Fe acquisition likely involves upregulated expression of Fe uptake genes such as *IRT1* and *FRO2*. These accessions combine efficient Fe uptake with strategies that minimize the physiological impact of Fe deficiency on growth and leaves. This diversity in tolerance strategies among the accessions underscores the complex nature of plant responses to Fe deficiency.

The common bean genotypes examined in this study originate from various regions of Türkiye, each with distinct soil properties (Berberoglu et al., 2020; Kük & Burgess, 2010). For instance, Bitlis, Hakkari, and Bingol share common characteristics that could contribute to the sensitivity of common bean genotypes to Fe deficiency. These regions, located in the eastern part of Türkiye, are characterized by challenging agricultural conditions, including mountainous terrain that results in rocky, shallow, and less fertile soils. The soils are often calcareous, with high lime content that leads to poor Fe availability due to high pH conditions, reducing Fe solubility and making it difficult for plants to absorb the necessary Fe. Additionally, these areas experience harsh climatic conditions, including cold winters and hot summers, which can further stress plants and exacerbate nutrient deficiencies. The limited agricultural infrastructure in these regions may also affect the ability to manage soil fertility and address nutrient deficiencies effectively. These factors collectively suggest that the challenging soil and environmental conditions in Bitlis, Hakkari, and Bingol might contribute to the sensitivity of common bean genotypes to Fe deficiency, as the plants are already under significant stress from their growing environment. Nigde, Duzce, and Elazig share several common characteristics that could contribute to the tolerance of common bean genotypes to Fe deficiency. These regions are known for more favorable agricultural conditions compared to the eastern parts of Türkiye. Nigde and Elazig, located in Central and Eastern Anatolia respectively, have relatively fertile soils that, while still calcareous, often have better nutrient management and irrigation practices, which can mitigate the effects of high pH on Fe availability. Duzce, located in the northwestern part of Türkiye, benefits from a more temperate climate and richer, more fertile soils due to its proximity to

the Black Sea. This region's soils tend to have better organic matter content and improved moisture retention, which can enhance nutrient uptake efficiency, including Fe. Furthermore, these areas generally have better-developed agricultural infrastructure, allowing for more effective management of soil fertility and the implementation of practices to correct nutrient deficiencies. These favorable conditions in Nigde, Duzce, and Elazig likely contribute to the higher tolerance of common bean genotypes to Fe deficiency observed in these regions. In conclusion, the calcareous and variable nature of soils, along with the presence of other abiotic stresses due to geographical differences, such as drought, cold or heat stress, might play crucial roles in the Fe deficiency tolerance of common bean genotypes in different regions of Türkiye. Taken together, this geographical variation in Fe deficiency tolerance among genotypes highlights the significant physiological responses of genetic variability to pedo-climatic factors.

Rhizosphere acidification is a critical aspect of plant response to nutrient stress, especially under Fe deficiency conditions. It involves the secretion of organic acids such as citrate and malate by plant roots, which play a vital role in enhancing Fe uptake from the soil. These acids effectively solubilize Fe, making it more available for plant uptake. Additionally, the pH of the root environment is crucial for nutrient availability and uptake. Fe availability, for instance, is significantly influenced by soil pH, with acidic conditions generally favoring Fe solubility. The pH of the root zone also affects the activity of enzymes involved in nutrient uptake processes (de Vos et al., 1986). Therefore, understanding and managing root zone pH is essential for optimizing nutrient uptake efficiency and overall plant health. Therefore, monitoring rhizosphere acidification provides insights into the efficiency of Fe acquisition strategies employed by plants, shedding light on their adaptation mechanisms to Fe-deficient environments. In this study, one notable challenge was the inability to assess rhizosphere acidification due to the rapid growth and size of the common bean plants within the experimental period. The plants became excessively large, making it impractical to separate them from the hydroponic system without causing damage. Even if separation were possible, their towering height

rendered them unstable. Despite the inability to measure rhizosphere acidification directly in this study, the focus on root and above-soil characteristics still yielded valuable insights into the response of common bean genotypes to Fe deficiency stress. Future studies could explore methods to overcome the challenges posed by plant size in hydroponic systems, allowing for a more comprehensive assessment of plant responses, including rhizosphere acidification dynamics.

In the Manhattan plot, it can be seen that there were two SNPs, on chromosome 2 and chromosome 7, that were significantly associated with FCR activity. On chromosome 4, chromosome 7, and chromosome 11, there were three significant SNPs associated with TRA. Finally, on chromosome 4, there was one SNP that was significantly associated with RFW.

In this study, the potential candidate genes associated with FCR activity in roots, or total root area under Fe deficiency displayed diverse functions encompassing abiotic and biotic stress responses, plant growth and development, as well as metabolism and biosynthesis. Additionally, numerous uncharacterized genes were identified, representing enzyme superfamilies, protein families involved in nucleic acid processing and regulation, protein modification, signaling pathways, cellular processes, and structural proteins. Gene ontology analysis was conducted to identify and categorize the biological processes associated with candidate genes linked to traits of interest, particularly FCR activity in roots, and total root area under Fe deficiency. Gene ontology analysis results (Table 3.13, Table 3.14, Table 3.15, Table 3.16, Table 3.17 and Table 3.18) revealed various biological processes associated with the potential candidate genes identified from the significant markers identified in this study. These GO results further helped to focus on the potential candidate genes that are related to abiotic stress response, ion transport, and root growth.

Notable potential candidate genes identified from the marker DArT-8208605 (FCR) can be grouped into two categories: genes related to root growth, and genes related to stress response. The genes related to root growth, such as *XYLOGLUCAN ENDOTRANSGLYCOSYLASE 7 (XTR7)* and *BAK1-ASSOCIATING RECEPTOR-*

LIKE KINASE 1 (BARK1) might play crucial roles in regulation of FCR activity in roots by influencing the overall architecture of the root system. This enhancement might lead to increased root surface area, stimulated root hair development and lateral root formation, which can contribute to a more extensive and efficient root network, optimizing the plant's ability to explore the soil for Fe. Consequently, these changes create additional sites for FCR activity, thereby bolstering the plant's ability to acquire Fe under deficient conditions. In addition, hemicellulose xyloglucan, which is an important component of the cell walls of vascular plants, plays a crucial role in controlling the cellulose microfibrils' ability to loosen and tighten, which allows for changes in cell shape throughout development and differentiation. By ensuring that cells may maintain their ultimate form after maturation, this mechanism maximizes structural integrity and functionality (Wan et al., 2018). Integrating genetic insights with the fundamental roles of xyloglucan sheds light on the intricate mechanisms governing root architecture and nutrient acquisition strategies under challenging environmental conditions like Fe deficiency. These candidate genes require further study to understand their potential relationship with Fe deficiency responses of plants in terms of root growth and development. The other notable candidate gene, which was related to stress response, was *PHYTOCYSTATIN 2 (CYS2)*. Phytocystatins belong to a superfamily of Cys proteases widely distributed among eukaryotes. They are are well known protease inhibitors that are involved in protective mechanisms of plants to biotic and abiotic stress factors (Mangena, 2020). A prior study focused on iTRAQ protein profile analysis of *Arabidopsis* roots found that two out of seven *Arabidopsis* phytocystatins, *CYS1* and *CYS2*, were up-regulated upon Fe deficiency (Lan et al., 2011). Besides, in another study, it was shown that both genes were up-regulated in response to various abiotic stresses such as drought, heat and wounding stress, indicating a possible function of *CYS1* and *CYS2* in Fe deficiency signaling or in the control of root development in response to environmental cues (Hwang et al., 2010).

One notable potential candidate genes identified from the marker DArT-3368423 (FCR) was a metal transporter, *CHLOROPLAST MANGANESE TRANSPORTER 1*

(CMT1). Manganese (Mn) transporters might be important in the context of Fe deficiency because Mn and Fe often utilize similar transport mechanisms, and some transporters can facilitate the movement of both metals, due to structural and chemical similarities of Mn and Fe. Additionally, Mn transporters might directly influence Fe homeostasis by regulating processes that are critical for Fe uptake and metabolism, thereby contributing to the plant's ability to cope with Fe deficiency(Höller et al., 2022). For example, the *Vacuolar Manganese Transporter (MTP8)* acts as a critical determinant for the tolerance to Fe deficiency-induced chlorosis. In a previous study, it was shown that *mtp8* mutants were hypersensitive to Fe deficiency when there is Mn present in the medium, and the diminished uptake of Fe by *mtp8* mutants in this medium was caused by an impaired ability to boost the FCR activity, so similar mechanisms might be valid for *CMT1* as well (Eroglu et al., 2017). Further studies are required to understand if *CMT1* has a role in Fe deficiency responses in common bean roots through FCR activity.

Notable potential candidate genes identified from the marker DArT-8210632 (FCR) were related to root growth, such as *ROOT INITIATION DEFECTIVE 3 (RID3)*, *ROOT MERISTEM GROWTH FACTOR 2 (RGF2),* and *FERONIA (FER).* From these genes, *FERONIA (FER)* emerges as a compelling candidate for FCR activity based on its diverse roles in root biology and stress response. *FER* encodes a synergid-expressed, plasma-membrane localized receptor-like kinase, which has several important functions including plant growth and development and biotic stress responses (Ji et al., 2020). Besides, a previous study showed that FER plays a crucial role in root hair (RH) development by modulating protein synthesis through the extracellular peptide(Zhu et al., 2020). Another previous study demonstrated that low nitrate conditions trigger RH elongation response through activation of the FERONIA by triggering the activation of nutrient sensing TOR Complex. The study also showed that FER is required to perceive limited nutrient availability (Pacheco et al., 2023). Notably, studies have shown that FER contributes to Cd tolerance by regulating genes involved in Fe uptake, such as *IRT1, bHLH38, NRAMP1, NRAMP3, FRO2,* and *FIT*, thereby reducing Cd-induced stress and improving overall plant

resilience to heavy metal toxicity (Zhou et al., 2021). The multifaceted functions of *FER* related to root hair growth, nutrient sensing, and Cd tolerance by regulating Fe uptake genes underscore its potential significance in FCR activity and its broader implications in plant adaptation to environmental challenges.

There is only one potential candidate gene related to fresh root weight under Fe deficiency, and it belongs to the Ubiquitin carboxyl-terminal hydrolase family. Ubiquitin-mediated processes are known to play crucial roles in plant development, stress responses, and nutrient homeostasis (Sharma et al., 2016). This finding suggests a potential link between the ubiquitin pathway and root growth under Fe deficiency stress, highlighting the importance of post-translational regulation in plant adaptive responses.

Notable potential candidate genes identified from the marker DArT- 8213104 (TRA) were *ALTERED XYLOGLUCAN 8 (AXY8),* which is related to root growth, and *PUMILIO 8 (PUM8),* which was a gene involved in the regulation of translation (Günl et al., 2011; Huh, 2021). Pumilio proteins are a class of RNA-binding proteins harboring Puf domains. Their roles are mostly unknown, but, recently, it was reported that Arabidopsis Pumilio proteins (APUM) are involved in biotic and abiotic stress and development via translational modification (Abbasi et al., 2011). In a previous study investigating the role of miRNAs and their target genes related to Fe-deficiency, *PUM* was identified as the predicted target gene of *miR395,* which was down-regulated under Fe-deficiency (Jin et al., 2021). miRNAs negatively regulate eukaryotes gene expression at post-transcriptional level via cleavage or/and translational inhibition of targeting mRNA. *PUM8* might have a role in regulation of Fe deficiency responses in roots, through miRNAs.

All of the notable candidate genes related to root FCR activity, root fresh weight and total root area under iron deficiency need further investigation to understand their potential roles in iron deficiency homeostasis in plants, and the identification of these candidate genes can be a starting point for future iron deficiency studies.

CHAPTER 5

CONCLUSIONS

In conclusion, this thesis provides a comprehensive analysis of the genetic and phenotypic responses of common bean genotypes to Fe deficiency. By utilizing a hydroponic system to simulate Fe-deficient conditions, we were able to identify key root traits linked to Fe deficiency tolerance. The application of GWAS using 7900 DArT-seq markers allowed for the identification of seven significant markers associated with FCR activity in roots, root fresh weight, and total root area. From these significant markers, a total of 158 potential candidate genes were identified related to root FCR activity, root fresh weight, and total root area under Fe deficiency. The gene ontology analysis of candidate genes near these markers revealed several critical biological processes involved in Fe homeostasis. After a detailed review of the literature, it was seen that some of these potential candidate genes might have roles in iron deficiency homeostasis. These findings not only enhance our understanding of the genetic mechanisms underlying Fe deficiency tolerance in common beans but also provide a valuable resource for breeding programs aimed at developing more resilient cultivars.

The identification of the most tolerant and sensitive accessions further underscores the potential for genetic improvement and offers a pathway towards mitigating the impacts of Fe deficiency in common bean cultivation. As future prospects, these potential candidate genes can be further characterized to deepen our understanding of the important pathways involved in Fe deficiency homeostasis in common beans. Future research should focus on validating these candidate genes and exploring their functional roles to fully harness their potential in improving Fe deficiency tolerance in common beans.

REFERENCES

Abbasi, N., Park, Y.-I., & Choi, S.-B. (2011). Pumilio Puf domain RNA-binding proteins in Arabidopsis. *Plant Signaling & Behavior*, *6*(3), 364–368. https://doi.org/10.4161/psb.6.3.14380

Adu, B. G., Akromah, R., Amoah, S., Nyadanu, D., Yeboah, A., Aboagye, L. M., Amoah, R. A., & Owusu, E. G. (2021). High-density DArT-based SilicoDArT and SNP markers for genetic diversity and population structure studies in cassava (Manihot esculenta Crantz). *PLOS ONE*, *16*(7), e0255290. https://doi.org/10.1371/journal.pone.0255290

Allen, L. H. (2013). Legumes. In *Encyclopedia of Human Nutrition* (pp. 74–79). Elsevier. https://doi.org/10.1016/B978-0-12-375083-9.00170-7

Altschul, S. F., Gish, W., Miller, W., Myers, E. W., & Lipman, D. J. (1990). Basic local alignment search tool. *Journal of Molecular Biology*, *215*(3), 403–410. https://doi.org/10.1016/S0022-2836(05)80360-2

BALOCH, F. S., & NADEEM, M. A. (2022). Unlocking the genomic regions associated with seed protein contents in Turkishcommon bean germplasm through genome-wide association study. *Turkish Journal of Agriculture and Forestry*. https://doi.org/10.3906/tar-2104-63

Baloch, F. S., Nadeem, M. A., Sönmez, F., Habyarimana, E., Mustafa, Z., Karaköy, T., Cömertpay, G., Alsaleh, A., Çiftçi, V., Sun, S., Chung, G., & Chung, Y. S. (2022a). Magnesium- a Forgotten Element: Phenotypic Variation and Genome Wide Association Study in Turkish Common Bean Germplasm. *Frontiers in Genetics*, *13*. https://doi.org/10.3389/fgene.2022.848663

Baloch, F. S., Nadeem, M. A., Sönmez, F., Habyarimana, E., Mustafa, Z., Karaköy, T., Cömertpay, G., Alsaleh, A., Çiftçi, V., Sun, S., Chung, G., & Chung, Y. S. (2022b). Magnesium- a Forgotten Element: Phenotypic Variation and Genome

Wide Association Study in Turkish Common Bean Germplasm. *Frontiers in Genetics*, *13*. https://doi.org/10.3389/fgene.2022.848663

Berberoglu, S., Cilek, A., Kirkby, M., Irvine, B., & Donmez, C. (2020). Spatial and temporal evaluation of soil erosion in Turkey under climate change scenarios using the Pan-European Soil Erosion Risk Assessment (PESERA) model. *Environmental Monitoring and Assessment*, *192*(8), 491. https://doi.org/10.1007/s10661-020-08429-5

Brachi, B., Morris, G. P., & Borevitz, J. O. (2011). Genome-wide association studies in plants: the missing heritability is in the field. *Genome Biology*, *12*(10), 232. https://doi.org/10.1186/gb-2011-12-10-232

Castro-Guerrero, N. A., Isidra-Arellano, M. C., Mendoza-Cozatl, D. G., & Valdés-López, O. (2016). Common Bean: A Legume Model on the Rise for Unraveling Responses and Adaptations to Iron, Zinc, and Phosphate Deficiencies. *Frontiers in Plant Science*, *7*. https://doi.org/10.3389/fpls.2016.00600

Chacón S, M. I., Pickersgill, B., & Debouck, D. G. (2005). Domestication patterns in common bean (Phaseolus vulgaris L.) and the origin of the Mesoamerican and Andean cultivated races. *Theoretical and Applied Genetics*, *110*(3), 432–444. https://doi.org/10.1007/s00122-004-1842-2

Clark, S. F. (2008). Iron Deficiency Anemia. *Nutrition in Clinical Practice*, *23*(2), 128–141. https://doi.org/10.1177/0884533608314536

Colangelo, E. P., & Guerinot, M. Lou. (2004). The Essential Basic Helix-Loop-Helix Protein FIT1 Is Required for the Iron Deficiency Response. *The Plant Cell*, *16*(12), 3400–3412. https://doi.org/10.1105/tpc.104.024315

Connolly, E. L., & Guerinot, M. (2002). Iron stress in plants. *Genome Biology*, *3*(8), reviews1024.1. https://doi.org/10.1186/gb-2002-3-8-reviews1024

Connorton, J. M., Balk, J., & Rodríguez-Celma, J. (2017). Iron homeostasis in plants – a brief overview. *Metallomics*, *9*(7), 813–823. https://doi.org/10.1039/C7MT00136C

de Vos, C. R., Lubberding, H. J., & Bienfait, H. F. (1986). Rhizosphere Acidification as a Response to Iron Deficiency in Bean Plants. *Plant Physiology*, *81*(3), 842–846. https://doi.org/10.1104/pp.81.3.842

Easlon, H. M., & Bloom, A. J. (2014). Easy Leaf Area: Automated digital image analysis for rapid and accurate measurement of leaf area. *Applications in Plant Sciences*, *2*(7). https://doi.org/10.3732/apps.1400033

Eroglu, S., Giehl, R. F. H., Meier, B., Takahashi, M., Terada, Y., Ignatyev, K., Andresen, E., Küpper, H., Peiter, E., & von Wirén, N. (2017). Metal Tolerance Protein 8 Mediates Manganese Homeostasis and Iron Reallocation during Seed Development and Germination. *Plant Physiology*, *174*(3), 1633–1647. https://doi.org/10.1104/pp.16.01646

Esquinas-Alcázar, J. (2005). Protecting crop genetic diversity for food security: political, ethical and technical challenges. *Nature Reviews Genetics*, *6*(12), 946–953. https://doi.org/10.1038/nrg1729

Günl, M., Neumetzler, L., Kraemer, F., de Souza, A., Schultink, A., Pena, M., York, W. S., & Pauly, M. (2011). AXY8 Encodes an α-Fucosidase, Underscoring the Importance of Apoplastic Metabolism on the Fine Structure of *Arabidopsis* Cell Wall Polysaccharides. *The Plant Cell*, *23*(11), 4025–4040. https://doi.org/10.1105/tpc.111.089193

Höller, S., Küpper, H., Brückner, D., Garrevoet, J., Spiers, K., Falkenberg, G., Andresen, E., & Peiter, E. (2022). Overexpression of *METAL TOLERANCE PROTEIN8* reveals new aspects of metal transport in *Arabidopsis thaliana* seeds. *Plant Biology*, *24*(1), 23–29. https://doi.org/10.1111/plb.13342

Huang, M., Liu, X., Zhou, Y., Summers, R. M., & Zhang, Z. (2019). BLINK: a package for the next level of genome-wide association studies with both

individuals and markers in the millions. *GigaScience*, *8*(2). https://doi.org/10.1093/gigascience/giy154

Huh, S. U. (2021). The Role of Pumilio RNA Binding Protein in Plants. *Biomolecules*, *11*(12), 1851. https://doi.org/10.3390/biom11121851

Hwang, J. E., Hong, J. K., Lim, C. J., Chen, H., Je, J., Yang, K. A., Kim, D. Y., Choi, Y. J., Lee, S. Y., & Lim, C. O. (2010). Distinct expression patterns of two Arabidopsis phytocystatin genes, AtCYS1 and AtCYS2, during development and abiotic stresses. *Plant Cell Reports*, *29*(8), 905–915. https://doi.org/10.1007/s00299-010-0876-y

Idoudi, M., Slatni, T., Laifa, I., Rhimi, N., Rabhi, M., Hernández-Apaolaza, L., Zorrig, W., & Abdelly, C. (2024). Silicon (Si) mitigates the negative effects of iron deficiency in common bean (Phaseolus vulgaris L.) by improving photosystem activities and nutritional status. *Plant Physiology and Biochemistry*, *206*, 108236. https://doi.org/10.1016/j.plaphy.2023.108236

Ji, D., Chen, T., Zhang, Z., Li, B., & Tian, S. (2020). Versatile Roles of the Receptor-Like Kinase Feronia in Plant Growth, Development and Host-Pathogen Interaction. *International Journal of Molecular Sciences*, *21*(21), 7881. https://doi.org/10.3390/ijms21217881

Jiménez, M. R., Casanova, L., Saavedra, T., Gama, F., Suárez, M. P., Correia, P. J., & Pestana, M. (2019). Responses of tomato (*Solanum lycopersicum* L.) plants to iron deficiency in the root zone. *Folia Horticulturae*, *31*(1), 223–234. https://doi.org/10.2478/fhort-2019-0017

Jin, L.-F., Yarra, R., Yin, X.-X., Liu, Y.-Z., & Cao, H.-X. (2021). Identification and function prediction of iron-deficiency-responsive microRNAs in citrus leaves. *3 Biotech*, *11*(3), 121. https://doi.org/10.1007/s13205-021-02669-z

Kanehisa, M., Furumichi, M., Sato, Y., Kawashima, M., & Ishiguro-Watanabe, M. (2023). KEGG for taxonomy-based analysis of pathways and genomes.

Nucleic Acids Research, *51*(D1), D587–D592. https://doi.org/10.1093/nar/gkac963

Kim, S. A., & Guerinot, M. Lou. (2007). Mining iron: Iron uptake and transport in plants. *FEBS Letters*, *581*(12), 2273–2280. https://doi.org/10.1016/j.febslet.2007.04.043

Kinsella, R. J., Kahari, A., Haider, S., Zamora, J., Proctor, G., Spudich, G., Almeida-King, J., Staines, D., Derwent, P., Kerhornou, A., Kersey, P., & Flicek, P. (2011). Ensembl BioMarts: a hub for data retrieval across taxonomic space. *Database*, *2011*(0), bar030–bar030. https://doi.org/10.1093/database/bar030

Kobayashi, T., & Nishizawa, N. K. (2012). Iron Uptake, Translocation, and Regulation in Higher Plants. *Annual Review of Plant Biology*, *63*(1), 131–152. https://doi.org/10.1146/annurev-arplant-042811-105522

Krishna, T. P. A., Maharajan, T., & Ceasar, S. A. (2023). The Role of Membrane Transporters in the Biofortification of Zinc and Iron in Plants. *Biological Trace Element Research*, *201*(1), 464–478. https://doi.org/10.1007/s12011-022-03159-w

Krohling, C. A., Eutrópio, F. J., Bertolazi, A. A., Dobbss, L. B., Campostrini, E., Dias, T., & Ramos, A. C. (2016). Ecophysiology of iron homeostasis in plants. *Soil Science and Plant Nutrition*, *62*(1), 39–47. https://doi.org/10.1080/00380768.2015.1123116

Krouma, A., Gharsalli, M., & Abdelly, C. (2003). Differences in Response to Iron Deficiency Among Some Lines of Common Bean. *Journal of Plant Nutrition*, *26*(10–11), 2295–2305. https://doi.org/10.1081/PLN-120024282

KÜK, M., & BURGESS, P. (2010). The Pressures on, and the Responses to, the State of Soil and Water Resources of Turkey. *Ankara Üniversitesi Çevrebilimleri Dergisi*, 199–211. https://doi.org/10.1501/Csaum_0000000036

Kumar, R. K., Chu, H.-H., Abundis, C., Vasques, K., Rodriguez, D. C., Chia, J.-C., Huang, R., Vatamaniuk, O. K., & Walker, E. L. (2017). Iron-Nicotianamine Transporters Are Required for Proper Long Distance Iron Signaling. *Plant Physiology*, *175*(3), 1254–1268. https://doi.org/10.1104/pp.17.00821

Lan, P., Li, W., Wen, T.-N., Shiau, J.-Y., Wu, Y.-C., Lin, W., & Schmidt, W. (2011). iTRAQ Protein Profile Analysis of Arabidopsis Roots Reveals New Aspects Critical for Iron Homeostasis . *Plant Physiology*, *155*(2), 821–834. https://doi.org/10.1104/pp.110.169508

Lasocki, S., Gaillard, T., & Rineau, E. (2014). Iron is essential for living! *Critical Care*, *18*(6), 678. https://doi.org/10.1186/s13054-014-0678-7

Li, G., Kronzucker, H. J., & Shi, W. (2016). The Response of the Root Apex in Plant Adaptation to Iron Heterogeneity in Soil. *Frontiers in Plant Science, 7*. https://doi.org/10.3389/fpls.2016.00344

Li, J., Cao, X., Jia, X., Liu, L., Cao, H., Qin, W., & Li, M. (2021). Iron Deficiency Leads to Chlorosis Through Impacting Chlorophyll Synthesis and Nitrogen Metabolism in Areca catechu L. *Frontiers in Plant Science, 12*. https://doi.org/10.3389/fpls.2021.710093

Ling, H.-Q., Bauer, P., Bereczky, Z., Keller, B., & Ganal, M. (2002). The tomato *fer* gene encoding a bHLH protein controls iron-uptake responses in roots. *Proceedings of the National Academy of Sciences*, *99*(21), 13938–13943. https://doi.org/10.1073/pnas.212448699

Lucena, J. J., & Hernandez-Apaolaza, L. (2017a). Iron nutrition in plants: an overview. *Plant and Soil*, *418*(1–2), 1–4. https://doi.org/10.1007/s11104-017-3316-8

Lucena, J. J., & Hernandez-Apaolaza, L. (2017b). Iron nutrition in plants: an overview. *Plant and Soil*, *418*(1–2), 1–4. https://doi.org/10.1007/s11104-017-3316-8

Mace, E. S., Xia, L., Jordan, D. R., Halloran, K., Parh, D. K., Huttner, E., Wenzl, P., & Kilian, A. (2008). DArT markers: diversity analyses and mapping in Sorghum bicolor. *BMC Genomics*, *9*(1), 26. https://doi.org/10.1186/1471-2164-9-26

Mangena, P. (2020). Phytocystatins and their Potential Application in the Development of Drought Tolerance Plants in Soybeans (Glycine max L.). *Protein & Peptide Letters*, *27*(2), 135–144. https://doi.org/10.2174/0929866526666191014125453

Maphosa, Y., & Jideani, V. A. (2017). The Role of Legumes in Human Nutrition. In *Functional Food - Improve Health through Adequate Food*. InTech. https://doi.org/10.5772/intechopen.69127

Marschner's Mineral Nutrition of Higher Plants. (2012). Elsevier. https://doi.org/10.1016/C2009-0-63043-9

Means, R. T. (2020). Iron Deficiency and Iron Deficiency Anemia: Implications and Impact in Pregnancy, Fetal Development, and Early Childhood Parameters. *Nutrients*, *12*(2), 447. https://doi.org/10.3390/nu12020447

Merry, R., Dobbels, A. A., Sadok, W., Naeve, S., Stupar, R. M., & Lorenz, A. J. (2022). Iron deficiency in soybean. *Crop Science*, *62*(1), 36–52. https://doi.org/10.1002/csc2.20661

Morrissey, J., & Guerinot, M. Lou. (2009). Iron Uptake and Transport in Plants: The Good, the Bad, and the Ionome. *Chemical Reviews*, *109*(10), 4553–4567. https://doi.org/10.1021/cr900112r

Mullins, A. P., & Arjmandi, B. H. (2021). Health Benefits of Plant-Based Nutrition: Focus on Beans in Cardiometabolic Diseases. *Nutrients*, *13*(2), 519. https://doi.org/10.3390/nu13020519

NADEEM, M. A., & BALOCH, F. S. (2023). Genome-wide Association Studies revealed DArTseq loci associated with seed traits in Turkish common bean

germplasm. *Turkish Journal of Agriculture and Forestry*, *47*(4), 479–496. https://doi.org/10.55730/1300-011X.3103

Nadeem, M. A., Gündoğdu, M., Ercişli, S., Karaköy, T., Saracoğlu, O., Habyarimana, E., Lin, X., Hatipoğlu, R., Nawaz, M. A., Sameeullah, M., Ahmad, F., Jung, B.-M., Chung, G., & Baloch, F. S. (2019). Uncovering Phenotypic Diversity and DArTseq Marker Loci Associated with Antioxidant Activity in Common Bean. *Genes*, *11*(1), 36. https://doi.org/10.3390/genes11010036

Nadeem, M. A., Habyarimana, E., Çiftçi, V., Nawaz, M. A., Karaköy, T., Comertpay, G., Shahid, M. Q., Hatipoğlu, R., Yeken, M. Z., Ali, F., Ercişli, S., Chung, G., & Baloch, F. S. (2018a). Characterization of genetic diversity in Turkish common bean gene pool using phenotypic and whole-genome DArTseq-generated silicoDArT marker information. *PLOS ONE*, *13*(10), e0205363. https://doi.org/10.1371/journal.pone.0205363

Nadeem, M. A., Habyarimana, E., Çiftçi, V., Nawaz, M. A., Karaköy, T., Comertpay, G., Shahid, M. Q., Hatipoğlu, R., Yeken, M. Z., Ali, F., Ercişli, S., Chung, G., & Baloch, F. S. (2018b). Characterization of genetic diversity in Turkish common bean gene pool using phenotypic and whole-genome DArTseq-generated silicoDArT marker information. *PLOS ONE*, *13*(10), e0205363. https://doi.org/10.1371/journal.pone.0205363

Nadeem, M. A., Habyarimana, E., Karaköy, T., & Baloch, F. S. (2021). Genetic dissection of days to flowering via genome-wide association studies in Turkish common bean germplasm. *Physiology and Molecular Biology of Plants*, *27*(7), 1609–1622. https://doi.org/10.1007/s12298-021-01029-8

Naranjo-Arcos, M. A., & Bauer, P. (2016a). Iron Nutrition, Oxidative Stress, and Pathogen Defense. In *Nutritional Deficiency*. InTech. https://doi.org/10.5772/63204

Naranjo-Arcos, M. A., & Bauer, P. (2016b). Iron Nutrition, Oxidative Stress, and Pathogen Defense. In *Nutritional Deficiency*. InTech. https://doi.org/10.5772/63204

Nsiri, K., & Krouma, A. (2023). The Key Physiological and Biochemical Traits Underlying Common Bean (Phaseolus vulgaris L.) Response to Iron Deficiency, and Related Interrelationships. *Agronomy*, *13*(8), 2148. https://doi.org/10.3390/agronomy13082148

Pacheco, J. M., Song, L., Kuběnová, L., Ovečka, M., Berdion Gabarain, V., Peralta, J. M., Lehuedé, T. U., Ibeas, M. A., Ricardi, M. M., Zhu, S., Shen, Y., Schepetilnikov, M., Ryabova, L. A., Alvarez, J. M., Gutierrez, R. A., Grossmann, G., Šamaj, J., Yu, F., & Estevez, J. M. (2023). Cell surface receptor kinase <scp>FERONIA</scp> linked to nutrient sensor <scp>TORC</scp> signaling controls root hair growth at low temperature linked to low nitrate in *Arabidopsis thaliana*. *New Phytologist*, *238*(1), 169–185. https://doi.org/10.1111/nph.18723

Pathania, A., Sharma, S. K., & Sharma, P. N. (2014). Common Bean. In *Broadening the Genetic Base of Grain Legumes* (pp. 11–50). Springer India. https://doi.org/10.1007/978-81-322-2023-7_2

Paul, B. T., Manz, D. H., Torti, F. M., & Torti, S. V. (2017). Mitochondria and Iron: current questions. *Expert Review of Hematology*, *10*(1), 65–79. https://doi.org/10.1080/17474086.2016.1268047

Przybyla-Toscano, J., Boussardon, C., Law, S. R., Rouhier, N., & Keech, O. (2021). Gene atlas of iron-containing proteins in *Arabidopsis thaliana*. *The Plant Journal*, *106*(1), 258–274. https://doi.org/10.1111/tpj.15154

Puig, S., Ramos-Alonso, L., Romero, A. M., & Martínez-Pastor, M. T. (2017). The elemental role of iron in DNA synthesis and repair. *Metallomics*, *9*(11), 1483–1500. https://doi.org/10.1039/C7MT00116A

Pushnik, J. C., Miller, G. W., & Manwaring, J. H. (1984). The role of iron in higher plant chlorophyll biosynthesis, maintenance and chloroplast biogenesis. *Journal of Plant Nutrition*, *7*(1–5), 733–758. https://doi.org/10.1080/01904168409363238

Ruiz-Espinoza, F. H., Murillo-Amador, B., García-Hernández, J. L., Fenech-Larios, L., Rueda-Puente, E. O., Troyo-Diéguez, E., Kaya, C., & Beltrán-Morales, A. (2010). FIELD EVALUATION OF THE RELATIONSHIP BETWEEN CHLOROPHYLL CONTENT IN BASIL LEAVES AND A PORTABLE CHLOROPHYLL METER (SPAD-502) READINGS. *Journal of Plant Nutrition*, *33*(3), 423–438. https://doi.org/10.1080/01904160903470463

Sánchez, M., Sabio, L., Gálvez, N., Capdevila, M., & Dominguez-Vera, J. M. (2017). Iron chemistry at the service of life. *IUBMB Life*, *69*(6), 382–388. https://doi.org/10.1002/iub.1602

Seethepalli, A., Dhakal, K., Griffiths, M., Guo, H., Freschet, G. T., & York, L. M. (2021). RhizoVision Explorer: open-source software for root image analysis and measurement standardization. *AoB PLANTS*, *13*(6). https://doi.org/10.1093/aobpla/plab056

Sharma, B., Joshi, D., Yadav, P. K., Gupta, A. K., & Bhatt, T. K. (2016). Role of Ubiquitin-Mediated Degradation System in Plant Biology. *Frontiers in Plant Science*, *7*. https://doi.org/10.3389/fpls.2016.00806

Smith, M. R., & Rao, I. M. (2021). Common bean. In *Crop Physiology Case Histories for Major Crops* (pp. 384–406). Elsevier. https://doi.org/10.1016/B978-0-12-819194-1.00012-8

Spielmann, J., Fanara, S., Cotelle, V., & Vert, G. (2023). Multilayered regulation of iron homeostasis in Arabidopsis. *Frontiers in Plant Science*, *14*. https://doi.org/10.3389/fpls.2023.1250588

Sun, M., & Shen, Y. (2024). Integrating the multiple functions of CHLH into chloroplast-derived signaling fundamental to plant development and adaptation as well as fruit ripening. *Plant Science*, *338*, 111892. https://doi.org/10.1016/j.plantsci.2023.111892

Tibbs Cortes, L., Zhang, Z., & Yu, J. (2021). Status and prospects of genome-wide association studies in plants. *The Plant Genome*, *14*(1). https://doi.org/10.1002/tpg2.20077

Uebersax, M. A., Cichy, K. A., Gomez, F. E., Porch, T. G., Heitholt, J., Osorno, J. M., Kamfwa, K., Snapp, S. S., & Bales, S. (2023). Dry beans (<scp> *Phaseolus vulgaris* </scp> L.) as a vital component of sustainable agriculture and food security—A review. *Legume Science*, *5*(1). https://doi.org/10.1002/leg3.155

Vasconcelos, M. W., & Grusak, M. A. (2014). Morpho-physiological parameters affecting iron deficiency chlorosis in soybean (Glycine max L.). *Plant and Soil*, *374*(1–2), 161–172. https://doi.org/10.1007/s11104-013-1842-6

Wan, J.-X., Zhu, X.-F., Wang, Y.-Q., Liu, L.-Y., Zhang, B.-C., Li, G.-X., Zhou, Y.-H., & Zheng, S.-J. (2018). Xyloglucan Fucosylation Modulates Arabidopsis Cell Wall Hemicellulose Aluminium binding Capacity. *Scientific Reports*, *8*(1), 428. https://doi.org/10.1038/s41598-017-18711-1

Wang, J., & Zhang, Z. (2021). GAPIT Version 3: Boosting Power and Accuracy for Genomic Association and Prediction. *Genomics, Proteomics & Bioinformatics*, *19*(4), 629–640. https://doi.org/10.1016/j.gpb.2021.08.005

Wang, Q., Liu, J., & Zhu, H. (2018). Genetic and Molecular Mechanisms Underlying Symbiotic Specificity in Legume-Rhizobium Interactions. *Frontiers in Plant Science*, *9*. https://doi.org/10.3389/fpls.2018.00313

Wei Jin, C., You, G. Y., & Zheng, S. J. (2008). The iron deficiency-induced phenolics secretion plays multiple important roles in plant iron acquisition

underground. *Plant Signaling & Behavior*, *3*(1), 60–61. https://doi.org/10.4161/psb.3.1.4902

Yamamoto, A., Nakamura, T., Adu-Gyamfi, J. J., & Saigusa, M. (2002). RELATIONSHIP BETWEEN CHLOROPHYLL CONTENT IN LEAVES OF SORGHUM AND PIGEONPEA DETERMINED BY EXTRACTION METHOD AND BY CHLOROPHYLL METER (SPAD-502). *Journal of Plant Nutrition*, *25*(10), 2295–2301. https://doi.org/10.1081/PLN-120014076

Zhang, X., Zhang, D., Sun, W., & Wang, T. (2019). The Adaptive Mechanism of Plants to Iron Deficiency via Iron Uptake, Transport, and Homeostasis. *International Journal of Molecular Sciences*, *20*(10), 2424. https://doi.org/10.3390/ijms20102424

Zhou, M., Zhang, L. L., Ye, J. Y., Zhu, Q. Y., Du, W. X., Zhu, Y. X., Liu, X. X., Lin, X. Y., & Jin, C. W. (2021). Knockout of FER decreases cadmium concentration in roots of Arabidopsis thaliana by inhibiting the pathway related to iron uptake. *Science of The Total Environment*, *798*, 149285. https://doi.org/10.1016/j.scitotenv.2021.149285

Zhu, S., Estévez, J. M., Liao, H., Zhu, Y., Yang, T., Li, C., Wang, Y., Li, L., Liu, X., Pacheco, J. M., Guo, H., & Yu, F. (2020). The RALF1–FERONIA Complex Phosphorylates eIF4E1 to Promote Protein Synthesis and Polar Root Hair Growth. *Molecular Plant*, *13*(5), 698–716. https://doi.org/10.1016/j.molp.2019.12.014

Zielińska-Dawidziak, M. (2015). Plant Ferritin—A Source of Iron to Prevent Its Deficiency. *Nutrients*, *7*(2), 1184–1201. https://doi.org/10.3390/nu7021184

Zocchi, G., De Nisi, P., Dell'Orto, M., Espen, L., & Gallina, P. M. (2007). Iron deficiency differently affects metabolic responses in soybean roots. *Journal of Experimental Botany*, *58*(5), 993–1000. https://doi.org/10.1093/jxb/erl259

APPENDICES

A. Plant Material

Table A.1 Passport data of 136 Turkish common bean accessions were used in this study.

Genotype Number	Name	Genotype Number	Name
1	Bingol-1	**69**	Tunceli-11
2	Bingol-6	**70**	Van-1
3	Bingol-7	**71**	Van-11
4	Bingol-11	**72**	Van-13
5	Bingol-16	**73**	Van-17
6	Bingol-18	**74**	Van-19
7	Bingol-25	**75**	Van-25
8	Bingol-33	**76**	Van-27
9	Bingol-36	**77**	Van-36
10	Bingol-44	**78**	Van-42
11	Bingol-45	**79**	Van-51
12	Bingol-52	**80**	Van-59
13	Bingol-53	**81**	Van-65
14	Bingol-58	**82**	Van-68
15	Bingol-60	**83**	Elazig-2
16	Bingol-61	**84**	Elazig-14
17	Bingol-63	**85**	Elazig-16
18	Bingol-65	**86**	Elazig-25
19	Hakkari-11	**87**	Elazig-27
20	Hakkari-13	**88**	Elazig-29
21	Hakkari-16	**89**	Elazig-39
22	Hakkari-20	**90**	Mus-1
23	Hakkari-23	**91**	Mus-2
24	Hakkari-28	**92**	Mus-15
25	Hakkari-31	**93**	Mus-18
26	Hakkari-37	**94**	Mus-22
27	Hakkari-38	**95**	Mus-27
28	Hakkari-39	**96**	Mus-28
29	Hakkari-43	**97**	Mus-39
30	Hakkari-44	**98**	Mus-41
31	Hakkari-51	**99**	Mus-42
32	Hakkari-55	**100**	Mus-43

Table A1 (cont'd)

33	Hakkari-65	**101**	Mus-46
34	Hakkari-69	**102**	Mus-48
35	Hakkari-71	**103**	Mus-50
36	Hakkari-76	**104**	Mus-53
37	Bitlis-5	**105**	Sivas-4
38	Bitlis-22	**106**	Sivas-12
39	Bitlis-35	**107**	Sivas-17
40	Bitlis-53	**108**	Sivas-18
41	Bitlis-66	**109**	Sivas-44
42	Bitlis-69	**110**	Sivas-69
43	Bitlis-76	**111**	Sivas-70
44	Bitlis-81	**112**	Bilecik-2
45	Bitlis-90	**113**	Bilecik-6
46	Bitlis-94	**114**	Bilecik-7
47	Bitlis-97	**115**	Bilecik-10
48	Bitlis-103	**116**	Balikesir-4
49	Bitlis-105	**117**	Balikesir-5
50	Bitlis-111	**118**	Balikesir-6
51	Bitlis-115	**119**	Balikesir-17
52	Bitlis-117	**120**	Balikesir-18
53	Bitlis-118	**121**	Balikesir-19
54	Bitlis-119	**122**	Balikesir-20
55	Bitlis-120	**123**	Duzce-1
56	Bitlis-121	**124**	Duzce-9
57	Bitlis-124	**125**	YLV-20
58	Malatya-13	**126**	YLV-21
59	Malatya-18	**127**	Erzincan-4
60	Malatya-28	**128**	Erzincan-5
61	Malatya-33	**129**	Bursa-1
62	Malatya-50	**130**	Bursa-22
63	Malatya-51	**131**	Nigde-Dermasyon
64	Malatya-52	**132**	Nigde-Derinkuyu
65	Malatya-59	**133**	**Akman***
66	Malatya-71	**134**	**Karacaşehir***
67	Tunceli-1	**135**	Elazig
68	Tunceli-5	**136**	**Goksun***
*Commercial cultivars.			

B. Normality Test and Distribution Plots

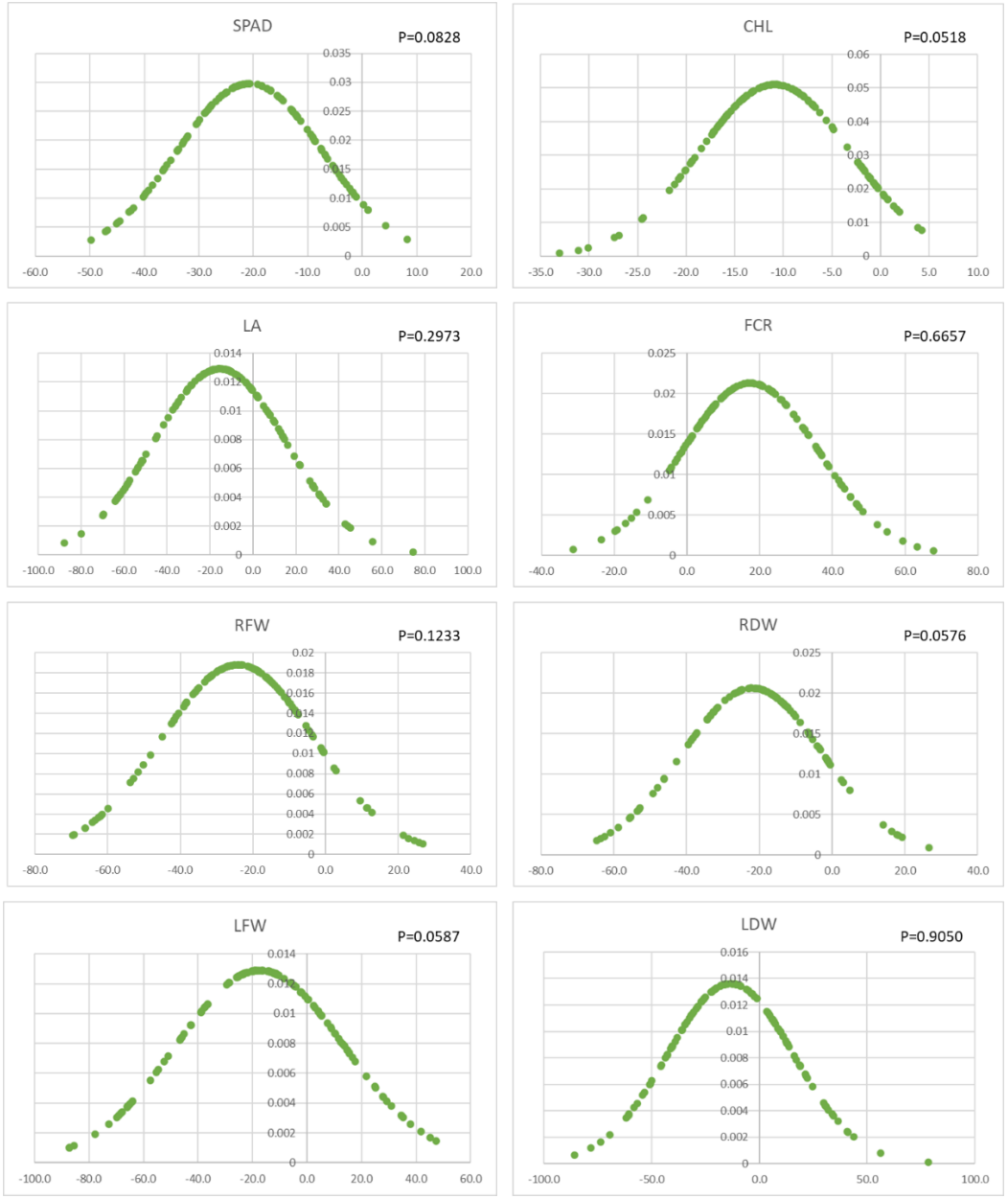

Figure B.1 Normal distribution analysis of relative change values of the studied traits.

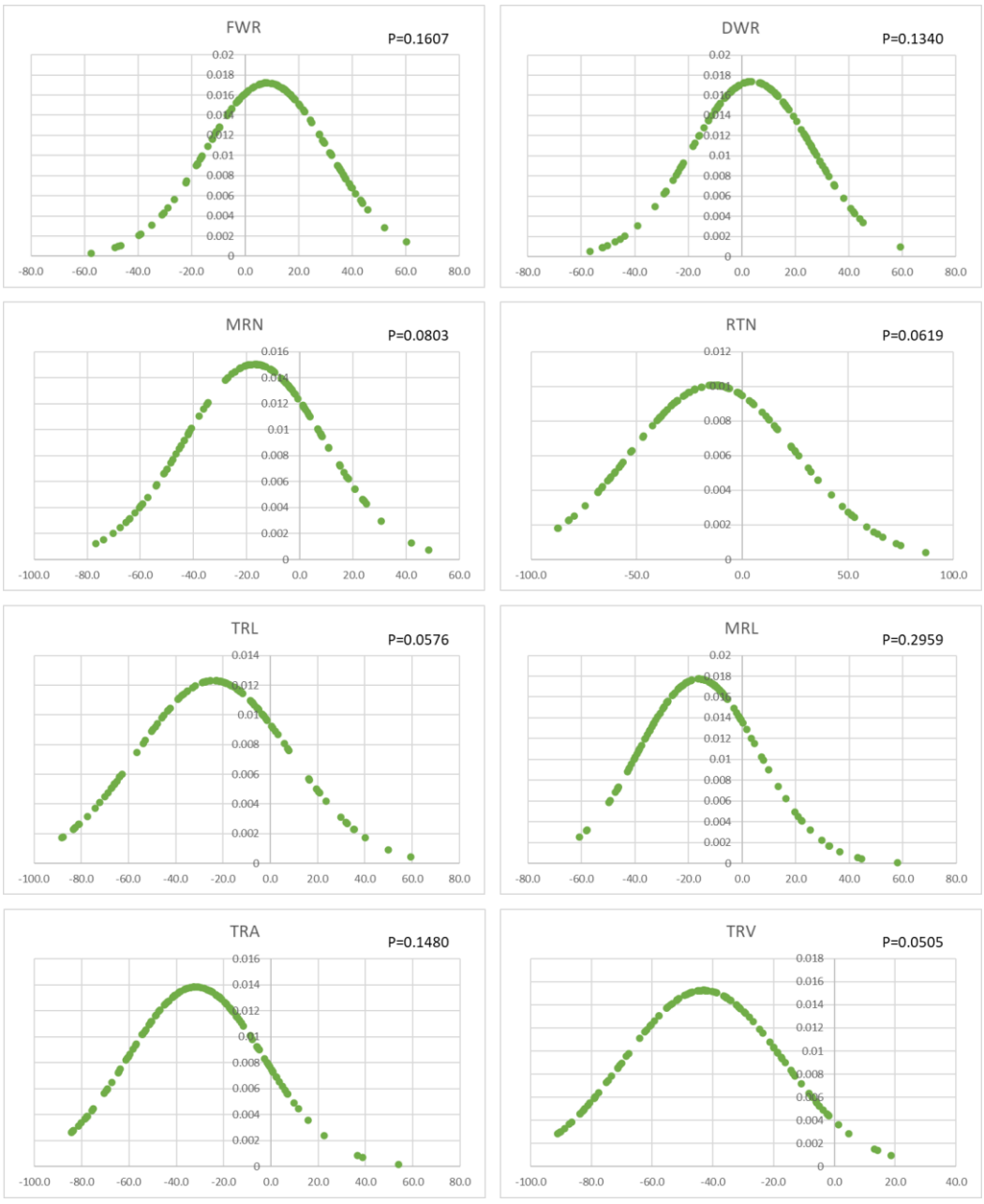

Figure B.2 Normal distribution analysis of relative change values of the studied traits.

C. Roots of the Most Sensitive and Tolerant Common Bean Accessions

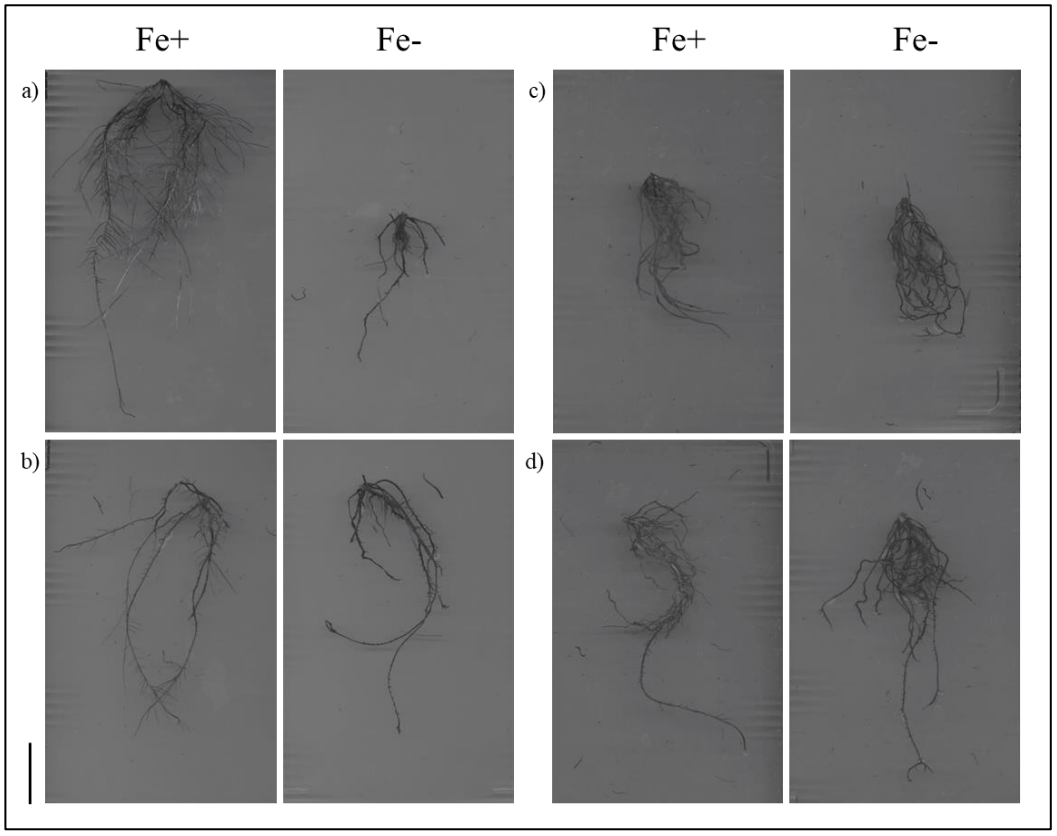

Figure C.1 Roots of the most sensitive and tolerant common bean accessions to Fe deficiency treatment. The most sensitive accessions are a) Bitlis-35, and b) Hakkari-23. The most tolerant accessions are c) Duzce-9, and d) Elazig. Bar represents 2 cm.